IMMUNE INFILTRATION IN OVARIAN CANCER AND ITS SIGNIFICANCE IN CHEMOTHERAPY

by

Charlotte Sum-Yee Lo

HBSc., The University of Toronto, 2010

A THESIS SUBMITED IN PARTIAL FULFILLMENT OF
THE REQUIREMENTS FOR THE DEGREE OF

MASTER OF SCIENCE

in

The Faculty of Graduate and Postdoctoral Studies

(Interdisciplinary Oncology)

THE UNIVERSITY OF BRITISH COLUMBIA
(Vancouver)

February 2015

Abstract

High grade serous carcinoma (HGSC), the most commonly diagnosed ovarian cancer subtype, is often presented as late stage disease with high recurrence rates, thus contributing to poor prognosis. Despite poor survival outcomes, the presence of tumour-infiltrating lymphocytes (TIL) in primary, untreated tumours is associated with increased survival. However, little is known about the phenotype and composition of TIL subsets in HGSC patients following treatment. In this thesis, we investigated the functional phenotype of TIL and the changes in immune composition in tumours over the course of chemotherapy.

In Chapter 2, we investigated the association of cytotoxic TIL with the presence of apoptotic tumour cells in primary tumours. By immunohistochemistry (IHC), we found that the majority of the CD8$^+$ T cells lack cytotoxic Granzyme B and that the presence of both CD8$^+$ and Granzyme B$^+$ TIL were not associated with the presence of apoptotic cleaved caspase-3$^+$ tumour cells. In Chapter 3, we investigated the composition of TIL subsets in HGSC following neoadjuvant chemotherapy in matching pre- and post-chemotherapy tumour samples. By IHC, we found an increased density of intraepithelial T cells, CD20$^+$ B cells, and TIA-1$^+$ and PD-1$^+$ TIL. In contrast, no significant change was found in the density of intraepithelial Granzyme B$^+$ TIL, FoxP3$^+$ T cells, or CD68$^+$ macrophages. Patients with high CD8$^+$ TIL density following chemotherapy showed prolonged survival. Thus, we found the immune response to cancer is dynamic, and TIL populations change during the course of treatment.

The results from this study indicate chemotherapy can alter the immunologic microenvironment in which tumour prior to chemotherapy lacking cytotoxic T cells can have increased infiltration of cytotoxicT cells and B cells, as well as PD-1$^+$ TIL. This study indicates the increased TIL infiltration following chemotherapy could be further enhanced with immunotherapies, such as tumour-specific vaccines and immune modulators (PD-1 blockade), to eradicate remaining tumour cells and reduce recurrences in HGSC. This work contributes to a better understanding of the effects of chemotherapy on TIL and this can lead to a more strategic development of immunotherapies in order to harness the anti-tumour immune response and

mitigate immunosuppression against cancer.

Preface

The research in this thesis was conducted with ethics approval from the UBC Ethics Board, Certificate REB# H12-00833. Funding for this study was supported by Canadian Institutes of Health Research (CIHR) and Congressionally Directed Medical Research Programs in the Department of Defence (DOD).

The research in this thesis was conducted by Charlotte Sum-Yee Lo. I designed and performed all the experiments in Chapter 2. I used a retrospective ovarian patient cohort that was previously designed and collected at the Deeley Research Centre. I performed all the optimizations, experiments, and data analyses.

I also designed and carried out the study in Chapter 3. I was responsible for identifying retrospective patients for the patient cohort relevant to the study, selecting tumour specimens, and designing the tissue microarray. I selected all the immune markers that were investigated, and I also optimized the triple-colour immunohistochemistry (CD3, CD8, TIA-1) protocol prior to the automated staining. The tissue microarray construction and automated serial single-stain immunohistochemistry were performed by Katy Milne, research assistant III, at the Deeley Research Centre. All the cell quantifications in the serial single-stain immunohistochemistry were performed by our collaborators, Drs. Blaise Clarke and Sanaz Sanii, at Princess Margaret Hospital, University Health Network, Toronto, ON. I conducted the data analyses and I consulted a biostatistician at BC Cancer Research Center, Aline Talhouk, for assistance with multiple testing analyses.

A version of Chapter 3 is being prepared for publication [Lo CS], Sanii S, Milne K, Talhouk A, Clarke BA, Nelson BH (2015). As indicated above, I designed the experiments for this project, performed data interpretation and analyses, and wrote the above manuscript.

Table of Contents

List of Tables

List of Figures

List of Abbreviations

APC	antigen presenting cell
ARID1A	AT-rich interactive domain 1A
ATP	adenosine tri-phosphate
BAX/BAK	Bcl-2-associated X/Bcl-2 homologous antagonist killer
BID	BH3 interacting domain death agonist
BRAF	B-Raf proto-oncogene, serine/threonine
BRCA1/2	breast cancer 1/2, early onset
Bregs	B regulatory cells
CAIS	British Columbia Cancer Agency's Information System
CCC	clear cell carcinoma
CCNE1	cyclin E1
CRT	calreticulin
CTL	cytotoxic T lymphocyte
CTLA-4	cytotoxic T-lymphocyte-associated protein 4
CTNNB1	catenin (cadherin-associated protein), beta 1
DAB	3, 3'-diaminobenzidine
DC	dendritic cell
DNA	deoxyribonucleic acid
EC	endometroid carcinoma
EOC	epithelial ovarian carcinoma
FIGO	Federation of Gynecology and Obstetrics
FFPE	formalin-fixed, paraffin-embedded
FoxP3	forkhead box P3
GM-CSF	granulocyte macrophage colony-stimulating factor
GzmB	granzyme B
ICD	immunogenic cell death

IFN-γ	interferon gamma
IHC	immunohistochemistry
IL-	interleukin
H&E	hematoxylin and eosin
HER2	human epidermal growth factor receptor 2
HGSC	high grade serous carcinoma
HMGB1	high-mobility group box 1
HNF-1B	hepatocyte nuclear factor-1 beta
HPF	high power fields
KRAS	Kirsten rat sarcoma viral oncogene homolog
KO	knocked down/out
LGSC	low grade serous carcinoma
LIF	leukemia inhibitory factor
LOH	loss of heterozygosity
MC	mucinous carcinoma
MDSC	myeloid derived suppressor cell
MECOM	MDS1 and EVI1 complex locus
MUC1	mucin 1
MYC	v-myc avian myelocytomatosis viral oncogene homolog
NF1	neurofibromin 1
NK	natural killer
NY-ESO-1	cancer/testis antigen 1
PARP	poly ADP ribose polymerase
pCR	pathological complete response
PIK3CA	phosophatidylinositol 3-kinase
PD-1	programmed cell death 1
PD-L1/2	programmed death ligand 1/2

PPP2R1A   protein phosphatase 2, regulatory subunit A, alpha

PTEN   phosphatase and tensin homolog

RAGE   receptor for advanced glycation end products

RB1   retinoblastoma 1

RNA   ribonucleic acid

RT-PCR   real-time polymerase chain reaction

STIC   serous tubal intraepithelial carcinioma

TAM   tumour associated macrophage

TCGA   the Cancer Genome Atlas

TIA-1   T cell restricted intracellular antigen 1

TIL   tumour infiltrating lymphocyte

TLR4   toll-like receptor 4

TMA   tissue microarray

TNF-α   tumour necrosis factor alpha

TP53   tumour protein p53

TRAIL   TNF-related apoptosis-inducing ligand

Treg   T regulatory cells

VEGF-A   vascular endothelial growth factor A

VGH   Vancouver General Hospital

Acknowledgements

I would first like to thank my supervisor Dr. Brad Nelson. He has been patient with me since I started, and has taken time to coach me through various facets of immunology. I am particularly grateful as he has never failed to stimulate critical thinking and provide constructive criticism in our meetings, and he has been a pillar of support throughout my studies. In the 4 years I have spent in his lab, he has given me numerous opportunities that have allowed me to develop a deeper understanding of cancer biology, immunology, and the elements involved in clinical studies. He has demonstrated that research benefiting patients involves a great deal of teamwork and collaboration amongst researchers and clinicians alike. I have come a long way as a graduate student and I thank Brad for mentoring me throughout the journey.

I would also like to extend my gratitude to my co-supervisor Dr. Yuzhuo Wang and all his lab members. He has always been supportive and keenly interested in my research. Of his lab members, I especially thank Margaret Sutcliffe for introducing me to the basics in pathology, Hui Xue, Rebecca Wu, and Yuwei Wang for teaching me about xenografts (and allowing me to realize that I am not too shabby at it), and students, Yanting Chiang and Iris Luk, for being supportive and helpful with experiments. I am truly grateful to the Wang lab for making me feel at home when I first started my graduate studies in Vancouver.

My research would not have been successful if it was not for the help of many others. Firstly, I would like to thank all past and present Nelson lab members for giving me intellectual guidance, advice on experiments, and technical support. I especially thank Katy Milne, who was always ready to help and has been great to work with. I would also like to express my gratitude to Dr. David Kroeger for being an integral member in supporting my research. He has never hesitated in providing me constructive criticism, was always available for scientific discussions, and constantly provided little reminders that my project was awesome. I would also like to thank Dr. Ron deLeeuw and Juzer Kakal for involving me in their animal studies, enabling me to learn the rigours of *in vivo* studies. Secondly, I would like to thank the other senior principal investigators of the Deeley Research Centre (DRC), Drs. Peter Watson, John Webb, and Julian

Lum. They have all given me important advice on pathology and immunology. Thirdly, I am incredibly grateful to those who were willing to bear with me and edit my thesis, specifically Katy Milne, Dr. David Kroeger, Ashley Westerback, Dr. Martin Isabelle, Dr. Lisa Johnson, and Jessica Pettigrew. I especially thank Ashley for being there for me whenever I needed it, as well as Martin and Lisa, who constantly gave me guidance in my project and career advice. I would also like to thank Jessica for lending a helping hand in times of need, especially when I was afflicted with vertigo. Lastly, I would like to thank other current and past members of the DRC who have contributed to my research and graduate school experience.

I would also like to express my appreciation for the members of my committee, Drs. Randy Gascoyne and Cheng-Han Lee. They have each provided advice on patient cohort selection, pathology, statistics on clinical data analyses, and support toward the completion of my thesis. They have always taken time from their busy schedule to give me guidance whenever possible, and for that, I am truly grateful.

I would also like to thank my collaborators at University Health Network, Drs. Blaise Clarke and Sanaz Sanii for a wonderful collaboration. My research would not have been possible without your help and the team camaraderie we have established. It was a pleasure to work with you.

To my friends and family members, there are no words to describe the support you have given me over these past four years. I could not have completed this Masters thesis without the love and care that my parents in Toronto and extended family members in Vancouver have given me. To my friends back in Toronto and my new found friends at BCCRC, I cannot thank-you enough for the mental support you have given me.

This journey has been challenging and rewarding at the same time. I have grown a lot over the past four years and I acknowledge that many have helped me grow and shape who I am today. Thank you to you all and I look forward to starting a new chapter in my life. I share a verse that has been dear to me throughout my studies:

Philippians 4:13 "For I can do everything through Christ, who gives me strength." NLT

Dedication

This thesis is dedicated to all the women who have battled against ovarian cancer. I also want to dedicate this to Uncle Kevin, who died of glioblastoma multiforme when I was 10 years old, and Uncle Stephen, who is in remission of liposarcoma. All of you have inspired me to pursue a career in science. May we find a better treatment not just for ovarian cancers, but all cancers.

1. Introduction

1.1. Ovarian cancer

Ovarian cancer is the eighth most commonly diagnosed cancer type in females in Canada[1]. The majority of ovarian cancers, approximately 62%, are diagnosed at late stage (stage III and IV), while early stage (stage I and II) tumours account for the remaining 38%[2]. The late detection of ovarian cancer has contributed to its poor prognosis, with a 5-year survival of 29% for women diagnosed at last stage[3]. Once treated as a single disease, ovarian cancer is now recognized as consisting of separate subtypes that involve the ovaries and other pelvic and abdominal tissues. With the advancement in genetic sequencing and a deeper knowledge of the different histopathological patterns, epithelial ovarian cancer (EOC) is presently classified into 5 subtypes with distinct genomic aberrations and molecular pathway perturbations. These specific characteristics provide opportunities for targeted therapies based on EOC subtype.

1.1.1. Pathology and clinical management of epithelial ovarian carcinoma subtypes

EOC is universally diagnosed using World Health Organization (WHO) classification and Federation of Gynecology and Obstetrics (FIGO) staging system. Tumours are classified based on morphology, as well as other pathological features, such as grade, stage, nuclear and tumour size, biomarker expression, and gene signatures. Grade is a score given for the histologic degree of abnormality of the tumour cells; the higher the grade, the more dissimilar the tumour cells appear in terms of appearance of the nuclei, mitotic rate, and structural organization of the cells compared to normal cells of the same tissue. Stage describes the size of the tumour and the extent of spread. The combination of grade and stage describes the aggressiveness and severity of the tumour. In the revised 2014 FIGO system, the stagings are defined as follows: stage I - tumour confined to one ovary, stage II – tumour involves one or both ovaries and extends to other pelvic areas such as uterus and fallopian tubes, stage III – tumour involving one or both ovaries with extensive spread to the pelvis and metastasis to retroperitoneal lymph nodes, or

surface of liver or spleen, and stage IV – tumour involving metastasis to other extra-abdominal organs such as liver and or spleen parenchyma.

There are five major subtypes of EOC (Figure 1): high grade serous carcinoma (HGSC), low grade serous carcinoma (LGSC), clear cell carcinoma (CCC), endometrioid carcinoma (EC), and mucinous carcinoma (MC). HGSC is the most common subtype and constitutes 67-68% of epithelial ovarian cancers, followed by CCC (10-12%), EC (6.8-11%), MC (2.7-3.5%), LGSC (3.5%), and others (2%)[2, 4].

HGSC accounts for 88% of advanced ovarian cancer (Stage III and IV) diagnoses[2]. It is histologically characterized by highly stratified epithelium with papillary pattern, slit-like glandular spaces and/or solid growth. The tumour cells are intermediate in size with the presence of multinucleated mononuclear giant cells[5]. HGSC has a high mitotic index, with ≥12 mitoses per 10 high power fields (HPF)[6, 7]. In addition to the marked high rates of mitosis, the presence of high nuclear atypia, irregular chromatin, and presence of macronucleoli are features characteristic of HGSC. *TP53* mutation is present in majority of (96%) the tumours and approximately 40% of HGSCs have genetic mutations or epigenetic loss of *BRCA1/2* mutations[8]. The majority of HGSC tumours are initially chemotherapy sensitive, and treatment commonly involves a combination of platinum and taxane therapy. Nonetheless, HGSC has a poor prognosis with a 5-year survival rate of 29% for stage IIIC patients and 13% for stage IV patients[9]. Moreover, many patients encounter multiple recurrences before succumbing to the disease[10].

Clear cell carcinoma (CCC) accounts for 12% of ovarian cancers in North America and is more prevalent in Asia, specifically Japan (14%)[2, 11]. CCC tumours consist of a mixture of clear, hobnail, and oxyphil cell types arranged in tubulocystic, papillary, and solid architectural patterns, with densely hyaline basement membrane material expanding the cores of the papillae and hyaline bodies[5, 12]. The tumour cells feature clear cytoplasm with a low mitotic index of <5 mitoses/10 HPF[5, 12, 13]. Although often diagnosed in early stage, CCC has an unfavourable prognosis due to high recurrence rates and chemotherapy resistance[14]. The presence of

endometriosis is associated with longer overall survival and lower instances of recurrences, and between 40-70% of CCC present with co-existing endometriosis[15, 16, 17]. Mutations involving AT-rich interactive domain 1A gene (*ARID1A*) and phosphatidylinositol 3-kinase (*PIK3CA*) are present in 50% and 43% of CCC cases respectively[18, 19, 20]. Apart from these genetic signatures, angiogenesis also appears to play an essential role in the survival of CCC. Accordingly, drugs like sunitnib, an inhibitor of angiogenesis, have become attractive therapies for targeting CCC[21]. A few studies have shown responses to sunitinib, which therefore warrants further investigation as a future therapy[22].

Endometrioid carcinoma (EC) is the third most common subtype and comprises of 11% of EOC[2]. ECs are normally diagnosed at stage I and II and confined to the ovary, thus surgery alone is sufficient for treatment. Similar to CCC, endometriosis is frequently found in association with EC, and is present in 23-54% of reported cases[16, 23, 24, 25]. These factors indicate EC is less aggressive compared to other EOC subtypes, and indeed low stage EC is associated with favourable outcome[2, 26]. Tumours display glandular architecture lined by a stratified non-mucin-containing cells with squamous differentiation[5, 12, 27]. The most common mutations in EC are related to the Wnt and PI3K signalling pathways. Mutations in *CTNNB1* and *PTEN* are present in 28% and 17% of low-grade ovarian ECs respectively[28]. By immunohistochemistry (IHC), beta-catenin is detectable in 38-80% of EC tumours, and this is almost always linked with *CTNNB1* mutations[29, 30]. Similar to CCC tumours, EC harbours *ARID1A* mutation, albeit at a lower frequency in comparison to CCC, *PIK3CA*, and *PP2R1A* mutations in 20-30%, 40%, and 7-12% of cases respectively[19, 31, 32, 33, 34]. The majority of tumours are treated by surgery alone, but advanced staged ECs are treated by platinum plus taxane based chemotherapy[12].

Mucinous carcinoma (MC), one of the least studied subtypes, accounts for only 3.5% of EOC[2]. Often diagnosed as stage I and II tumours, MCs are borderline tumours that are large (>13cm) but confined to the ovary[2, 27, 35]. These tumours resemble endocervix, gastric pylorus, and intestine with the majority of MC tumours displaying gastrointestinal differentiation[5]. The presence of mucin within tumour cells is a prominent feature in primary MC, although this can

3

be absent in recurrent tumours[12]. MCs often harbour *KRAS* mutations at codon 12 between 50-75% of cases, but with no detectable *BRAF* mutations[36, 37, 38]. *HER2* amplification and overexpression is seen in approximately 15% of MCs[39, 40]. The occurrence of *KRAS* mutations and *HER2* amplification is mutually exclusive, indicating possible subclonal populations of MC that activates Ras and ErbB signalling pathways respectively. Surgery is the first-line treatment for early stage MC tumours, and prognosis for MC patients with low-stage disease is favourable. However, metastasis and recurrence of MC tumours is associated with poor prognosis and platinum-based chemotherapy is the only treatment option[41, 42].

Low grade serous carcinoma (LGSC), now recognized as a separate subtype from HGSC, is rare and accounts for 3.5% of EOC[2]. It is characterized by micropapillary or cribriform pattern with low malignant potential in >50% of the tumour[6, 7]. The tumour cells exhibit uniform, round, and oval nuclei and low mitotic index of <12 mitoses /10 HPF[6, 7]. In contrast to HGSC, LGSC does not harbour *BRCA* mutations, and *TP53* mutations occur in less than 10% tumours[27, 43]. Furthermore, LGSC lacks the chromosomal instability and genetic aberrations of HGSC[5, 27]. Instead, *BRAF* and *KRAS* mutations are found in 33% and 35% of LGSC respectively, and are mutually exclusive[44]. Because of the recent reclassification as a separate subtype, much is still unknown about effective treatments and prognosis. One study indicated favourable prognosis with a median survival of 21 years, however, poor survival was associated with recurrent disease[45].

The recent reclassification of EOC subtypes has contributed to a better understanding of the separate diseases. Genetic mutations and corroborating immunohistochemical staining patterns have shed light on the signalling pathways and histological morphologies unique to each subtype. These new findings have allowed for reproducible diagnoses and identification of potential targeted therapies[26, 46, 47]. For example, the presence of lymphocytes in the tumour epithelium is associated with increased survival primarily in HGSC, thus allowing opportunities to use immunotherapies in treatment[48, 49, 50, 51]. In contrast, angiogenesis plays a prominent role in CCC and inhibitors, such as sunitinib, are more applicable in the treatment of CCC[21]. Therefore,

molecular aberrations unique to each subtype can be used for developing more effective targeted treatment.
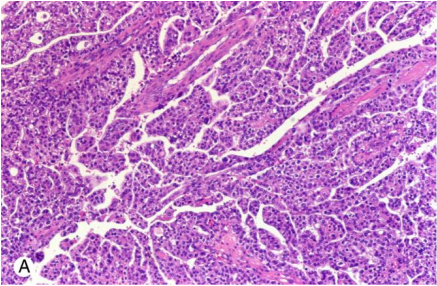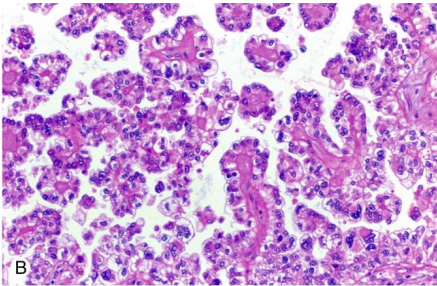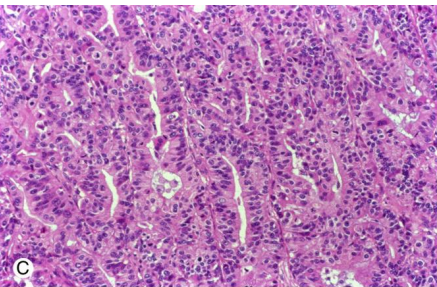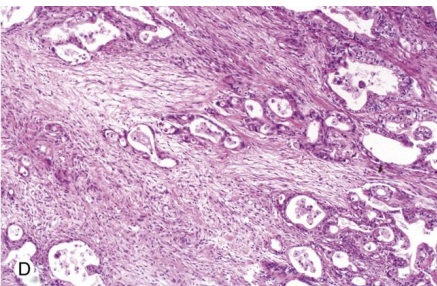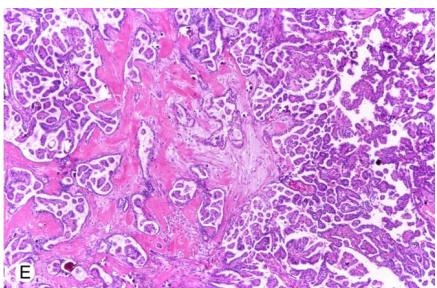
EOC subtype	EOC Immunohistochemistry	Mutations
HGSC		• TP53 in 96% cases • BRCA1/BRCA2 • High genomic instability
CCC		• ARID1A • PIK3CA
EC		• CTNNB1 • PTEN • ARID1A
MC		• KRAS • HER2
LGSC		• TP53 in 10% cases • no BRCA1/BRCA2 • lack of genomic instability

Figure 1. Five subtypes of EOC and subtype-specific genetic mutations (IHC taken from Gilks et al, 2009, Hum Pathol)

1.1.2. High grade serous carcinoma (HGSC)

HGSC is the most prevalent subtype of ovarian cancer, accounting for 70% of EOCs and 90% of ovarian cancer deaths[2, 4, 52]. A major contributor to the poor prognosis in HGSC is the lack of sensitivity and specificity in the detection of the disease[10]. The presenting symptoms of HGSC are typically nonspecific, and commonly suggest abdominal and gastrointestinal diseases, which are frequently present in post-menopausal women independent of the presence of cancer. Commonly reported symptoms include abdominal fullness, dyspepsia or indigestion, early satiety, and bloating. Bloating is caused by an increase in ascites fluid that increases the pressure within the pelvic space. Patients who experience these symptoms often present with stage III/IV disease. However, patients diagnosed with stage I/II disease are typically asymptomatic with a proportion experiencing pelvic pain due to ovarian torsion. Diagnoses involve physical examinations, visualizations by X-ray computed tomography (CT) scans, and serological detection of the tumour marker, CA-125. Currently, CA-125 is the standard diagnostic tumour marker in the clinic. Despite being elevated in 80% of HGSC patients and widely employed in diagnostic tests, CA-125 is also elevated in other cancers and conditions such as pregnancy, endometriosis, pelvic inflammatory disease, menstruation and benign cysts[10]. Thus, CA-125 is neither specific nor sensitive enough to be a stand-alone diagnostic marker for HGSC. Rather, a diagnosis is determined using the combined information collected from pelvic examinations, imaging, and CA-125 testing [53]. Although CA-125 alone is insufficient in determining HGSC diagnosis, it is useful in indicating response to chemotherapy and monitoring for relapses. Significant decreases in CA-125 in conjunction with reduction in tumour size seen on CT scans can reliably indicate a favourable response to chemotherapy, while a rise in CA-125 correlates with disease progression and relapse[54, 55]. The procedures utilized for the detection of HGSC have remained stagnant and a need for more sensitive and specific testing methods is of paramount importance so that earlier detection and treatment of HGSC can improve survival.

1.1.3 Molecular genetics of HGSC

Genetic aberrations unequivocally distinguish HGSC from other EOC subtypes. The genetic hallmarks of HGSC consist of chromosomal instability, and *TP53* and *BRCA1/2* mutations[56]. *TP53* is the most prevalently mutated gene in HGSC, accounting for 70-95% of cases[8, 57, 58, 59]. In a recent large-scale genome sequencing study by the Cancer Genome Research Atlas Network, *TP53* mutation was reported in 303/316 HGSC samples[8]. The product of *TP53*, p53, induces cell arrest, DNA repair, and apoptosis of cells with damaged DNA due to exposure to environmental and cellular stress[60]. This indicates the importance of p53 in cell regulation and, thus, genomic abnormalities in *TP53* leads to tumourgenesis. Missense mutations and deletions, as well as nonsense mutations are found in 55% and 25% of cases, respectively[57, 58]. Mutation type is often reflected in the immunohistochemical staining pattern of p53. Missense mutations result in an accumulation of mutant p53 within the nuclei of tumour cells, thus tumours display strong and diffuse p53 staining. Deletion and nonsense mutations do not stain for p53 because of the encounter of early stop codons and truncation of the proteins[43, 57, 58]. Despite the strong correlation between mutational status and p53 immunohistochemical staining, especially for missense mutations, wildtype *TP53* in HGSC tumours were found to exhibiting a wide range of p53 expression with some displaying similar IHC patterns as mutated *TP53*[59]. Therefore, without genetic testing in conjunction with IHC information, tumours harbouring wildtype *TP53* but exhibit strong, diffuse positive p53 staining or loss of p53 expression can be mistaken as harbouring missense or deletion/nonsense *TP53* mutations respectively. A larger study correlating *TP53* mutational status and IHC p53 expression pattern is needed to replicate and confirm the findings regarding wildtype TP53 expression in HGSCs and validate the sensitivity and accuracy of the loss of p53 expression with deletion and nonsense mutations.

The second most commonly mutated family of tumour suppressor genes is *BRCA*. It is associated with an increased risk of developing HGSC by 40-60% for *BRCA1* carriers and 11-27% *BRCA2* carriers[61, 62, 63, 64]. In the Cancer Genome Atlas (TCGA) study, germline *BRCA1* (chromosome 17q21) and *BRCA2* (chromosome 13q12-q13) mutations were found in 9% and

8% of cases respectively, while somatic mutations accounted for a further 3% of cases[8]. In smaller studies, *BRCA1* is mutated in 14-19% of cases, while *BRCA2*, is found mutated in approximately 5-6% of cases[65, 66]. In congruence with the study above, one Canadian study found the prevalence of germline *BRCA* mutations to be 16.4%, with *BRCA1* and *BRCA2* mutated in 10.9% and 5.5% of HGSCs respectively[67]. The wildtype BRCA proteins are involved in error-free repair of double stranded breaks in DNA via homologous recombination, and mutations in BRCA genes can result in an accumulation of double stranded breaks from defective DNA repair protein complexes[68]. *BRCA* mutation is autosomal dominant, thus mutation in one allele leads to the production of defective BRCA proteins. Interestingly, a study from Vancouver General Hospital (VGH) showed 44% of cases with *BRCA1* mutation had positive p53 expression by IHC[66]. Besides genetic mutations, epigenetic loss of *BRCA1* through hypermethylation is observed in 11.5% of cases in a TCGA study, and 18% in HGSC cases in a VGH study[8, 66]. In contrast, epigenetic loss of *BRCA2* is less commonly seen[69]. Interestingly, 89% of cases with epigenetic loss of *BRCA1* had positive p53 expression by IHC[66]. Moreover, HGSCs with epigenetic loss of *BRCA1* had an increase in *PI3KCA* copy number, while mutational loss of *BRCA1* had abrogated *PTEN* mRNA expression, and these were mutually exclusive[66]. Collectively, these studies are beginning to identify possible subgroups of HGSC based on genetic differences. HGSCs with *BRCA* mutations have moderate occurrences of positive p53 expression and an attenuated *PTEN* mRNA expression, while tumours with epigenetic loss of *BRCA* frequently have positive p53 expression and an increase in *PI3KCA* copy number. Chromosomal instability, such as aneuploidy, is not associated with *BRCA1* status, suggesting that a defect in homologous repair is not the only contributor to genomic instability in HGSC[70]. Several studies have shown an increased recurrence free and overall survival in *BRCA* carriers[71, 72]. It is suggested that the benefit is due to elevated sensitivity towards chemotherapy, leading to a greater response to treatment[73].

Other genomic aberrations seen are amplification in copy number, deletions, and increased expression of mRNA and miRNA. Amplification of *CCNE1*, *MYC*, and *MECOM* is

seen in 20% of tumours, while deletion of *PTEN*, *RB1*, *NF1* is observed in 2% of cases, with *RB1* and *NF1* being more commonly mutated[8]. The high prevalence of mutations in *TP53* and *BRCA1/2* in HGSC tumours distinguishes HGSC from other forms of EOC. When the pathological diagnosis of EOC by histology is uncertain, as it is often the case with mixed serous tumours, genetic testing for these mutations can provide additional information for the correct diagnosis of HGSC.

1.1.4. Etiology of HGSC

Different theories for the development of HGSC have been proposed. Earlier theories postulated that inflammation of the ovary was the culprit of HGSC development[56]. The "incessant ovulation hypothesis" proposed that during ovulation, the continuous rupture and inflammation of the ovarian serous epithelium lead to the development of ovarian cancer. Another theory is that the high levels of reactive oxygen species released during ovulation lead to DNA damage and cause the malignant transformation of the cells of the ovarian epithelium[74]. Despite these theories, cases with precursor lesions confined to the ovaries are low in numbers, suggesting that the ovary is not the tissue of origin for HGSC[75].

A more recent proposal is that repeated exposure to inflammatory agents within the retrograde flow from the endometrium to the fallopian tube during menstruation leads to the malignant transformation of cells[76, 77]. Over time, the repeated exposure to inflammatory agents causes first acute, then chronic inflammation of the cells in the fallopian tube. One study found a higher concentration of inflammatory cytokines interleukin 8 (IL-8), IL-12, IL-1, granulocyte macrophage colony-stimulating factor (GM-CSF), leukemia inhibitory factor (LIF), and tumour necrosis factor alpha (TNF-α) in the fluid from hydrosalpinx compared to normal follicular fluid[78]. Furthermore, TNF-α, IL-1, GM-CSF, and IL-8 were found to be overexpressed in ovarian carcinomas compared to normal ovarian tissue[79]. These results suggest that inflammation at the fallopian tube is a plausible hypothesis for HGSC development.

The most compelling evidence for the tissue of origin in HGSC comes from prophylactic

surgeries of BRCA carriers. During these surgeries, fallopian tubes and ovaries were removed. Histological investigation revealed cells with similar appearance to HGSC were found at the fimbrae of the fallopian tubes[80]. These occult carcinomas found in the fallopian tube are known as serous tubal intraepithelial carcinoma (STIC). STICs were observed in 6% to 39% of HGSC cases, and 43% to 100% of HGSC cases had fallopian tube involvement[80, 81, 82, 83]. In a recent study, *TP53* mutations were found in 27/29 (93%) HGSC cases with concurrent STICs that had p53 staining patterns typical of HGSC tumours[84]. These findings prompted Piek et al.to propose that HGSC develops from the shedding of malignant cells from STICs, located on the fallopian tube, leading to seeding on the ovary and subsequent development into HGSC[85]. The involvement of STICs in the development of HGSC provides strong rationale for the removal of both ovaries and fallopian tubes in BRCA-positive carriers to reduce the risk of developing ovarian cancer. Indeed, studies have shown a reduced risk of ovarian cancer by 96% in BRCA carriers through prophylatic surgery[86, 87]. Tubal ligations, which are surgical sterilizations of the fallopian tubes, have been shown to decrease the risk of ovarian cancer[88, 89, 90, 91]. Collectively, these studies have led to a renaming of "high grade serous ovarian carcinoma" to "high grade serous carcinoma".

1.1.5. Treatment advancements in HGSC

Standard treatment for HGSC

The standard treatment for most late stage HGSCs is a combination of surgery and chemotherapy. Surgery serves two important purposes: to remove as much tumour as possible and to provide a subtype-specific pathological diagnosis[92]. Surgical resection can include: hysterectomy (removal of the uterus), bilateral salpingo-oophorectomy (removal of both fallopian tubes and ovaries), omentectomy (removal of the omentum), and removal of other abdominal or pelvic areas and adjacent lymph nodes[92]. The success of the surgery can have a significant impact on patient survival. Patients who have most of their tumour removed at the time of surgery are classified as optimally debulked, while patients with residual disease greater

than 1 cm are classified as suboptimally debulked. Several studies have reported patients who are optimally debulked had a higher 5-year survival rate and a lower rate of recurrences[93, 94, 95, 96]. In one study, patients who had less than 1 cm of residual disease following surgery had a median survival of 33.9 months compared to patients with more extensive residual disease post-surgery with a median survival of 22.4 months[96].

Following tumour debulking surgery, cytotoxic drugs are administered to treat residual disease (known as adjuvant chemotherapy). Chemotherapy plays an important role in the survival of HGSC patients. A clinical study showed suboptimally debulked patients had a longer survival (median survival of 38 months) with taxane agent included in the chemotherapy regimen compared to those who did not receive taxane (median survival of 24 months)[97]. These studies indicate that in advanced disease, both surgery and chemotherapy are vital to the treatment of HGSC.

The current standard chemotherapy used for HGSC treatment is a combination of platinum and taxane chemotherapy. Prior to the 1980s, the combination of cisplatin and cyclophosphamide were the main therapeutic agents for the treatment of ovarian cancers[98]. Similar to many chemotherapeutic agents that modify DNA, cisplatin, a platinum-based antineoplastic agent, acts to form intra-strand cross-links with the DNA[10]. In the 1980s-1990s, the discovery of paclitaxel, a taxane drug, from the bark of the Pacific yew tree led to the advances in chemotherapy-based treatment of ovarian cancers[98]. The mechanism of activation of paclitaxel involves the stabilization of tubulin polymer formation[99]. The superior efficacy of cisplatin plus paclitaxel over cisplatin plus cyclophosphamide was demonstrated in a number of clinical trials which in 1998 led to the universal acceptance of platinum-based plus taxane chemotherapy as the standard treatment[100, 101, 102]. In 1979, carboplatin, an analogue of cisplatin, was introduced as a better alternative to cisplatin[98]. Two randomized trials showed that carboplatin plus paclitaxel was just as effective as cisplatin plus paclitaxel, but with fewer side effects, including reduced nausea, leukopenia, and nephropathy[103, 104]. These findings led to the current standard chemotherapy treatment regimen of carboplatin plus paclitaxel.

Recently, there has been a shift in the scheduling and dosing of chemotherapy, in the hopes of improving treatment for HGSC. Prior to the 2000s, the standard protocol was adjuvant therapy (debulking surgery followed by subsequent chemotherapy), but a shift towards neoadjuvant therapy (chemotherapy followed by debulking surgery) is occurring in many clinics. At VGH, neoadjuvant chemotherapy is a treatment option for HGSC patients with stage IIIC or IV HGSC disease who present with severe disseminated disease at the time of the exploratory laparotomy or primary surgery. Neoadjuvant chemotherapy begins with the administration of 3-4 cycles of chemotherapy to resolve the ascites and reduce tumour burden in patients. A good response to treatment, as indicated by a significant decrease in CA-125 and tumour size by CT scans, is subsequently followed by a second surgery, referred to as interval debulking. Following interval debulking, patients are given several more rounds of chemotherapy until they are negative for tumour. The efficacy of neoadjuvant chemotherapy has been compared with that of adjuvant chemotherapy, and studies have reported mixed results in the efficacy and survival benefit of neoadjuvant compared with adjuvant chemotherapy. A few studies have indicated that neoadjuvant chemotherapy is associated with inferior survival compared to conventional adjuvant chemotherapy[105, 106]. Several other studies (one randomized and four retrospective), comparing adjuvant and neoadjuvant therapy in stage IIIC and IV advanced ovarian cancer patients, found similar overall survival (29-47 v.s. 30-46 months) and progression free (12-14 v.s. 12-18 months) survival between the two groups[107, 108, 109, 110]. Despite similar survival outcomes, all the studies were unanimous in stating that neoadjuvant therapy had a higher rate of optimal tumour debulking, as well as lower morbidity and post-operative complications[107, 108, 109, 110, 111]. Neoadjuvant patients had a higher rate of optimal tumour debulking (80-95% of cases) compared to adjuvant patients (55-71% of cases)[107, 108]. Furthermore, patients with neoadjuvant chemotherapy had lower rates of peri-operative and post-operative complications such as blood loss, OR time, length of hospital stay, admissions to intensive care units, and deaths[107, 108, 111]. Although these studies indicate that there is no added survival benefit with neoadjuvant chemotherapy, it nonetheless increases the percentage of cytoreduction (amount of

tumour debulked) achieved and lowers the morbidity rates to allow for a better quality of care for patients.

Chemotherapy resistance

The potential of increased chemotherapy resistance due to earlier exposure to chemotherapy in the neoadjuvant setting has been raised, but little research has been done to address this. There is currently one study that has compared chemoresistance between neoadjuvant and adjuvant chemotherapies[112]. In this retrospective study, they compared chemoresistance rates in 95 neoadjuvant-treated patients with 330 adjuvant-treated patients and found resistance to be higher in neoadjuvant patients[112]. Resistance to platinum therapy, measured by recurrence at 6 months from the completion of the first platinum-based chemotherapy, was significantly higher in neoadjuvant-treated patients (44.2%) compared to adjuvant-treated patients (31.2%). However, statistical significance was lost when multivariate logistic regression was used to control for factors that are known to be associated with recurrence, signifying resistance is influenced by multiple factors. In addition, two other studies indicated that chemoresistance increased as the number of treatment cycles increased prior to interval debulking[105, 113]. Although a few studies have suggested neoadjuvant chemotherapy is associated with increased chemoresistance in HGSC tumours, platinum resistance also occurs in approximately 50% of the patients treated with adjuvant chemotherapy, indicating that chemoresistance is influenced by multiple factors. As more neoadjuvant chemotherapy is being utilized, this will provide more opportunities for studies to compare the incidences of chemoresistance between neoadjuvant and adjuvant chemotherapies.

DNA repair chemotherapy targets

Novel chemotherapeutic drugs that target DNA repair pathways in HGSC, have emerged as alternative options for clinical management of HGSC. Poly ADP ribose polymerase (PARP) inhibitors, such as olaparib, have undergone phase II clinical trials in HGSC[114, 115]. PARP

inhibitors exploit the fact that many HGSC are dysfunctional in homologous recombination owing to *BRCA* mutations. In normal cells, damaged DNA can be repaired either by homologous recombination using BRCA proteins or by PARP through single-strand DNA repair[116, 117]. In HGSC patients with dysfunctional BRCA, cells have to rely on PARP to repair DNA damage. PARP inhibitors lead to synthetic lethality by inhibiting the single strand repair pathway in BRCA-deficient tumour cells, thus rending both DNA repair pathways non-functional, resulting in cellular apoptosis[118].

HGSC treatment has improved over the years. From altering the combination and type of cytotoxic chemotherapy agents, to the sequence of treatment, the management of HGSC has improved the survival outcome of these patients. Although studies have shown similar survival outcomes as patients treated with adjuvant chemotherapy, neoadjuvant chemotherapy is effective in reducing peri-operative and post-operative complications for patients with advanced stage disease. Additionally, neoadjuvant chemotherapy allows for higher rates of cytoreduction for patients where optimal debulking would have been unachievable with adjuvant chemotherapy. Thus, neoadjuvant chemotherapy may be the appropriate treatment for those with presentation of advanced disease, while adjuvant therapy is more suited for patients diagnosed with early stage disease.

1.2. The dichotomous role of the immune system in cancer

The immune system has been recognized as an important player in cancer, both as a suppressor and promoter. The importance of the immune system in keeping cells in check and preventing tumourgenesis is demonstrated in early studies showing immunodeficient mice were more susceptible to carcinogen-induced and spontaneous tumour formation than immunocompetent mice[119, 120]. The primary cell type involved in the direct killing of tumour cells are the T lymphocytes (T cells); of a lesser focus in this thesis, natural killer (NK) cells can also directly kill tumour cells. Besides direct killing, other cell types that support immunity against cancer include dendritic cells (DCs), which are responsible for presenting tumour

antigens for T cell recognition, and B lymphocytes (B cells), which can also present tumour antigens as well as produce antibodies against them. In contrast, the immune system can also promote tumourgenesis and tumour survival by infiltrates such as M2 macrophages, myeloid derived suppressor cells (MDSC), and T regulatory (Treg) cells. By understanding the complex immune network in relationship to cancer development and progression, we can improve on designing immunotherapies in favour of an active and robust anti-tumour immune response in the treatment of cancers that are susceptible to immune infiltration, such as HGSC. Herein, the immune subsets involved in anti- and pro-tumour immunity, as well as immunosuppression will be discussed.

1.2.1. Anti-tumour immunity

The immune system can play an active role in the eradication of cancer. Studies have shown that the immune system can recognize tumours leading to regression[121, 122, 123]. The endogenous anti-tumour response involves many players: dendritic cells (DC), T cells, B cells, and NK cells. The immune response typically begins with DCs as antigen-presenting cells (APC) that can phagocytose cells and process and present tumour antigens to T cells and B cells[124]. Tumour antigens can be mutated proteins, non-mutated overexpressed proteins on the cells' surfaces, or antigens that are expressed in neoplastic tissue[125, 126]. The presentation of tumour antigens to T cells is followed by T cell proliferation and an immune response against the tumour. Other immune cells also play a role in anti-tumour immunity, which will be further discussed below.

CD8+ T cells and cytotoxicity

T cells are the main immune cells that actively kill tumour cells. Effector CD8+ T cells do so by secreting cytotoxic enzymes or binding to death receptors and inducing apoptosis of target cells. T cells contain vesicles that house cytotoxic molecules such as perforin and granzymes, which are released to the target cell upon T cell recognition[127]. When the T cell receptor (TCR) binds to complementary antigen presented on the MHC complex of target cells,

antigen recognition is established and an immunological synapse is formed. Cytotoxic granules are subsequently mobilized and released from T cells. Perforin is a protein responsible for forming pores on the cell membrane and allowing for entry of granzymes into target cells[128]. Granzymes, such as granzyme B, are serine proteases that cleave caspase-3 and 7 to activate the apoptotic pathway in target cells[129, 130, 131]. Granzyme B (GzmB) also induces apoptosis by promoting the release of cytochrome c from the mitochondria through cleavage of BH3 interacting domain death agonist (BID) and allowing the opening of Bcl-2-associated X/ Bcl-2 homologous antagonist killer (BAX/BAK) channels located on the mitochondrial outer membrane[132, 133, 134]. The released cytochrome C binds to apoptosomes, which then activate caspases and result in apoptosis. Clinical studies have found that the presence of GzmB$^+$ T cells in ovarian cancer is associated with improved survival[48, 135], suggesting that CD8$^+$ T cells use GzmB as a mechanism to kill malignant ovarian cancer cells. In this thesis, we use GzmB as a marker for identifying activated cytotoxic CD8$^+$ T cells within the tumour.

T cells also possess alternative mechanisms to eradicate their target cells. One of these mechanisms is through T cell intracellular antigen-1 (TIA-1), a RNA-binding protein that is expressed in T cells, NK cells, and macrophages, and possesses functions such as DNA fragmentation, RNA splicing, translational repression of certain mRNA, and sequestering of mRNA into stress granules[136, 137, 138, 139, 140, 141, 142]. In clinical studies, TIA-1 is correlated with prolonged survival in colon and ovarian cancers, however, in B-cell lymphoma, low TIA-1$^+$ infiltrates are associated with better outcomes[49, 143, 144]. Currently, little is known of the mechanism by which TIA-1 mediates cytotoxicity of target cells, but a few studies have shown it can induce cell death by DNA fragmentation and RNA splicing of Fas mRNA[136, 137]. TIA-1 was first discovered to be a pro-apoptotic protein when a lysosome targeting motif was found near the carboxyl-terminal domain[137]. Kawakami et al. found DNA fragments when digitonin-permeabilized thymocytes were incubated with recombinant TIA-1, suggesting TIA-1$^+$ T cells may induce apoptosis in target cells by nucleolysin activity. In addition to harbouring nucleolysin activity, TIA-1 has been shown to contain three RNA-motifs that allow for

recognition and binding of mRNA to execute RNA splicing[145]. Recent studies have found that TIA-1 is involved in splicing Fas transcripts and allows for the production of the isoform of Fas that is inserted into the cell membrane[146, 147, 148]. Additionally, TIA-1 is found to sequester house-keeping mRNA from being translated at times of cell stress to allow for translation of mRNA responsible for recovering stress[140, 142]. Collectively, these studies indicate TIA-1 has multiple functions depending on the cell type and the state of the cell. More functional studies are needed to elucidate the role of TIA-1 in cytotoxicity and the biological events that occur when encountered with cancer cells.

B cells in anti-tumour immunity

The role of B cells in cancer immunology has also garnered interest. Many studies in the current literature consider B cells as tumour-promoting lymphocytes that inhibit effector T cell functions against tumours. These B cells are better known as regulatory B cells (Bregs) for their role in immune suppression. Studies in tumour-bearing mice that lacked B cells found reduced tumour growth compared to their wildtype counterparts[149, 150, 151, 152]. B cells have been found to inhibit T cell proliferation, induce Treg differentiation, and secrete suppressive cytokines such as IL-10[151, 153]. On the contrary, DiLillo et al showed that the selective depletion of CD20+ B cells (instead of using murine models that were completely deficient of B cells) led to an increase in tumour growth and greatly impaired CD4+ and CD8+ T cell activation[154]. CD20+ B cells have also been shown to be involved in tumour antigen presentation to T cells[155, 156, 157, 158]. In one study, CD40-activated B cells that were pulsed with melanoma cell lysates stimulated autologous T cells that were specific for melanoma-associated antigens, suggesting APC functions present in B cells[159]. Activated B cells can also enhance the expansion of TIL when cultured with anti-CD3 and low doses of IL-2[160].

Clinical studies have shown that B cells are associated with good prognosis in lung, cervical, breast and ovarian cancers[49, 161, 162, 163, 164]. Specifically in a HGSC study, CD20+ B cells in the tumour exhibited a IgD-IgM-IgG+ phenotype, which is indicative of prior exposure to

antigen[164]. Within the tumour, CD20^{+} B cells were located in close proximity to CD8^{+} T cells, and patients with both intraepithelial CD20^{+} B cells and CD8^{+} T cells had increased survival compared to patients who had CD20^{+} B cells or CD8^{+} T cells alone[164]. This may suggest that certain B cell subsets cooperate with T cells in anti-tumour immunity. A colorectal cancer study also found activated, memory CD20^{+} B cells in the tumour and with elevated levels in the tumour compared to peripheral blood of matched patients[165]. In contrast, colon metastases lacked intraepithelial CD20^{+} B cells, but contained more regulatory B cells, identified as CD24^{high}CD38^{high}. Lastly, B cells can produce antibodies against tumour antigens such as HER-2/neu, cancer-testis antigens, and MUC1[165, 166, 167, 168]. Collectively, these studies imply there may be two subsets of B cells: Bregs, similar to Tregs, are involved in tumour progression and immunosuppression, whereas effector B cells are involved in anti-tumour immune responses through antigen-presentation and tumour antibody production.

The immune system has developed multiple ways to eradicate tumour cells by various cytotoxic mechanisms found in T cells, such as the release of GzmB and TIA-1. Immune subsets that support effector T cell function, such as DCs and B cells, through presentation of tumour antigens and antibody production, are integral to the effectiveness of the anti-tumour immune response. Thus, a network of effector TIL subsets produces the most effective immune response against cancer.

1.2.2. Immunosuppression

The immune system also has components that promote tumour progression. Immunosuppressive cell types include T regulatory cells (Tregs), tumour-associated macrophages (TAMs), and myeloid-derived suppressor cells (MDSCs). Besides immunosuppressive cells, immune checkpoint receptors, such as cytotoxic T-lymphocyte antigen 4 (CTLA-4) and programmed cell death 1 (PD-1) are presented on T cell surfaces and are responsible for inhibiting T cell functions. Tregs, TAMs, and immune checkpoint receptors are discussed below.

Regulatory T cells (Tregs)

Tregs have been studied extensively for their immunosuppressive role in a variety of diseases, including cancer. Classically identified by expression of the transcription factor FoxP3, their presence has been correlated with poor prognosis in ovarian cancer[169]. Tregs promote tumour immunosuppression by four major mechanisms: 1) secretion of immunosuppressive cytokines such as IL-10 and transforming growth factor β (TGF-β), 2) active killing of CTLs, 3) metabolic disruption of CTLs, and 4) suppression of DCs[170]. The primary mechanism utilized by Tregs is the release of IL-10, TGF-β, and IL-35 to inhibit CTLs, thus promoting tumour progression[171, 172, 173]. Tregs are also able to directly kill CTLs by releasing GzmB, activating the TNF-related apoptosis-inducing ligand (TRAIL) pathway in CTL, and through galectin-1[174, 175, 176, 177]. Lastly, Tregs suppress DCs by upregulation of indoleamine 2,3,-dioxygenase (IDO) in DCs through direct binding of cytotoxic T-lymphocyte antigen 4 (CTLA-4) on Tregs to CD80/ CD86 on DCs[178]. The upregulation of IDO results in an increased catabolism of tryptophan that leads to the suppression of CTLs. Tregs elicit immunosuppression within the tumour microenvironment, therefore their recruitment into the tumour microenvironment is essential to their effectiveness. Both the tumour cells themselves and TAMs recruit Tregs into the tumour by releasing the chemokine CCL2[169, 179]. Hypoxia also leads to the recruitment of Tregs through up-regulation of CCL28 by tumour cells, which binds to the CCR10 receptors on Tregs[180]. The tumour microenvironment also promotes the expansion of Tregs and converts naïve CD4$^+$ T cells into Tregs by the stimulation of IL-10, TGF-β, adenosine from tumour cells, immunosuppressive DCs, and monocytes[181, 182, 183, 184, 185]. Tregs play a central role in opposing the CTL response to cancer, and their ability to induce immune suppression with multiple mechanisms makes tumour eradication a challenge.

Tumour-associated macrophages (TAMs)

Macrophages can both stimulate and suppress the immune system, and this is carried out by two separate types of macrophages. M1-polarized macrophages are involved in clearing

infections and are considered immune stimulatory[186]. They are activated by IFN-γ and other immunostimulatory cytokines such as IL-12 and IL-23. In contrast, M2-polarized macrophages are considered to be immunosuppressive. They are involved in tissue repair and scavenging cellular debris, and are activated by IL-4, IL-10, and IL-13. Macrophages that are known to promote tumour invasion, progression, and metastasis exhibit an M2 phenotype and are referred as TAMs[187, 188, 189]. Their presence has been associated with poor survival in several cancer types[190, 191, 192]. In ovarian cancer, TAMs found in ascites fluid have been associated with poor prognosis and tumour progression[193]. Additionally, several studies have reported an increase in the presence of TAMs in malignant ovarian cancer compared to borderline and benign tumours, further indicating that TAMs play a more prominent role as the cancer becomes more advanced[194, 195, 196]. The most commonly used marker for macrophage detection is CD68, while CD163 and CD206 are more specific to TAMs. Studies have found high CD163+ TAMs, CD163/CD68, and CD206/CD68 cell ratio are associated with decreased survival[195, 197, 198]. Similar to Tregs, TAMs are recruited by the tumour through the expression of CCL2 and colony stimulating factor 1 (CSF-1)[188, 194, 199]. TAMs exhibit their immunosuppressive activities by releasing CCL18 and CCL22, which recruit Tregs into the tumour and promote angiogenesis[51, 169, 200, 201]. In addition, TAMs contribute to tumour immunosuppression by binding of CD206 to CA-125 to increase levels of IL-10, an immunosuppressive cytokine, and decreasing the levels of the T cell chemoattractant CCL3[202]. Interestingly, a study has indicated chemotherapy can induce TAM differentiation. In this study, treatment of some ovarian cancer cell lines with cisplatin and carboplatin was found to induce M2-like differentiation from monocytes[203]. TAMs, like Tregs, can heavily influence the effectiveness of the anti-tumour immune response, therefore, therapies tailored to decreasing TAMs within the tumour microenvironment can lead to improved responses to immunotherapy.

Immune-checkpoint receptors

Another class of immunosuppressive factors that hinder the function of CTLs are

immune-checkpoint receptors, such as CTLA-4 and programmed cell death protein 1 (PD-1). The expression of ligands involved in checkpoint inhibition is dysregulated in cancer. CTLA-4 is expressed on T cells and shares the same ligands (CD80 and CD86) as the co-stimulatory receptor, CD28, that activates T cells[204, 205]. CTLA-4 confers T cell inhibition or dampens the activity of T cells by binding to and sequestering CD80 and CD86 from contact with CD28[206, 207]. Antibodies against CTLA-4, such as ipilimumab and tremelimumab, have shown clinical responses in 25% of melanoma patients[208, 209]. A phase III clinical trial with ipilimumab found 18% of the patients survived beyond two years compared to patients who received a melanoma antigen-specific peptide vaccine alone[210]. Currently, a phase II trial using ipilimumab to treat recurrent platinum sensitive ovarian cancer patients is being conducted[211].

A second immune-checkpoint receptor is PD-1, which is expressed on activated T cells, B cells, and myeloid cells[212, 213]. Its main mechanism of tumour immunosuppression is through the induction of T cell exhaustion by binding PD-1 on T cells with programmed cell death ligand 1 and 2 (PD-L1 & PD-L2), which dampens immune response by CTLs[213]. A few studies have found that the overexpression of PD-L1 on tumour and tumour-associated myeloid cells is associated with poor survival[214, 215, 216]. In ovarian cancer, patients with low PD-L1 expression had a longer overall survival (80 months) compared to patients with high PD-L1 expression (53 months)[217]. Tumours upregulate PD-L1 as an adaptive response to the anti-tumour immune response[217, 218, 219]. This is illustrated in a study where increased PD-L1 expression was found to be correlated with increased TIL and upregulated IFN-γ expression in melanoma[219]. Not only does the overexpression of PD-L1 contribute to immune inhibition of CTLs, the receptor PD-1 is also upregulated on T cells. Several studies have reported increased expression of PD-1 on CD8+ T cells and TIL in different cancers, as well as on tumour-reactive T cells in ovarian cancer[217, 220, 221, 222]. In one study, CD8+ T cells specific for NY-ESO-1, a tumour antigen expressed in ovarian cancer, were also PD-1 positive[223]. Moreover, these tumour-reactive T cells appear to be exhausted when stimulated with NY-ESO-1 peptides, as they expressed an additional exhaustive marker, lymphocyte-activation gene 3 (LAG-3). Another study also found that PD-1 expression

was found on tumour-reactive T cells in melanoma; however, these T cells were not exhausted and were able to elicit an immune response against autologous tumour[221]. These studies suggest that although PD-1 is involved in T cell exhaustion, it could also be a potential marker for identifying tumour-reactive T cells.

The number of mechanisms in which the immune system can suppress or inhibit the anti-tumour response indicates the immunosuppressive immunity has evolved along with the anti-tumour immunity. These immunosuppressive, and ultimately tumour promoting, cell types must be eliminated for the T cell-mediated response against tumours to be effective.

1.2.3. Tumour infiltrating lymphocytes in ovarian cancer

The importance of the immune system in the survival of ovarian cancer patients was first reported by Zhang et al, who showed that the density of intraepithelial T cells, using the common T cell co-receptor CD3 as a marker, was independently associated with increased progression-free and overall survival[224]. These lymphocytes that reside in the tumour were known as tumour-infiltrating lymphocytes (TIL). Increased presence of intraepithelial CD3^{+} T cells also correlated with elevated expression of cytokines involved in immunity, such as IFN-γ, IL-2, and secondary lymphoid-tissue chemokine, by mRNA and protein expressions using real-time polymerase chain reaction and IHC respectively. This was then followed by a study that found intraepithelial CD8^{+} T cells (a primary receptor expressed on cytotoxic T cells), but not CD4^{+} T cells, were associated with increased survival[50]. Upon further analysis, a population of immunosuppressive Tregs was found in the CD4^{+} population, and a high ratio of CD8^{+} T cells to CD25^{+} Tregs was associated with increased survival. The relationship between TIL and survival has also been assessed in the different subtypes of EOC. The presence of intraepithelial CD3^{+} and CD8^{+} T cells was correlated with prolonged survival in HGSC tumours, but not in EC or CCC tumours[48]. These studies implicate T cells as markers of anti-tumour immune response that favour the survival of patients with HGSC subtype.

Another study systematically examined the relationship of several TIL markers and

22

the survival of HGSC patients. It confirmed that the presence of CD8^{+} T cells was associated with survival, as were TIA-1^{+} TIL and CD20^{+} B cells[49]. Moreover, HGSC patients who possess both CD20^{+} B cells in addition to CD8^{+} T cells within their tumours exhibited a better survival compared to patients with CD8^{+} T cells alone[164]. These B cells also expressed markers for antigen presentation, suggesting B cells provide a support to T cells in tumour antigen recognition for anti-tumour immunity.

Similar to TIL studies in other cancers, infiltrates like FoxP3^{+} Tregs, M2 macrophages, and MDSCs are associated with poor outcome in HGSC. CD4^{+} CD25^{+} FoxP3^{+} Tregs have been reported to be associated with decreased survival in ovarian cancer[169, 225]. Besides the infiltrates from the adaptive immune system, immune cells from the innate system also contribute to poor prognosis. Macrophages, specifically tumour-associated macrophages (TAMs), can actively suppress effector T cells in cancer and an increased abundance of them is associated with reduced survival[226, 227]. MSDCs have been associated with poor prognosis due to their immunosuppressive function in many cancers, including ovarian cancer in both clinical and pre-clinical studies[228, 229, 230].

These clinical studies imply that there is a multifaceted relationship between the immune system and HGSC. Many of the lymphocytes from the adaptive immune system, including effector T cells, CD20^{+} B cells, and cytotoxic immune cells, can kill tumour cells and are involved in anti-tumour immunity, which leads to prolonged survival. On the contrary, Tregs and cells from the innate immune system promote tumour progression in HGSC and are associated with poor outcome. These studies provide the basis for molecular studies to investigate the mechanisms that explain these associations.

1.3. The effects of chemotherapy on the immune response to cancer

Chemotherapy has traditionally been thought to be detrimental to the immune system, inhibiting the growth of immune cells as well as cancer cells[231, 232]. Indeed, for many years,

myeloablative chemotherapy has been used to destroy the immune systems of acute leukemia patients to prepare for transplantation of new haemopoietic stem cells[233, 234, 235]. However, the negative stigma of the impact of chemotherapy on the immune system is slowly disappearing and certain chemotherapy regimens are now accepted as being immune stimulatory. One of the earlier chemotherapeutic agents used in ovarian cancer, cyclophosphamide, has been reported to elicit an immune response against tumours in mice[236]. It has also been found to suppress Treg function and restore proliferative capacity in effector T cells and NK cells[237, 238]. Furthermore, dose-dense chemotherapy, which involves low dose but frequent administration of chemotherapy, has been reported to reduce immunosuppression and recruit macrophages and CD8+ T cells into the tumours of ovarian cancer patients[239]. These studies implicate that standard treatment, such as chemotherapy, can be used to tip the balance in favour of tumour regression. By understanding the dynamics of the immune system during the course of standard treatment, we can begin to design novel therapeutics that harness the immune system's anti-tumour response in combination with standard therapy to increase the efficacy of treatment against HGSC.

1.3.1. Chemotherapy and immunogenic cell death

Originally described by Guido Kroemer and Laurence Zitvogel, immunogenic cell death (ICD), is the release of immunostimulatory molecules during tumour cell death[240]. Studies have shown that ICD can be induced by many different types of chemotherapy and radiation, however not all types of cell death are immunostimulatory. Apoptosis (programmed cell death) of tumour cells during chemotherapy elicits a stimulatory immune response and is considered to be an integral part of ICD (Figure 2). When tumour cells apoptose in response to chemotherapy treatment and undergo ICD, molecules such as calreticulin (CRT), adenosine tri-phosphate (ATP), and nonhistone chromatin protein high-mobility group box 1 (HMGB1) are released[241, 242, 243]. These molecules stimulate the recruitment of DCs to take up tumour antigens and present to naïve T cells from neighbouring draining lymph nodes[244, 245]. These naïve T cells are educated to recognize new tumour antigens and become CTLs that migrate into the tumour to initiate an

immune response against the remaining therapy-resistant tumour cells[240].
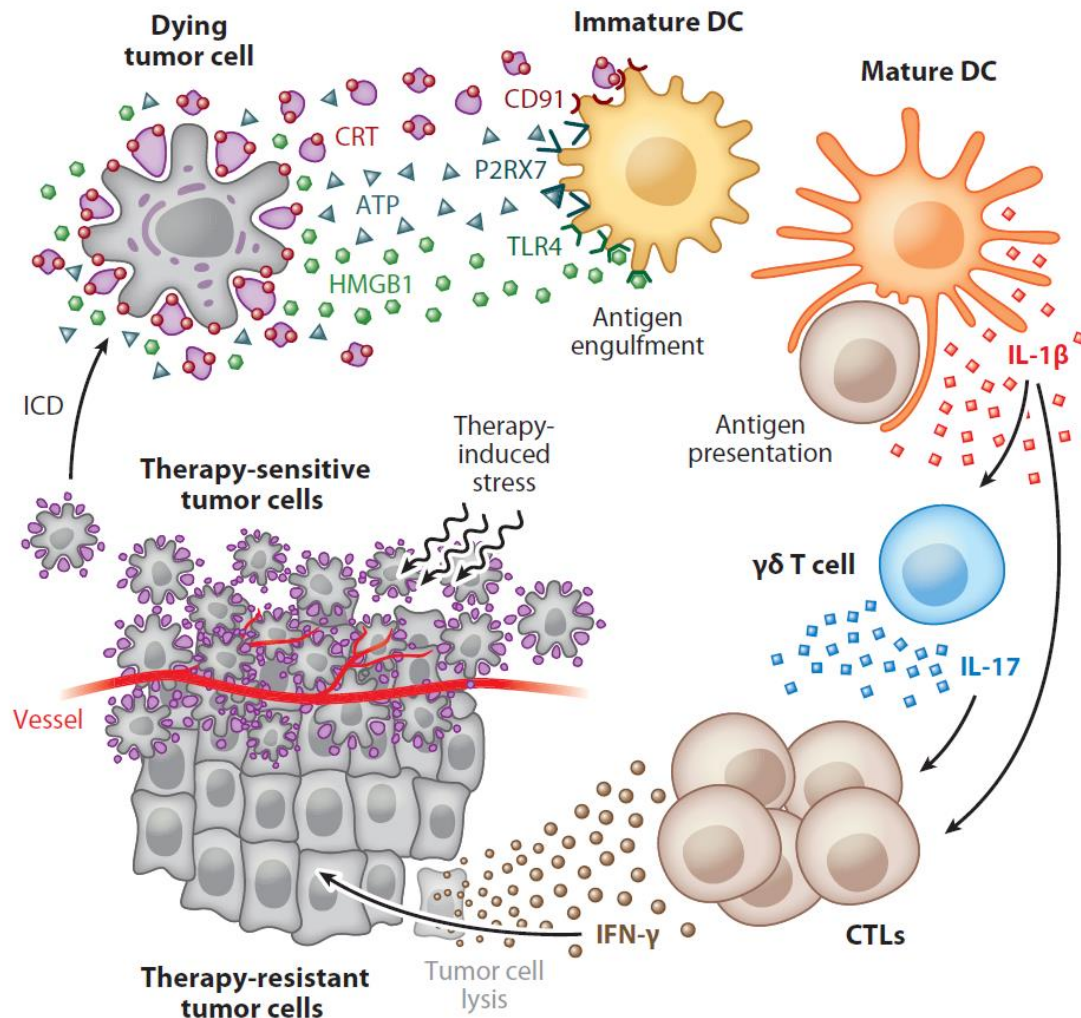
Figure 2. ICD following chemotherapy elicits anti-tumour immunity. (Figure taken from Kroemer et al, 2013, Ann Rev Immunol)

Many studies have emerged identifying the chemotherapeutic agents that can induce an anti-tumour immune response against cancer. Anthracycline, commonly used in the treatment of breast cancer, has been shown to enhance a strong immune response against cancer in both *in vitro* and *in vivo* studies[242, 245, 246]. In mice, anthracycline was reported to induce the release of ATP from dying cancer cells, and resulted in the recruitment and stimulated the differentiation

25

of CD11c^{+}CD11b^{+}Ly6C^{hi} DCs[245]. These DCs were able to engulf tumour antigens and therefore, increase the presence of TIL within the tumour bed. Evidence indicates another ICD molecule, CRT, is also released following anthracycline administration in both *in vitro* and *in vivo* experiments[247, 248]. In addition, autophagy plays a role in the release of ATP from dying cells, which attracts DCs to the site of tumour cell death[246]. Both the inhibition of autophagy (using bafilomycin A1 and 3-hydroxychloroquine to reduce levels of released ATP) and the blockade of CRT (using specific anti-CRT antibody) abrogated the immunogenicity of tumours in mice[242, 246].

ICD-associated molecules

The three main immunostimulatory molecules that are released from cells undergoing ICD are CRT, ATP and HMGB1. CRT is a Ca^{2+}-binding chaperone that is located in the lumen of the endoplasmic reticulum[249]. When tumour cells are undergoing the early phases of cell death, CRT is translocated to the plasma membrane and triggers an immunogenic response[242, 250]. DCs recognize the exposed, surface CRT and engulf these apoptotic tumour cells to present tumour antigens to T cells. The role of CRT in the stimulation of immune responses is best described in a study where CT26, a murine colon cancer cell line, that had CRT knocked down (KO) using siRNA and was treated with mitoxantrone, a type of antineoplastic therapeutic, inhibited its phagocytosis by DCs in both *in vitro* and *in vivo* experiments[242]. The attenuated release of CRT from siRNA KO of mitoxantrone-treated CT26 cells was reversed when recombinant CRT was administered, and phagocytotic activity of the DCs was similar to that of mitoxanetrone-treated CT26 cells with wildtype CRT. KO of other proteins that mediate CRT's surface exposure, such as PI3K p110α, ER stress kinase PERK, caspase-8, Bax, and Bak, by shRNA or siRNA also decreased the surface exposure of CRT from dying cells[248, 251]. In clinical studies, CRT surface exposure is correlated with improved immune responses[252, 253]. In acute myeloid leukemia, autologous T cells from patients who had surface CRT expression on their dying tumour cells were able to produce significant levels of IFN-γ when incubated with autologous DCs[252]. In contrast, T cells from patients who did not have CRT surface expression were unable

to upregulate IFN-γ production. In conclusion, CRT is one of the main ICD molecules that elicits an immune response via stimulation of DCs in response to chemotherapy, and its presence can determine the effectiveness of T cell recognition and response to the tumour following chemotherapy.

The second ICD molecule is ATP, well known as the energy currency of cells, which is often released when cells undergo stress. This molecule can attract macrophages for apoptotic clearance and stimulates phagocytes as an "eat me" signal in response to cell death[254]. The release of extracellular ATP from dying cancer cells is dependent on autophagy[240]. A study inhibiting autophagy reported that ATP secretion from dying tumour cells was reduced, along with a reduced immune response[246]. They observed that autophagy-competent CT26 cells implanted in immunocompetent mice, had increased DC and T cell infiltration into the tumour following chemotherapy administration. The recruitment of DCs and T cells was re-established in autophagy-deficient tumours during chemotherapy when mice were given inhibitors to extracellular ATP-degrading enzymes that artificially increased extracellular ATP. Given these points, autophagy is an important catabolic mechanism in tumour cells that allows DCs and effector T cells to recognize chemotherapy-induced cell death.

Lastly, HMGB1 is the most abundant nonhistone chromatin protein that plays a role in ICD[240]. HMGB1 is released by damaged cells that are undergoing apoptosis, necrosis, and necroapoptosis. In the past, it was widely known for being released during necrosis, however, recent additional studies have provided evidence that HMGB1is released during apoptosis as well[255, 256]. HMGB1 mainly triggers a proinflammatory response by binding to TLR4 and Receptor for Advanced Glycation end products (RAGE) on DCs[249, 257]. Once bound, phagosomes that contain potential tumour derived antigens are trafficked towards vesicles that process antigens for presentation and divert the phagosomes from being fused with lysosomes, which could lead to the degradation of these antigens[258]. The importance of HMGB1 in its ability to stimulate DCs is highlighted when the depletion of TLR4, and the neutralization of HMGB1 with antibodies abrogates the ability of DCs to present tumour antigens[244]. In the same manner

as CRT and ATP, HMGB1 activates DCs to process and present tumour antigens to T cells and activate an adaptive immune response against cancer.

1.3.2. The effects of platinum and taxane chemotherapy in ICD

Not all chemotherapeutic agents can induce ICD by apoptosis, and a few *in vitro* studies have investigated as to whether platinum and taxane therapies can induce ICD and elicit an anti-tumour immune response[259, 260]. A few studies reported that oxaliplatin and cisplatin were able to trigger HMGB1 release from apoptotic cells from colon cancer cell lines, although only oxaliplatin was also able to induce calreticulin exposure[259, 260]. Surprisingly, cisplatin was unable to induce ICD on its own, despite up-regulation of HMGB1 release from apoptotic cells, and was only able to induce ICD when the cell lines were subjected to endoplasmic reticulum stress[259, 260]. The addition of endoplasmic reticulum stress inducer, tunicamycin, allowed for calreticulin exposure to the cell surface and induced ICD in cisplatin-treated cells[259]. From the above studies, it appears that the loss of one ICD signal abrogates the ICD response, as shown in cisplatin's inability to induce an immune response due to the a lack of CRT surface exposure in treated cells despite HMGB1 being present on the surface of dying cells[243]. To date, no study has investigated whether paclitaxel can induce calreticulin and HMGB1 release. The role of ICD in carboplatin and paclitaxel chemotherapy needs to be elucidated, as studies using anthracycline have indicated the importance of ICD in eliciting an anti-tumour immune response. If ICD is the primary mechanism in which cytotoxic drugs elicit an endogenous T cell response against tumours, then the ability of carboplatin and paclitaxel drugs to promote immunogenicity in cancer would follow similar mechanisms that increase the release of CRT, ATP, and HMBG1 from dying tumour cells.

1.3.3. The effects of chemotherapy on TIL

Clinical studies involving patients treated with chemotherapy further support the idea that ICD can enhance anti-tumour immune responses. Very few studies have investigated the

changing dynamics in immune composition due to chemotherapy in human tumours. To study this, most of the clinical studies have utilized tumours from patients treated with neoadjuvant chemotherapy and compared TIL infiltration prior to and following chemotherapy to assess the anti-tumour immune response. Though sparse overall, the majority of these studies were done in breast cancer[261, 262, 263]. In one breast cancer study, patients who responded to anthracycline therapy showed decreased intraepithelial Tregs in their post-chemotherapy tumours compared to their matching pre-chemotherapy tumours[262]. This was quickly followed by a subsequent study from the same group which found that a decrease in FoxP3^{+} Tregs and an increase in CD8^{+} T cells in the post-chemotherapy tumours from breast cancer patients were associated with increased survival[263]. There has only been one study, by Polcher et al, which assessed changes in TIL following carboplatin and docetaxel chemotherapy in HGSC[264]. In 29 HSGC patients, they saw an increase in the mean intraepithelial CD4^{+}, CD8^{+}, and GzmB^{+} T cells in post chemotherapy tumours compared to the pre-chemotherapy tumours. Contrary to the breast cancer studies, Polcher et al did not find a change in FoxP3^{+} Tregs following chemotherapy. Surprisingly, CD8^{+} T cells, as well as the ratio of CD8^{+}/FoxP3^{+} T cells did not correlate with survival in their analysis. Instead, a high Granzyme B^{+}/FoxP3^{+} cell ratio was strongly associated with increased progression-free survival compared to patients with a low Granzyme B[+]/FoxP3^{+} T cell ratio in the tumour epithelium (median 17.88 v.s. 11.24 months respectively). Collectively, these studies indicate that an increase in T effector cells over immunosuppressive Tregs confers a more favourable outcome.

Other studies have associated the presence of TIL in pre-chemotherapy tumours with response to anthracycline treatment. Two studies in breast cancer discovered that high TIL infiltration was found in pre-treated tumours of patients who had complete pathological responses compared to patients without a complete pathological response to anthracycline treatment[265, 266]. Complete pathological response (pCR) is defined as an absence of all invasive disease in resected breast tumour tissue when examined by histopathology. In a triple negative breast cancer study, pCR was significantly higher in tumours that had a higher TIL

infiltration (37%) than those that had lower TIL infiltration (16%)[265]. Another study found TIL gene signatures in pre-chemotherapy tumours were associated with increased sensitivity to anthracycline[267]. Another study investigated the association between intraepithelial TIL density and responses to platinum-based chemotherapy in HGSC and found high stromal $CD3^+$ and $CD8^+$ T cells were predictive of responses to therapy, with a mean of 21 $CD3^+$ T cells/HPF and 9 $CD8^+$ T cells/HPF in chemosensitive tumours versus 8 $CD3^+$ T cells/HPF and 4.6 $CD8^+$ T cells/HPF in chemoresistant tumours[268]. Studies investigating the correlation between TIL and response to chemotherapy and infiltration following chemotherapy indicate the immune system plays a role in the changing dynamics of cancer during standard treatment.

These clinical studies implicate that effector T cells play a pivotal role in treatment outcome and ultimately survival. Unlike the experimental studies that focus on elucidating the mechanism by which cytotoxic drugs trigger the release of ICD signals, these clinical studies reveal the importance of T cells over an extended period of chemotherapy exposure. Furthermore, chemotherapy is associated with relieving immunosuppression within the tumour microenvironment as observed through a decrease in Tregs in some settings. The immunological network does not involve only T cells; other immunological players and factors such as B cells, TIA-1, PD-1, and PD-L1 are also associated with survival. These new studies promote further investigation and validation of the change in composition of T cells as well as other immune markers during the course of chemotherapy.

1.4. Rationale and aims

The immune system is in constant interaction with tumours. A robust immune response against cancer requires a host of effector immune infiltrates and cytokines that favour an active cytotoxic response. This requires phagocytosis of tumour cells by DCs, antigen processing and presentation by DCs and B cells, and stimulation of CTLs by APCs with newly acquired tumour antigens followed by killing of tumour cells by activated CTLs. The active cytotoxic killing of tumour cells is predominantly carried out by activated CTLs. Thus, the ability of CTLs to

recognize tumour and release cytotoxic molecules against tumour cells are important aspects to consider. GzmB has been the most studied cytotoxic molecule in effector T cells and its release into target cells activates apoptosis via caspases. In the first experimental chapter of my thesis (Chapter 2), we investigate if CD8^{+} TIL, which are associated with good prognosis, express GzmB in HGSC. We would expect CD8^{+} GzmB^{+} TIL to be actively involved in tumour killing and therefore be surrounded by apoptotic tumour cells positive for cleaved Caspase-3 expression. This chapter will address whether intraepithelial CD8^{+} TIL are indeed cytotoxic in HGSC.

All advanced stage HGSC patients undergo standard treatment consisting of surgery and chemotherapy. Several studies have now revealed that TIL composition undergoes changes during the course of chemotherapy. These studies have shown chemotherapy can elicit an active immune response against tumour cells, involving antigen presenting DCs and cytotoxic T cells, through the release of ICD molecules in dying tumour cells. In addition, breast cancer studies have shown a reduction of Tregs in post-chemotherapy tumours following anthracycline therapy, suggesting a decrease in immunosuppression in the tumour microenvironment. These studies demonstrate that chemotherapy can activate key infiltrates involved in tumour progression as well as reduce the immunosuppressive mechanisms that allow for tumour survival and progression, thus tipping the immune response in favour of tumour regression. In Chapter 3, we investigate the change in the composition of immune infiltrates following carboplatin and paclitaxel chemotherapy in HGSC. In this study, we utilize tumours from neoadjuvant patients and compare pre- and post-chemotherapy tumours to observe a direct change. Toward the long-term goal of developing effective immunotherapies for HGSC, these two chapters focus on identifying the major changes in immune infiltrates that occur during standard treatment of this challenging disease.

2. Determining the functional status of CD8^{+} TIL in HGSC

2.1. Background

It has been well established that the immune system plays a role in patient survival in high grade serous carcinoma (HGSC). Clinical studies have found patients who have increased CD3^{+} and CD8^{+} T cells in their tumours have improved overall survival[48, 49, 50, 224, 269]. In one study, patients with increased intraepithelial CD8^{+} T cells had a median survival of 55 months compared to patients with less intraepithelial CD8^{+} T cells who had a median survival of 26 months[50]. The association of increased CD8^{+} T cells with prolonged survival in HGSC implies that CD8^{+} T cells may play an active role in anti-tumour immunity.

One of the primary mechanisms that CD8^{+} T cells use to kill target cells is by inducing apoptosis via the release of granzyme B (GzmB). Cytotoxic killer CD8^{+} T cells (CTLs) contain granules that house cytotoxic molecules such as perforin and GzmB[127]. These cytotoxic molecules are released upon recognition of virus infected cells, foreign cells, and cancer cells by CTLs. Perforin is responsible for creating pores on the outer membrane of target cells and

Charlotte S. Lo[1,2,3], Katy Milne[3], Yuzhuo Wang[2,4], Brad H. Nelson[1,3,5]

[1]Department of Medicine, Interdisciplinary Oncology Program, University of British Columbia, Vancouver, BC, Canada

[2]Department of Experimental Therapeutics, BC Cancer Research Centre, BC Cancer Agency, Vancouver, BC, Canada

[3]Deeley Research Centre, BC Cancer Agency, Victoria, BC, Canada

[4]Vancouver Prostate Centre, Vancouver, BC, Canada

[5]Department of Medical Genetics, University of British Columbia, Vancouver, BC, Canada

allowing entry of GzmB[128]. GzmB, a serine protease, enters target cells and cleaves pro-caspases which activates the caspase-dependent apoptotic pathways, leading to cell death[129, 131]. The presence of GzmB has been found in different cancer types, including ovarian cancer, and its presence has been associated with improved survival[48, 135, 270, 271]. These studies indicate that CTLs may use GzmB to kill tumour cells.

In this study, we investigate the prevalence of CD8^{+} GzmB^{+} TIL in HGSC. We identified the presence of intraepithelial and stromal CD8^{+} GzmB^{+} and CD8^{+} GzmB^{-} T cells using multi-colour immunohistochemistry (IHC) in a small cohort of 38 HGSC patients. We also correlated the presence of TIL subsets with the presence of cleaved caspase-3^{+} apoptotic tumour cells. Based on prior studies, we hypothesize that there would be an increased cytotoxic CD8^{+} GzmB^{+} T cell population in tumours that have increased intraepithelial CD8^{+} T cells, as well as an increased abundance in neighbouring cleaved casapse-3^{+} apoptotic tumour cells.

2.2. Methods

2.2.1. Patient cohort

A retrospective cohort of patients with ovarian cancer was compiled for this study. All patients were previously recruited for the Immune Response to Ovarian Cancer (IROC) research program. Patient cases that were pathologically diagnosed as LGSC, HGSC mixed subtype tumours (mucinous, endometrioid, clear cell), and HGSC with undifferentiated/transitional tumours were excluded from the analysis. All patients underwent adjuvant chemotherapy, and tumour samples were obtained at the time of primary surgery prior to chemotherapy. A total of 38 HGSC patient cases were analysed. Only patients with a pathological diagnosis of high grade serous/papillary subtype were included.

Formalin-fixed paraffin-embedded (FFPE) tumour samples were obtained and a tissue microarray (TMA) previously constructed was used for this study. Each patient case contained duplicate 1 mm cores. Some patient cases (n=7) contained duplicate cores from more than

one tumour; these were subsequently quantified and the mean of the all the tumour sites were calculated for those patient cases.

2.2.2. Multicolour immunohistochemistry

A CD8, GzmB, and cleaved caspase-3 triple-stain IHC was manually performed. A microtome (Model: Microm HM-355S) was used to section at 4 μm sections onto Superfrost plus slides (Fisher Scientific, Cat# 12-550-15). Tissue sections were incubated overnight at 37°C to allow them to adhere securely to the slides. Sections were deparaffinized in xylene, followed by a series of ethanol and distilled water (dH$_2$O) washes to hydrate the tissue prior to staining. Following rehydration, heat-induced epitope retrieval was subsequently performed using a decloaking chamber (Decloaking Chamber Plus, Biocare Medical, Concord, CA, USA, Cat# DC08-1180) in a 1:10 dilution of Diva decloaking reagent (Biocare Medical, Concord, CA, USA, Cat# DV2004MX). The decloaking chamber was set for antigen retrieval at 125°C at the following settings: P1 at 125°C, P2 at 100°C with fan on, and P2 at 80°C with fan off. Following antigen retrieval, sections were washed with dH$_2$O and incubated, for 5 minutes at room temperature, with Peroxidased-1 (Biocare Medical, Concord, CA, USA, Cat# PX968H), a commercial hydrogen peroxidase solution to block endogenous peroxidase activity. The sections were then washed in TBS-tween buffer and incubated for 10 minutes with Background Sniper (Biocare Medical, Concord, CA, USA, Cat# BS966H), a blocking reagent used to reduce nonspecific background staining, at room temperature. Sections were washed once more in TBS-tween buffer prior to adding anti-CD8 mouse monoclonal antibody (1:200, Cell Marque, Rocklin, CA, USA, Cat# 108M-95, Clone C8/144B) and anti-GzmB rabbit polyclonal antibody (1:300, Abcam, Cambridge, MA, USA, Cat# ab4059) diluted in antibody diluent (1% BSA in 0.1% TBST), and incubated for 30 minutes at room temperature. Sections were washed again with TBS-tween buffer and then incubated with MACH2 Double Stain 1 containing anti-mouse AP polymer and anti-rabbit HRP polymer reagents (Biocare Medical, Concord, CA, USA, Cat# MRCT523) for 30 minutes at room temperature. Sections were washed again with TBS-tween buffer and signals were detected using 3, 3'-diaminobenzidine (DAB) (Betazoid DAB

chromogen kit, Biocare Medical, Concord, CA, USA, Cat# BDB2004) and Warp Red (Warp Red chromogen kit, Biocare Medical, Concord, CA, USA, Cat# WR806) chromogens. Sections were incubated with DAB for 3 minutes at room temperature, and washed in dH_2O. Then the sections were incubated with Warp Red for 8 minutes at room temperature, and washed in dH_2O.

Next, antibodies were denatured with glycine SDS buffer (25mM glycine-HCl, 10% SDS, pH 2) for 45 minutes at 50°C. Sections were washed with TBS-tween buffer and incubated with anti-cleaved caspase-3 rabbit polyclonal antibody (1:500, Cell Signaling, Beverly, MA, USA, Cat# 9661). They were followed by TBS-tween buffer washes and incubated with MACH2 anti-rabbit HRP polymer reagent (Biocare Medical, Concord, CA, USA, Cat# RHRP520) for 30 minutes at room temperature. Sections were washed in TBS-tween buffer and secondary antibody was detected with Vina Green reagent (Vina Green chromagen kit, Biocare Medical, Concord, CA, USA, Cat# BRR807A), then washed with dH_2O. Sections were stained with hematoxylin solution (1:10, Biocare Medical, Concord, CA, USA, Cat# CATHE-H) for 90 seconds at room temperature to visualize tissue architecture and washed in dH_2O. Then, sections were incubated with Tacha's Bluing Solution (Biocare Medical, Concord, CA, USA, Cat# HTBLU-M) for 30 seconds and washed once more. Finally, sections were air-dried and cover-slipped using EcoMount mounting media (Biocare Medical, Concord, CA, USA, Cat# EM897L). Human tonsil tissues were used as positive controls for the primary antibodies. An optimization TMA consisting of human tonsil, liver, and cancerous (breast and ovarian) tissues were used for single-stain and no-antibody stain controls. Tumour tissues from mice that received adoptive transfer (7 days post-treatment) from another experiment were used as positive controls for the staining of GzmB and cleaved caspase-3 antibodies (both antibodies are reactive to human and murine tissues).

2.2.3. Imaging and quantitative assessment of the immune infiltrates

For the multicolour stains, slides were imaged using the Vectra automated imaging system (Perkin Elmer, USA). Initially, we attempted to quantitate these TIL subsets in both the tumour epithelium and stroma using the automated imaging analysis from the inForm software.

35

The software is developed to quantitate single- and double-positive cells in different tissue compartments. First, we trained inForm to differentiate between tumour epithelium and stroma using a representative set of images showing different HGSC tumour sites. This was followed by training inForm to segregate the cell components (cell membrane, cytoplasm, and nucleus), and quantify single- and double-positive cells in the different tissue compartments. The spectra for each chromogen in the triple-colour images were separated by inForm software and positive cells were quantitated if they contained a certain spectra representative of the stained chromogen. When inForm was used for automated quantification, we found that inForm did not accurately segregate the tumour epithelium from the stroma because differences in tissue architecture in ovary/fallopian tube and omentum tissues. Hence, we decided to forgo our automated analysis.

We opted to manually count CD8^{+}, GzmB^{+}, and CD8^{+} GzmB^{+} TIL in the tumour epithelium and stroma, as well as cleaved caspase-3^{+} tumour cells. The mean was calculated for all the cell subsets. Patients with cores from more than one tumour sites had their cell counts averaged from all tumour sites.

2.2.4. Statistical analysis

Associations between the presences of different TIL subsets and between the presences of TIL v.s. cleaved caspase-3^{+} tumour cells were analysed. Absolute cell counts were used in Spearman's rank correlations. All statistical analysis was performed using GraphPad Prism 6.0 (GraphPad, La Jolla, CA, USA). *P*-values less than 0.05 were considered significant.

2.3. Results

2.3.1. Patient characteristics

We studied 38 HGSC patients in the IROC prospective cohort. The patient characteristics are listed in Table 1. Briefly, the majority of the patients had stage IIIC (73.7%) tumours, while the remaining patients were diagnosed with stage IV (15.8%), stage III (2.6%),

stage IIIB (2.6%), and stage IIC (2.6%). One case had no known stage or other clinical information available. All patients had grade 3 tumours. Most of the patients had suboptimally debulked tumours (76.3%) at time of their primary surgeries, while a smaller proportion had optimally debulked tumours (21.1%). The primary surgical specimens quantitated for each case were predominantly from a single tumour site, however, some cases had samples from two tumour sites. Most of the primary tumours quantitated were from the omentum (50.0% of cases), with the ovary as the second most common tumour site (34.2%). The remainder of the tumours were from the fallopian tube (26.3%), peritoneum (5.3%), or abdominal wall (2.6%). All but two of the patients received adjuvant chemotherapy (94.7%); one patient opted for alternative therapy, while another had no available clinical data.

Table 1. Patient characteristics of the IROC Prospective adjuvant-treated cohort

Characteristics	IROC Prospective Cohort (n=38)
Age (years)	
Mean	65 ± 29
Median	66
Range	40-83
Grade – no (%)	
1	0
2	0
3	38 (100%)
Stage – no. (%)	
IIC	1 (2.6%)
III	1 (2.6%)
IIIB	1 (2.6%)
IIIC	28 (73.7%)
IV	6 (15.8%)
Unknown	1 (2.6%)
Pre-chemotherapy tumour – no. (%)	
Omentum	19 (50.0%)
Ovary	13 (34.2%)
Fallopian tube	10 (26.3%)
Peritoneum	2 (5.3%)
Abdominal wall	1 (2.6%)
Debulking Status – no. (%)	
Optimal	8 (21.1%)
Suboptimal	29 (76.3%)
Unknown	1 (2.6%)
Chemotherapy – no. (%)	
Adjuvant	36 (94.7%)
No chemotherapy	1 (2.6%)
Unknown	1 (2.6%)

2.3.2. Prevalence of CD8$^+$ GzmB$^+$ T cells in HGSC

We evaluated the prevalence of intraepithelial CD8$^+$ GzmB$^+$ cytotoxic T cells in HGSC. Representative IHC images of CD8$^+$ GzmB$^+$, CD8$^+$, and GzmB$^+$ TIL are shown in Figure 3. In 36 patient cases that contained CD8$^+$ T cells in the tumour epithelium, CD8$^+$ GzmB$^+$ T cells comprised 2% of the intraepithelial CD8$^+$ T cell population (Figure 4A). Similarly, in 37 patient cases that contained CD8$^+$ T cells within the stroma, CD8$^+$ GzmB$^+$ T cells comprised 2% in the CD8$^+$ T cell population. Thus, we found an overall paucity of CD8$^+$ GzmB$^+$ T cells in HGSC tumours. Next, we asked if the presence of CD8$^+$ GzmB$^+$ T cells was correlated with the presence of increased CD8$^+$ T cells or GzmB$^+$ immune cells. We found a weak positive correlation between intraepithelial CD8$^+$ GzmB$^+$ T cells and intraepithelial CD8$^+$ T cells (r=0.3643, P=0.0245) (Figure 4B). In contrast, we found there was no significant correlation between the presence of intraepithelial CD8$^+$ GzmB$^+$ T cells and intraepithelial GzmB$^+$ TIL (r=0.2835, P=0.0846) (Figure 4C). When we investigated if these correlations also exist in total cell counts (intraepithelial and stromal), we found that the presence of total CD8$^+$ GzmB$^+$ T cells was not correlated with the presence of total CD8+ or GzmB+ TIL (Appendix A).

2.3.3. Evaluating the association between TIL and apoptotic tumour cells

We were interested in the prevalence of apoptotic tumour cells and its correlation with the presence of CD8$^+$ T cells and GzmB$^+$ immune cells. Specifically, we assessed if there was a higher abundance of cleaved caspase-3$^+$ apoptotic tumour cells in tumours with high infiltration of intraepithelial CD8$^+$ T cells and GzmB$^+$ immune cells. We observed there was no significant correlation between the abundance of cleaved caspase-3$^+$ apoptotic tumour cells with the presence of intraepithelial CD8$^+$ T cells (r=0.2001, P=0.2283) (Figure 5A) . In contrast, the presence of cleaved caspase-3$^+$ apoptotic tumour cells was not associated with the presence of intraepithelial GzmB$^+$ immune cells (r=0.1037, P=0.5357) (Figure 5B). Representative IHC images of cleaved caspase-3$^+$ tumour cells are shown in Figure 5C.
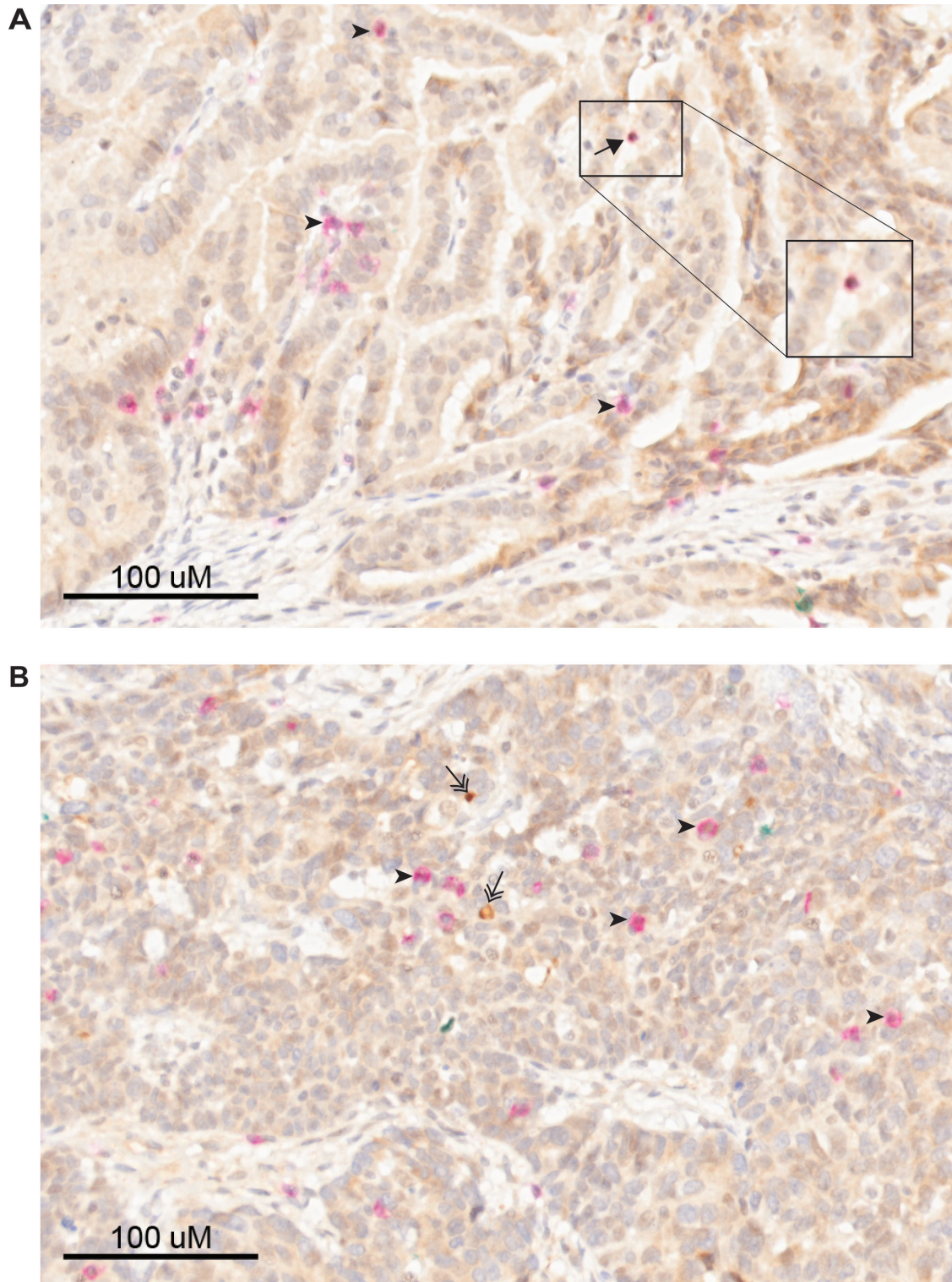
Figure 3. Immunohistochemical staining of CD8+ GzmB+ T cells in HGSC. (**A**) Few intraepithelial CD8+ GzmB+ T cells (arrow) were present among CD8+ T cells (red, arrowheads). (**B**) CD8+ GzmB- T cells (red, arrowheads) and GzmB+ TIL (brown, double arrowheads). Magnification, 200X.
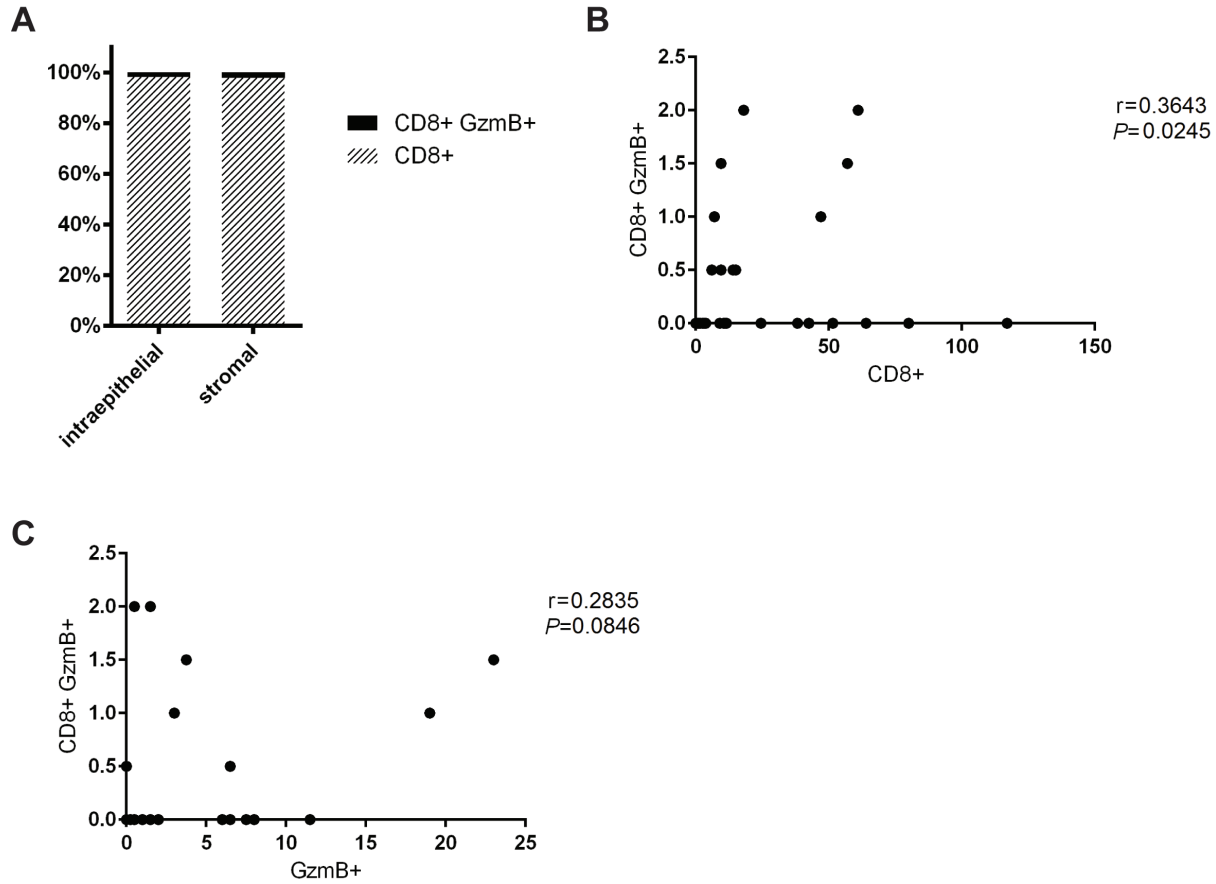
Figure 4. **Prevalence of intraepithelial CD8⁺ GzmB⁺ TIL in HGSC**. (**A**) Composition of intraepithelial CD8⁺ GzmB⁺ T cells in intraepithelial CD8⁺ T cell population. (**B**) Spearman's r correlation between the presence of intraepithelial CD8⁺ GzmB⁺ T cells and CD8⁺ T cells. (**C**) Spearman's r correlation between the presence of intraepithelial CD8⁺ GzmB⁺ T cells and GzmB⁺ TIL.
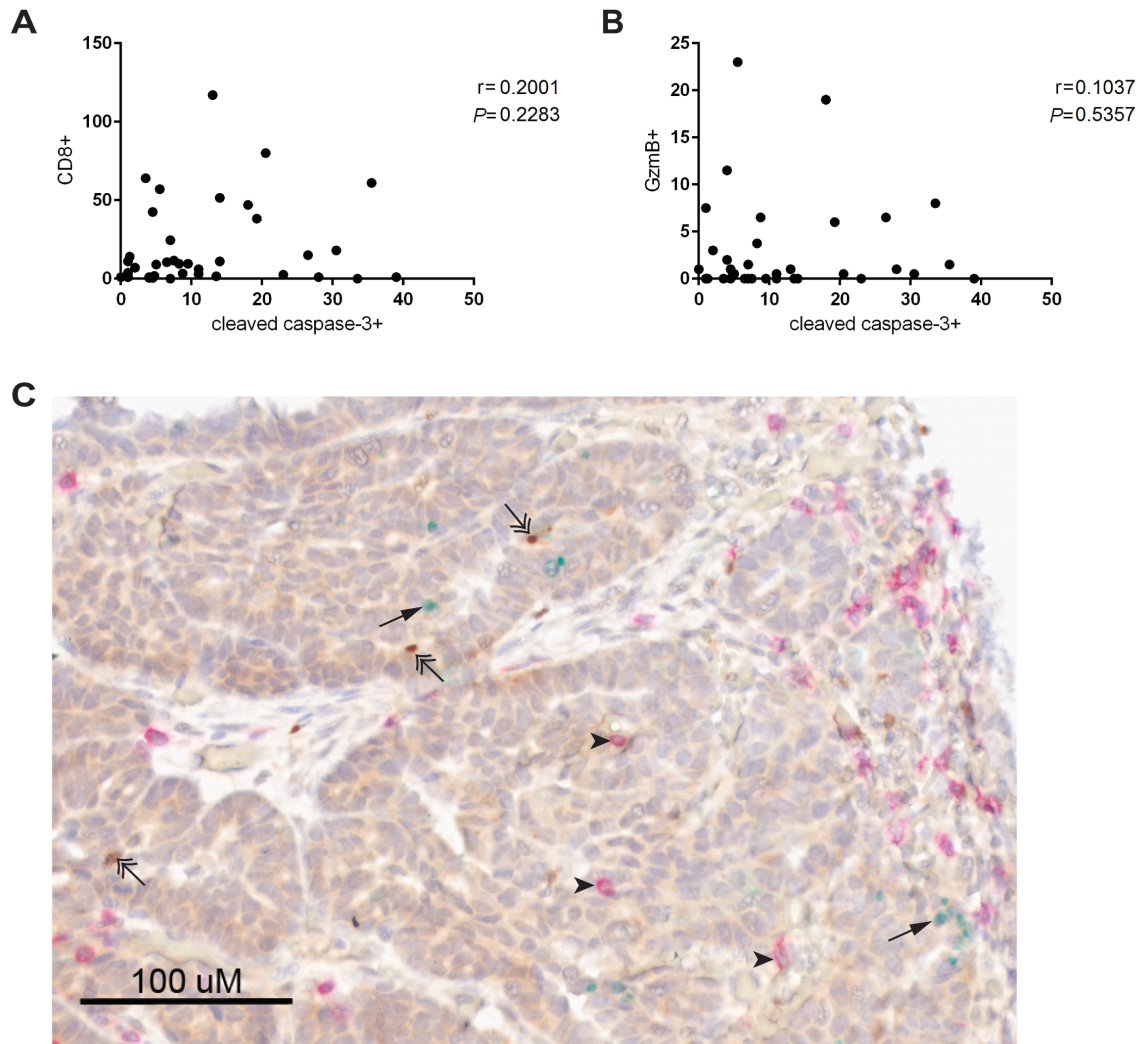
Figure 5. cleaved caspase-3⁺ apoptotic tumour cells in HGSC. (**A**) Spearman's r correlation between the presence of intraepithelial CD8⁺ T cells and cleaved caspase-3⁺ tumour cells. (**B**) Spearman's r correlation between the presence of intraepithelial GzmB⁺ TIL and cleaved caspase-3⁺ tumour cells. Strength of the correlation is shown in r value and statistical significance is indicated by P value. Statistical significance is indicated with *P*<0.05. (**C**) Representative IHC staining of cleaved caspase-3⁺ tumour cells (green, arrows) in IROC073. CD8⁺ GzmB⁻ T cells (red, arrowheads) and CD8⁻ GzmB⁺ TIL (brown, double arrowheads) are also shown. Magnification, 200X.

2.4. Discussion

In this study, we found that CD8⁺ GzmB⁺ CTLs were exceedingly rare in HGSC tumour epithelium. The positive association between the presence of intraepithelial CD8⁺ T cells and survival in patients has been indicated in a number of clinical studies[48, 49, 50, 51, 269]. Studies have

shown that tumour-specific CTLs can kill autologous tumour cells, indicating that CTLs are responsible for direct tumour eradication[123, 272, 273]. It is well established that CD8^{+} T cells utilize GzmB to actively kill their target cells[274, 275, 276]. From these previous studies, it was predicted that CD8^{+} GzmB^{+} T cells would be the dominant subset within the CD8^{+} T cell population in tumours with high intraepithelial CD8^{+} T cell density. However, we found that few CD8^{+} GzmB^{+} T cells were present in HGSC tumours. The lack of CD8^{+} GzmB^{+} T cells may be due to immunosuppression from the tumour. CTLs would be unfavourable for tumour survival therefore limiting their localization in the tumour epithelium would prevent T cell mediated tumour killing. Perhaps chemotherapy, which has been shown to alleviate tumour suppression, would allow for easier access of the tumour epithelium by CTLs and there would be an increased infiltration of CD8^{+} GzmB^{+} T cells[237, 262, 263]. This issue will be explored in the next chapter.

Besides GzmB release, CD8^{+} T cells have alternative methods of inducing apoptosis in cancer cells, such as Fas/FasL activation and RNA splicing by cytotoxic TIA-1 enzyme. The Fas ligand (FasL) on T cells binds to Fas receptors (Fas) on the tumour cells and activates the apoptotic pathway in the tumour cells[277]. Less is known about TIA-1, but a handful of biochemical studies have found that TIA-1 fragments DNA in target cells which leads to apoptosis[136, 137]. Although less is known of TIA-1's mechanism, besides being associated with cytotoxic granules, studies have found TIA-1 to be associated with improved survival in colon and ovarian cancers[49, 135, 143]. TIA-1 may play a more important role in T-cell mediated tumour cytotoxicity, as recently indicated by a higher prevalence of TIA-1^{+} TIL compared to GzmB^{+} in HGSC[49]. Another alternative is that CD8^{+} T cells use a combination of these cytotoxic mechanisms to mediate anti-tumour immunity. To further explore GzmB and TIA-1 mechanisms, flow cytometry assessing GzmB and TIA-1 from co-cultures of CTL (isolated from patient tumours) with autologous tumour can indicate whether GzmB and TIA-1 are released upon tumour interaction. Additionally, GzmB enzyme-linked immunospot assay (ELISPOT) can also asses GzmB release from CTLs.

We also did not observe significant levels of cleaved caspase-3^{+} tumour cells. The

activation of caspase-3 to induce apoptosis is a transient event which could easily be missed by IHC staining at a single time point. Thus, our methods only detect tumour cells undergoing apoptosis at the time of primary surgery.

In summary, our results indicate that there is a paucity of intraepithelial CD8$^+$ GzmB$^+$ T cells in HGSC tumours despite some tumours displaying high intraepithelial CD8$^+$ T cell infiltration. We also found that tumours with high TIL do not have increased presence of cleaved caspase-3$^+$ apoptotic tumour cells. Together, this suggests that CTLs may kill tumour cells through multiple mechanisms (TIA-1, Fas-FasL and caspase-independent pathways) or chemotherapy might induce CTL activation and killing in which case lead CD8$^+$ T cells to be positively correlated with prolonged survival.

3. The effects of chemotherapy on immune infiltrates in HGSC

3.1. Background

High grade serous carcinoma (HGSC) is the most aggressive subtype of ovarian cancer and accounts for 70% of all diagnosed epithelial ovarian cancers[2]. The current standard treatment for HGSC is a combination of surgery and carboplatin plus paclitaxel chemotherapy. In the past, adjuvant therapy, surgery followed by chemotherapy, was the standard treatment protocol; however, neoadjuvant therapy, chemotherapy followed by surgery, is becoming a common treatment in many cancer clinics. Studies that have compared the efficacy between adjuvant and neoadjuvant therapies have found no significant differences in overall survival[107, 108, 109, 110]. Despite the similar survival outcomes between the two therapies, neoadjuvant therapy improves post-surgical outcomes such as higher rates of optimal tumour debulking, resolving

---

Adapted from: Charlotte S. Lo[1,2,3], Sanaz Sanii[4], Katy Milne[3], Aline Talhouk[4], Yuzhuo Wang[2,5], Blaise A. Clarke[4], Brad H. Nelson[1,3,6] (Manuscript in preparation)

[1]Department of Medicine, Interdisciplinary Oncology Program, University of British Columbia, Vancouver, BC, Canada
[2]Department of Experimental Therapeutics, BC Cancer Research Centre, BC Cancer Agency, Vancouver, BC, Canada
[3]Deeley Research Centre, BC Cancer Agency, Victoria, BC, Canada
[4]Princess Margaret Hospital, University Health Network, Toronto, ON, Canada
[5]Vancouver Prostate Centre, Vancouver, BC, Canada
[6]Department of Medical Genetics, University of British Columbia, Vancouver, BC, Canada

ascites, and lower post-operative complications in patients with advanced stage disease. Thus, more translational research on neoadjuvant therapy is needed as this is becoming increasingly important and applicable in the clinical setting.

The association between the presence of TIL and survival in HGSC has been well established. In several clinical studies, the increased presence of CD3^{+} and CD8^{+} T cells, CD20^{+} B cells, and other cytotoxic immune cells expressing TIA-1 have been correlated with prolonged survival[48, 49, 50, 224]. Recently, a number of murine studies have suggested that chemotherapy can enhance the anti-tumour immune response by eliciting immunogenic cell death (ICD) in tumour cells[241, 242, 243, 245]. Certain chemotherapies, particularly anthracycline, have been shown to induce apoptotic tumour cells to release ICD molecules, such as calreticulin, ATP, and HMGB1[240]. These ICD molecules are recognized by immature dendritic cells (DCs), which engulf apoptotic tumour cells. Activated DCs then process and present new tumour antigens on their cell surfaces. These new tumour antigens are recognized by naïve T cells which in turn become activated effector T cells with the potential to eradicate any remaining cancer cells. A few clinical studies comparing pre- and post-chemotherapy samples from neoadjuvant-treated patients have found an increase in CD8^{+} T cells following chemotherapy[262, 263, 264]. Additionally, a decrease in FoxP3^{+} Treg infiltration in post-chemotherapy tumours in breast cancer was reported by Ladoire et al, and patients who had a high CD8^{+}/FoxP3^{+} T cell ratio showed a prolonged survival[262, 263]. In ovarian cancer, Polcher et al. found CD8^{+} and GzmB^{+} immune cells increased following carboplatin plus docetaxel treatment in post-chemotherapy tumours, but FoxP3^{+} Treg infiltration remained unchanged[264]. Together, these studies suggest the immune system is stimulated during standard treatment and may play a role in tumour eradication.

In this study, we compare TIL composition in matched pre- and post-chemotherapy tumours from neoadjuvant-treated HGSC patients. We performed immunohistochemistry (IHC) using a comprehensive panel of immune markers that focused on T cells, B cells, macrophages, cytotoxic cells, and the T cell exhaustion marker PD-1, to identify the immune cell phenotypes present in the tumour epithelium. Based on the limited clinical studies investigating changes

in TIL following chemotherapy, we hypothesize that there would be an increase in anti-tumour immune cells such as T cells (CD3$^+$, CD8$^+$), B cells (CD20$^+$), and cytotoxic immune cells (GzmB$^+$, TIA-1$^+$), and a decrease in immunosuppressive FoxP3$^+$ Tregs and PD-1$^+$ immune cells following chemotherapy.

3.2. Methods

3.2.1. Patient cohort selection

A retrospective patient cohort receiving neoadjuvant carboplatin plus paclitaxel chemotherapy was identified and collected for this study (Figure 6). Patients (1245 patient cases) who received surgery for gynecological disease at Vancouver General Hospital (VGH) between 2004-2012 were first broadly selected based on these surgical terms: debulking, interval debulking, exploratory laparotomy, oophorectomy, hysterectomy, bilateral salpingo-oophorectomy, intraperitoneal port, and removal of pelvic mass. The diagnostic pathologies of the patients were identified using the British Columbia Cancer Agency's (BCCA) Cancer Agency Information System (CAIS). Patients diagnosed with subtypes other than HGSC were excluded from the study (804 out of 1256 patient cases); this included LGSC, which has recently been classified as a distinct subtype from HGSC. Patients who received adjuvant chemotherapy were also excluded from the patient cohort (188 out of 441 HGSC patient cases). The exclusion criteria further included patients who had interval debulking for recurrent tumours, radiation, or had been diagnosed with any other cancers less than 5 years prior to diagnosis with HGSC. Patients who received interval debulking from VGH, but had pre-chemotherapy biopsies outside of VGH were also excluded as there was no access to these pre-chemotherapy biopsies (179 out of 253 neoadjuvant HGSC patient cases). These exclusions narrowed the initial 1245 patient cohort to 74 cases that had possible pre- and post-chemotherapy tumours available from OvCaRe's tumour bank (BC Ovarian Cancer Research Team (Vancouver, B.C.)). A request was sent to OvCaRe for formalin-fixed, paraffin embedded (FFPE) tissue blocks for these cases. Of

these 74 requested cases, 31 had inaccessible pre- or post-chemotherapy biopsies: 24 cases had unavailable pre-chemotherapy core-needle biopsies and 7 cases had missing pathology reports on CAIS. Of note, in our post-chemotherapy Kaplan-Meier survival analysis, we used an additional set of post-chemotherapy tumours from 18 of 24 cases with unavailable pre-chemotherapy core needle biopsies but still had available post-chemotherapy tissues. In continuation with our matching cohort selection, the elimination of the 31 cases further narrowed the cohort to 43 HGSC neoadjuvant-treated patient cases with available FFPE tissue from both pre-chemotherapy biopsies and post-chemotherapy surgical resections. 17 of the 43 matched HGSC neoadjuvant-treated patient cases did not have sufficient viable tumour present within the pre- and/or post-chemotherapy FFPE blocks and were therefore excluded in the matched sample analysis. The inclusion of these tumours in the tissue microarray (TMA) or as whole sections would have eliminated the remaining tumour present in the original blocks. The tumours that had sufficient viable tumour present in the FFPE blocks for whole sectioning (but not for TMA construction) were, however, included in the analysis. In the end, a total of 26 HGSC neoadjuvant-treated patients for the matching patient cohort were included in this study. Patients received carboplatin plus paclitaxel chemotherapy.
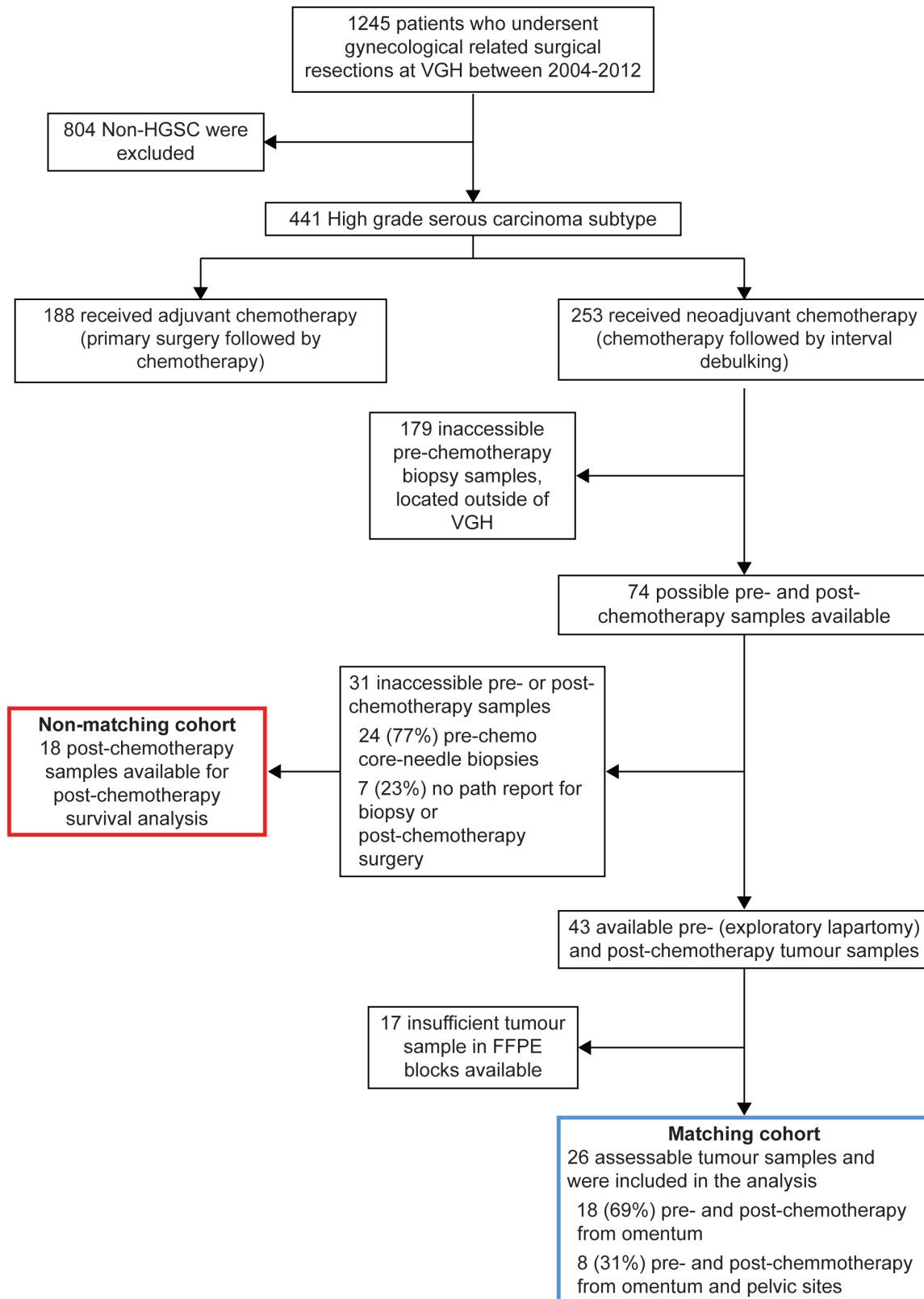
Figure 6. **The process of selecting neoadjuvant patients for the study cohorts**.

A typical neoadjuvant-treated patient from the study cohort was first diagnosed with gynecological malignancy by cytology using fine needle aspiration. The patient then received exploratory laparotomy, a surgery of the abdominal region, as a form of primary surgery. During exploratory laparotomy, complete debulking or removal of the tumour was intended but unachievable due to disseminated disease within the abdomen. A biopsy of the tumour, omentum being the dominant sampling site, was obtained for pathological diagnosis prior to the termination of the surgery (Figure 7), and the patient was reported to have undebulkable disease. After recovery from the unsuccessful primary surgery, the patient was given 3-4 cycles of chemotherapy (starting dose: paclitaxel = 175 mg/m^2, carboplatin = AUC x (GFR + 25)) with each cycle administered every 21-28 days (GOOVCATX protocol, BCCA). Significant tumour reduction from a well-tolerated response to chemotherapy was immediately followed by a second surgery, referred to as interval debulking, to remove all residual abdominal tumour. Finally, the patient was given several more cycles of chemotherapy until CT scans indicated the patient was negative for tumour.

Adjuvant Therapy
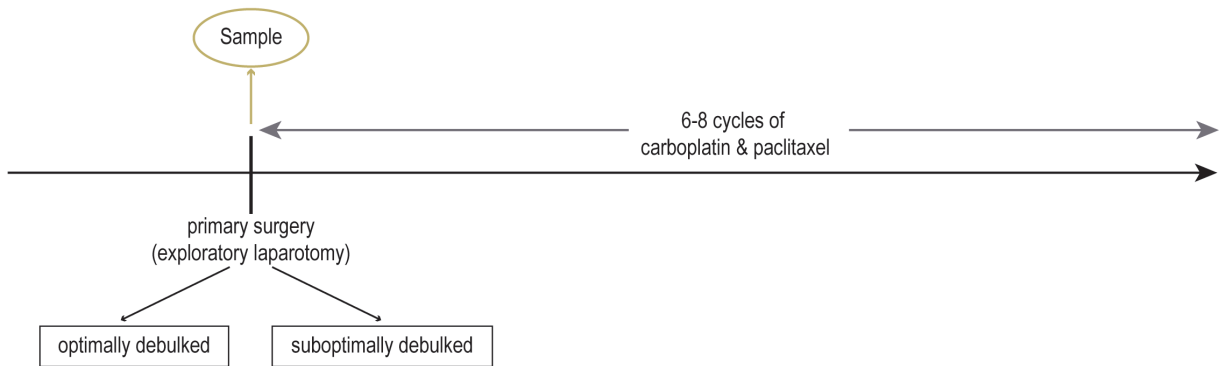
Neoadjuvant Therapy
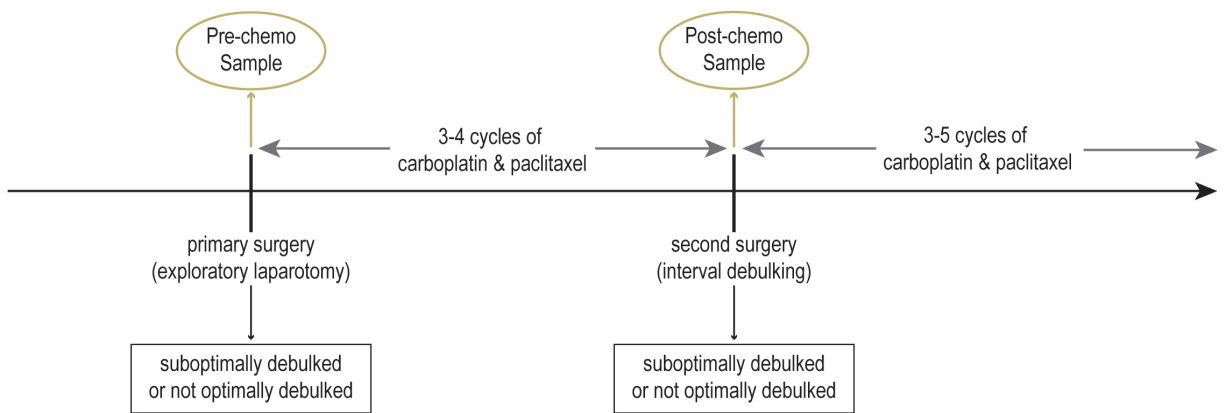
Figure 7. **Pre- and post-chemotherapy sample selection of neoadjuvant patients**. Previous TIL studies used tumour samples obtained at the time of primary surgery prior to carboplatin plus paclitaxel chemotherapy. In this study, pre- and post-chemotherapy tumour samples were collected at the time of primary surgery and interval debulking respectively.

3.2.2. Tissue microarray

FFPE blocks from the final patient cohort (26 cases) were for TMA construction. Tissue areas containing viable tumour were identified from diagnostic hematoxylin & eosin (H&E) slides and selected by a pathologist (B.A.C.) for TMA construction. Whenever tumour was present, pre- and post-chemotherapy samples from pelvic and extra-pelvic sites were included in the TMA. Pelvic sites, defined as the location from which the primary tumour arose, include ovary and fallopian tube, pelvic tumour, and adnexa. Extra-pelvic sites are areas of tumour metastasis, which include omentum, peritoneum, myometrium, uterus, intra-abdominal wall and umbilical nodules, and cul-de-sac. The orientation of the FFPE tumour samples on the TMA was

randomized and a TMA map was generated. A tissue microarray was constructed consisting of 1

mm duplicate cores of epithelial regions (identified on H&E stained slides) using a manual tissue

microarrayer (Beecher Instruments, Sun Prairie, WI, USA). Tissue blocks containing tumour

areas less than 1 mm in diameter were omitted from the TMA to avoid exhausting the tumour

in the original FFPE blocks. Instead, whole sections were sectioned from these tissue blocks

containing enough viable tumour for a series of immunohistochemical single-stains. TMA or

whole sections were used in subsequent immunohistochemistry (IHC) experiments.

3.2.3. Immunohistochemistry

Sections from the TMA or whole sections were stained with antibodies against 15

immune and functional markers (Table 2). All TMAs and FFPE blocks were consecutively

sectioned at 4 µm onto Superfrost plus slides (Fisher Scientific, Cat# 12-550-15) using a

microtome (Model: Microm HM-355S). Tissue sections were incubated overnight at 37°C to

allow for them to adhere securely to the slides. Sections were deparaffinized in xylene, and

passed through a series of graded reagent alcohols to distilled water washes to hydrate the tissue

prior to automated IHC staining using the Ventana Discovery XT autostainer (Ventana, Tucson,

AZ, USA). All the markers, except CD103 and PD-1, were stained using the Ventana Discovery

XT autostainer. The tissue sections were stained sequentially according to the order that is

presented in Table 1. All kits and reagents used were obtained from Ventana (Ventana, Tucson,

AZ, USA). The Ventana's standard Cell Conditioning 1 (CC1) protocol was used for antigen

retrieval. The CC1 protocol consists of heat-induced antigen retrieval with a commercial Tris-

based antigen retrieval buffer, CC1 (Ventana, Tucson, AZ, USA, Cat# 950-124). All blocking

steps, to block non-specific binding in the tissue, were included in the Discovery DABMap kit

(Ventana, Tucson, AZ, USA, Cat# 760-124), which was used for detecting proteins of interest

with 3, 3'-diaminobenzidine (DAB). All antibodies were diluted in Antibody Diluent (Ventana,

Tucson, AZ, USA, Cat# 250-018), a buffered solution at pH=7.2-7.4, and diluted antibodies

were manually added to the slides according to the concentrations indicated in Table 2, before

proceeding with the automated staining. Antibodies were incubated for 60 minutes at room

temperature followed by distilled water (dH$_2$O) washes. A cross-adsorbed biotinylated goat α-mouse immunoglobulin (IgG) secondary antibody or goat α-rabbit immunoglobulin (IgG) secondary antibody (Jackson Immunoresearch, West Grove, PA, USA, Cat# 115-065-003 & 111-065-003) was manually added onto the slides at dilutions of 1:250 and 1:500 respectively. Secondary antibodies were incubated for 32 minutes at room temperature and followed by dH$_2$O washes. The DABMap kit was used to detect the bound secondary antibodies with DAB, and this was followed by counterstaining with hematoxylin (Ventana, Tucson, AZ, USA, Cat# 760-2021) and bluing solution (Ventana, Tucson, AZ, USA, Cat# 760-2037) . Slides were then dehydrated in increasing alcohol dilutions and xylene prior to cover-slipping with Cytoseal-60 mounting media (Richard Allan, Kalamazoo, MI, USA, Cat# 23-244256). Human tonsil and liver tissues were used as positive controls for all the primary antibodies. A tissue section from the TMA stained without primary antibodies was used as a negative control.

Staining for CD103 and PD-1 was performed on Biocare Medical's Intellipath FLX autostainer (Biocare Medical, Concord, CA, USA). Tissue sections were incubated overnight at 37°C and deparaffinized in xylene followed by a series of graded alcohol washes. Heat-induced epitope retrieval was subsequently performed using Decloaking Chamber Plus (Biocare Medical, Concord, CA, USA, Cat# DC08-1180), and in a 1:10 dilution of Diva decloaking reagent (Biocare Medical, Concord, CA, USA, Cat# DV2004MX). The decloaking chamber was set for antigen retrieval at 125°C at the following settings: P1 at 125°C, P2 at 100°C with fan on, and P2 at 80°C with fan off. Following antigen retrieval, sections were incubated for 5 minutes at room temperature with Peroxidased-1 (Biocare Medical, Concord, CA, USA, Cat# PX968H), a commercial hydrogen peroxidase solution to block endogenous peroxidase activity. They were then washed with a TBS-tween wash buffer and incubated for 10 minutes at room temperature with Background Sniper (Biocare Medical, Concord, CA, USA, Cat# BS966H), a blocking reagent used to reduce nonspecific background staining. Sections were washed in TBS-tween buffer and anti-CD103 rabbit monoclonal antibody and anti-PD-1 mouse monoclonal antibody (Table 2) were incubated for 30 minutes at room temperature. All antibodies were diluted

in Da Vinci Green diluent (Biocare Medical, Concord, CA, USA, Cat# PD900L). Sections were washed again with TBS-tween buffer and followed by a 30-minute incubation at room temperature with the following secondary antibodies: MACH2 anti-rabbit HRP and MACH2 anti-mouse HRP polymer reagents (Biocare Medical, Concord, CA, USA, Cat# RHRP520H & MHRP520G) for anti-CD103 and anti-PD-1 antibodies respectively. Following subsequent buffer washes, secondary antibodies were detected using DAB reagent (intelliPATH FLX DAB Chromagen kit, Biocare Medical, Concord, CA, USA, Cat# IPK 5010 G80) for 5 minutes at room temperature and washed with dH$_2$O. Sections were stained with hematoxylin solution (Biocare Medical, Concord, CA, USA, Cat# CATHE-H) (1:10 dilution) to visualize tissue architecture, and washed once more with dH$_2$O. Sections were incubated with Tacha's Bluing Solution (Biocare Medical, Concord, CA, USA, Cat# HTBLU-M) for 30 seconds and washed once more. Slides were air-dried and cover-slipped using EcoMount mounting media (Biocare Medical, Concord, CA, USA, Cat# EM897L). Human tonsil and liver tissues were used as positive controls for the primary antibodies. A section stained without primary antibodies was used as a negative control.

Table 2. α-human antibodies for single-colour immunohistochemistry. Tissue sections were stained in sequential order as displayed in the following table.

Antigen	Clone	Supplier	Cat. No.	Source	Dilution
CD3	SP7	Spring Bio	M3074	Rabbit	1:150
CD4	SP35	Spring Bio	M3354	Rabbit	1:150
CD8	SP16	Spring Bio	M3162	Rabbit	1:100
Granzyme B	n/a	Abcam	ab4059	Rabbit	1:50
TIA-1	TIA1	Abcam	ab2712	Mouse	1:50
cleaved Caspase-3	n/a	Cell Signalling	9661	Rabbit	1:50
FoxP3	ebio7979	eBioscience	14-7979	Mouse	1:50
CD20	n/a	Spring Bio	E2560	Rabbit	1:300
CD68	PG-M1	LabVision	MS1808	Mouse	1:50
CD56	123C3.D5	LabVision	MS204	Mouse	1:50
CD1a	O10	LabVision	MS1856	Mouse	1:50
MHC Class I	EMR8-5	MBL	D226-3	Mouse	1:500
MHC Class II	CR3/43	Affinity Bioreagents	MAI-25914	Mouse	1:50
CD103	EPR4166(2)	Epitomics	550258	Rabbit	1:1500
PD-1	NAT105	Cell Marque	315M-94	Mouse	1:200

3.2.4. Quantitative assessment and analysis of immune infiltrates

Stained slides were reviewed and positive cells were manually counted by two pathologists (B.A.C. & S.S.), who were blinded to the patients' clinical data and treatment statuses. For the TMA stains, the absolute cell count of immune infiltrates in the intraepithelial and stromal compartments were scored by either one of the pathologists. The pathologists reviewed the slides together and arrived at a consensus of the scoring. For the whole section scoring, an equivalent of two 1 mm core areas containing tumour were identified and scored for intraepithelial and stromal immune infiltrates. Total tumour cells present within the cores were also calculated. The mean intraepithelial, stromal, and tumour counts between duplicate cores were calculated. Comparisons of the immune infiltrates were analysed for 4 characteristics: intraepithelial density (division of the absolute intraepithelial cell count by tumour cell count and

expressed as a density out of 100 tumour cells), total cell count (summation of intraepithelial and stromal cell counts), absolute intraepithelial cell count, and absolute stromal cell count. Analysis was performed on 26 patient cases with pre- and post-chemotherapy tumours from a combination of both pelvic and extra-pelvic sites, as well as a subset of 18 patient cases with pre- and post-chemotherapy tumours in extra-pelvic sites.

3.2.5. Imaging

For the single stains, slides were imaged using the Aperio imaging system (Leica Biosystems, Germany) and image snapshots were taken at 100X and 200X magnification using the downloadable Imagescope software.

For multicolour stains, slides were imaged using the Vectra automated imaging system (Perkin Elmer, USA). The spectra for each chromogen was separated by inForm software (Perkin Elmer, USA) to produce unmixed images. Unmixed images are individual images that contain a single marker/chromogen; therefore, a triple-stain would have three separate unmixed images. Composite images (a single image containing a composite of all the unmixed images) were also produced. For each image core, unmixed and composite images were produced by inForm. Unmixed images were used to guide manual scoring of TIL subsets.

3.2.6. Statistical analysis

The Wilcoxon matched pairs test was used for statistical analysis and was performed using GraphPad Prism 6.0 (GraphPad, La Jolla, CA). A biostatistician (A.T.) performed multiple testing using the false discovery rate method for all markers and for all measurements: intraepithelial density, total cell count, and absolute intraepithelial and stromal cell count. Power analysis was performed on all the markers (except cleaved capase-3, MHC I and II) for intraepithelial cell density in the matched cohort (n=26) (Appendix B). *P* values were adjusted according to the results from multiple testing analysis. *P*-values ≤0.05 were considered significant.

3.2.7. Heat-map

Heat-maps were generated using the online software CIMminer (Genomics and Bioinformatics Group, NCI, discover.nci.nih.gov/cmiminer/). Three heat-maps were generated to illustrate the changes in TIL densities and for comparing TIL densities present in only pre- or post-chemotherapy tumours. In the heat-map that illustrates changes in TIL densities, differences between TIL densities in pre- and post-chemotherapy tumours were calculated (i.e. post-chemotherapy density – pre-chemotherapy density). In the second and third heat-maps, only the densities from the pre- or post-chemotherapy tumours were used. Heat-maps were generated using the One Matrix CIM and hierarchical clustering algorithm with complete linkage method and Euclidean distances. The use of hierarchical clustering algorithms in immune markers can be found in Zucchetto et. al[278].

3.2.8. Kaplan-Meier analysis

Survival analysis was performed using Graphpad Prism 6.0. To investigate whether changes in TIL correlated with survival, we categorized the patients into increased (≥2-fold increase and *de novo* responses), decreased (≥2-fold decrease), or "no change" (no TIL present in tumours and sustained responses) in TIL response following chemotherapy. The log-rank (Mantel-Cox) test was used to compare survival between the three groups. For survival analysis on TIL densities in post-chemotherapy tumours, cut-offs to separate between low and high TIL densities were determined using the downloadable X-tile software (Rimm Lab, Yale School of Medicine). The patients were categorized based on low and high TIL densities and Kaplan-Meier curves were produced for the following TIL markers: CD3, CD8, CD20, TIA-1, PD-1, and FoxP3.

3.3. Results

3.3.1. Patient cohort and treatment

A cohort of 26 HGSC patients with matching pre-chemotherapy biopsies and post-

chemotherapy surgical specimens was used for the study. Patients received neoadjuvant chemotherapy at VGH from 2004-2012. The clinical and histological characteristics of the cohort are summarized in Table 3. The majority of the patients had well differentiated tumours (88.4%), whereas others were diagnosed with poorly differentiated serous carcinoma (7.7%), or a mixture of well differentiated and poorly differentiated serous carcinoma (3.8%). Most of the patients had grade 3 tumours (61.5%), while one patient had grade 2 tumour (3.8%), and the remaining patients did not have their tumour grades reported (34.6%). The majority of the patients had stage IIIC disease (80.8%), whereas the remaining patients were recorded as stage III (11.5%), or stage IV (7.7%). The most common biopsy procedure for obtaining pre-treatment tissue was exploratory laparotomy (73.1%), followed by omentectomy (26.9%), bilateral salpingo-oophorectomy (15.4%), hysterectomy (7.7%), or omental core biopsy (3.8%). Most biopsies were obtained from the omentum (73.1%), whereas others were taken from ovary (26.9%), colon and abdominal regions (23.1%), fallopian tubes (19.2%), other metastatic regions (19.2%), peritoneum (7.7%), pelvic tumour (7.7%), or uterus (7.7%).

All 26 patients received carboplatin plus paclitaxel chemotherapy as their neoadjuvant chemotherapy regimen. Patients had between 3 to 6 cycles (mean=4) of chemotherapy prior to interval debulking. The majority of the patients responded well to chemotherapy (88.5%); however, one patient responded poorly (3.8%), and two cases had no indication of response in their medical narratives (7.7%). The mean serum CA-125 prior to chemotherapy was 7,314.10 kU/L (median=1,522 kU/L; range=28-130,000 kU/L), which dropped to a mean of 72.18 kU/L after chemotherapy (median=36 kU/L; range=7.8-370 kU/L). During interval debulking surgery, most patients were optimally debulked (61.5%), while the remaining patients were suboptimally debulked (38.5%). Most post-chemotherapy tumour samples were resected from the omentum (69.2%), followed by ovary (57.7%), fallopian tube (46.2%), other metastatic regions (27%), colon and abdominal regions (23.1%), or uterus (19.2%).

Table 3. **Clinical characteristics of the neoadjuvant patient cohort**

Characteristics	Matched Neoadjuvant Patients
Age – yr	
Mean	61
Median	60
Range	44-82
Histologic type and grade – no. (%)	
High grade serous carcinoma	23 (88.4%)
Poorly differentiated serous	2 (7.7%)
High grade serous carcinoma & poorly differentiated serous	1 (3.8%)
Grade – no. (%)	
1	0
2	1 (3.8%)
3	16 (61.5%)
Not reported	9 (34.6%)
Stage – no. (%)	
III	3 (11.5%)
IIIC	21 (80.8%)
IV	2 (7.7%)
Method of biopsy – no. (%)	
Bilateral salpingo-oophorectomy	4 (15.4%)
Hysterectomy	2 (7.7%)
Laparotomy	19 (73.1%)
Laparoscopy	2 (7.7%)
Omentectomy	7 (26.9%)
Omental core biopsy	1 (3.8%)
Pre-chemotherapy tumour – no. (%)	
Ovary	7 (26.9%)
Fallopian tube	5 (19.2%)
Omentum	19 (73.1%)
Peritoneum	2 (7.7%)
Pelvic tumour	2 (7.7%)
Uterus	2 (7.7%)
Colon & Abdomen	6 (23.1%)
Other	5 (19.2%)

Table 3. Clinical characteristics of the neoadjuvant patient cohort (continued)

Characteristics	Matched Neoadjuvant Patients
Post-chemotherapy tumour – no. (%)	
Ovary	15 (57.7%)
Fallopian tube	12 (46.2%)
Omentum	18 (69.2%)
Uterus	5 (19.2%)
Colon & Abdomen	6 (23.1%)
Other	7 (26.9%)
Number of chemotherapy cycles prior to interval debulking	
Mean	4
Range	3-6
Serum CA-125 at entry (kU/L)	
Mean	7314.10
Median	1522
Range	28-130 000
Serum CA-125 before interval debulking surgery (kU/L)	
Mean	72.18
Median	36
Range	7.8-370
Response to Chemotherapy	
Well	23 (88.5%)
Poor	1 (3.8%)
No indication in medical narratives	2 (7.7%)
Interval debulking status – no. (%)	
Optimal	16 (61.5%)
Suboptimal	10 (38.5%)

Laparotomy comprises of subspecifc procedures such as bilateral salpingo-oophorectomy, hysterectomy, and omentectomy.

3.3.2. Changes in immune cell infiltration following chemotherapy

To determine the effects of chemotherapy on TIL in HGSC, we performed IHC with a comprehensive panel of immune markers and enumerated different TIL subsets in tumour samples collected before and after chemotherapy. The cohort consisted of 26 patients with matching pre-chemotherapy biopsies and post-chemotherapy specimens, thus allowing for a direct comparison of changes in TIL during treatment. Tissue specimens were stained using H&E to assess the amount of viable malignant tissue in each sample. Pre-chemotherapy samples typically contained a high proportion of viable tumour cells. By contrast, the majority of post-chemotherapy tumour samples exhibited histological features indicative of a response to treatment, including the presence of histiocytes or foamy macrophages, scattered clusters of tumour cells, extensive areas of fibrotic stroma, and high abundance of immune infiltrate clusters in the stroma (Figure 8). The extent of these features varied widely between patients, indicating a high degree of heterogeneity, with some post-chemotherapy samples showing high tumour viability and others showing extensive morphological changes.
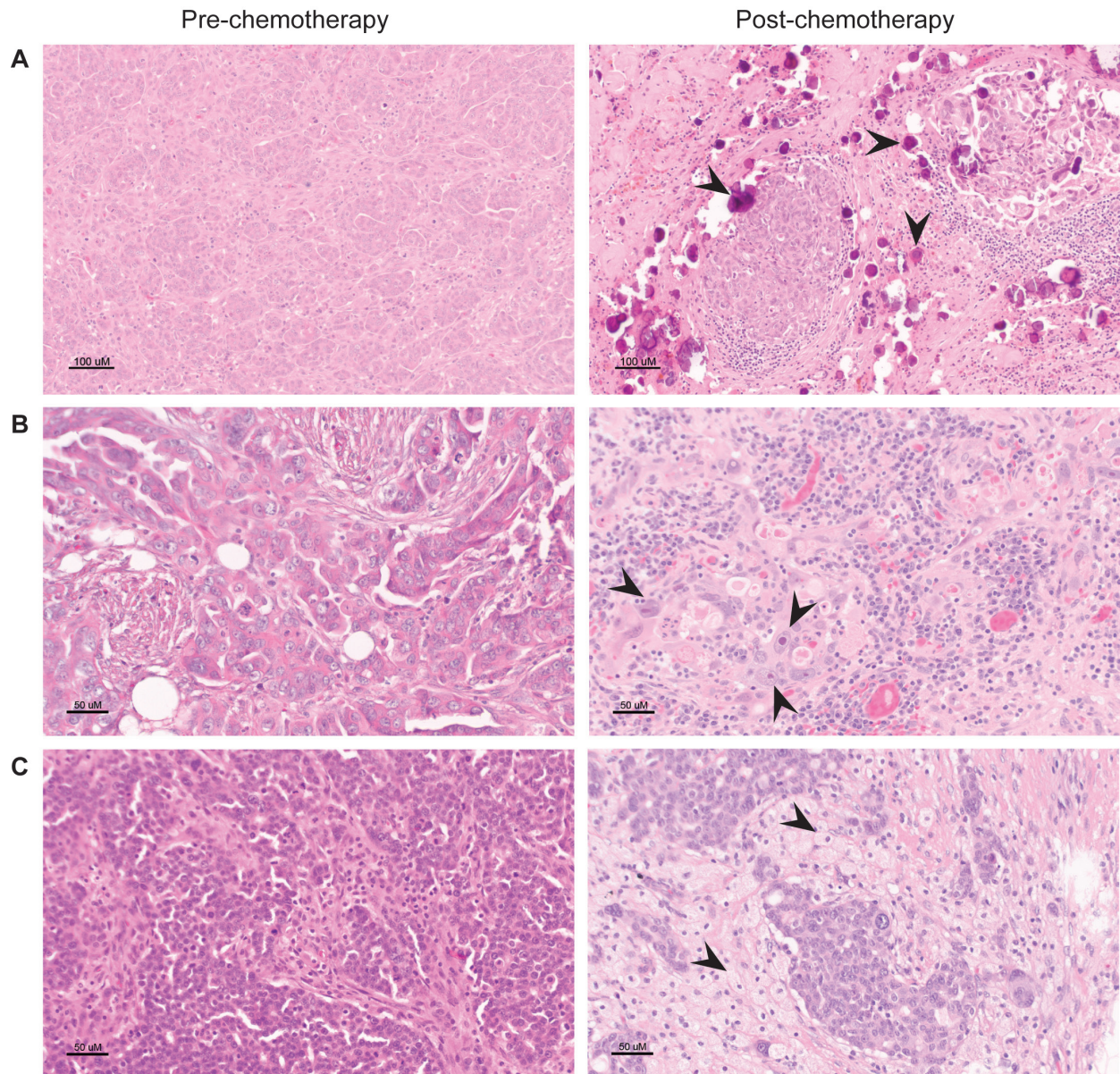
Figure 8. **Morphological changes due to the effects of chemotherapy**. Higher frequency of morphological changes in post-chemotherapy tumours compared to matching pre-chemotherapy tumours of neoadjuvant HGSC patients. (**A**) psammoma bodies (**B**) atypical cell morphology (**C**) histocytes. Arrows represent the cell types included above. Original magnification, (**A**) 100X, (**B & C**) 200X.

We assessed the extent of apoptotic tumour cell death by performing IHC for cleaved caspase-3, which is an indicator of caspase-mediated apoptosis. We found that very few tumour cells with intact nuclei expressed cleaved caspase-3 in either pre- or post-chemotherapy tumours, and their abundance did not change following treatment (Figure 9). In contrast, there were more apoptotic bodies seen in pre-chemotherapy tumours, and these decreased significantly in post-chemotherapy tumours (p=0.0007) (Figure 9 and Table 4).   These apoptotic bodies were often difficult to distinguish the original cell types, but appeared to include tumour cells, granulocytes, and mononuclear inflammatory cells. An increased number of cleaved caspase-3[+] apoptotic bodies was often found in areas of necrosis and inflammation. Despite a decrease in the number of viable tumour cells observed in post-treated tumours, the lack of overall cleaved caspase-3[+] apoptotic bodies found within the tumour epithelium suggest that most of the remaining malignant cells were not undergoing cell death at the time of interval debulking. Alternatively, the selection of viable tumour areas for our TMA construction might contribute to this observed phenomenon as well.
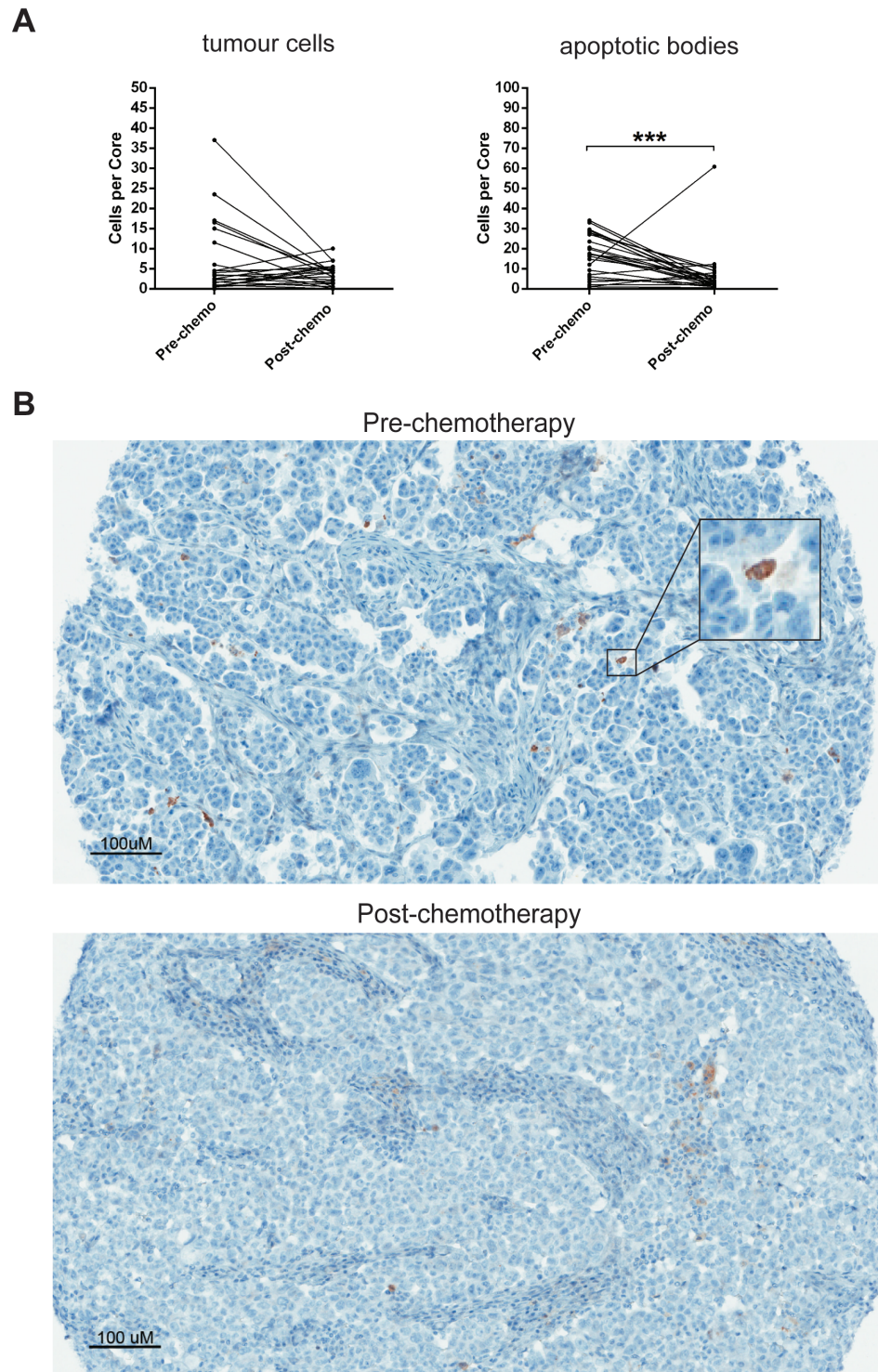
Figure 9. **cleaved caspase-3 expression in tumour and apoptotic bodies following chemotherapy**. (**A**) Paired comparison of cleaved caspase-3 expression on tumour cells and apoptotic bodies in pre- and post-chemotherapy from matched patient samples (n=25). *P* values were calculated using the Wilcoxon matched pairs test with Pratt's method. (**B**) Representative immunohistochemical staining pattern of cleaved caspase-3 expression prior to and after chemotherapy from a neoadjuvant patient. Magnification, 100X.

Next, we performed IHC for several immune cell markers. The surface markers used to identify the immune cell types included: dendritic cells (CD1a-marker of immature DCs), T cells (CD3, CD4, CD8), B cells (CD20), NK cells (CD56), and macrophages (CD68). We also included functional markers such as intraepithelial-associated integrin molecule $a_E b_7$ (CD103), Tregs (FoxP3), cytotoxic markers (Granzyme B (GzmB), TIA-1), T cell exhaustion (PD-1), and MHC I and II. Representative IHC images of T cells and B cells and functional markers from one patient are shown in Figures 10 and 11 respectively. TIL were enumerated by licensed pathologists who were blinded with regard to treatment status. TIL were enumerated separately in the epithelial and stromal regions of the tumour. Due to the wide variability in the amount of viable tumour epithelium between samples, we also used intraepithelial TIL densities, in addition to absolute cell counts, when comparing samples. Intraepithelial TIL densities were calculated by dividing the absolute intraepithelial TIL count by the number of epithelial tumour cells. We observed increases in intraepithelial T cells ($CD3^+$, $CD4^+$, $CD8^+$) following chemotherapy. $CD3^+$ T cells were frequently found in pre-chemotherapy tumours (mean=11.17 $CD3^+$ T cells/100 tumour cells), and the presence of $CD3^+$ TIL significantly increased in post-chemotherapy tumours (mean=24.33 $CD3^+$ T cells/100 tumour cells, P=0.014) (Figure 12 and Table 4). Similarly, $CD8^+$ T cells were commonly present in pre-chemotherapy tumours (mean=10.39 $CD8^+$ T cells/100 tumour cells), and increased in infiltration following chemotherapy (mean=20.38 $CD8^+$ T cells/100 tumour cells, P=0.0147). Pre-chemotherapy tumours also had $CD4^+$ TIL (mean=7.084 $CD4^+$ T cells/100 tumour cells), and they significantly increased following treatment (mean=20.41 $CD4^+$ T cells/100 tumour cells, P=0.01087). In contrast to T cells, intraepithelial $CD20^+$ B cells were lower in abundance in pre-chemotherapy tumours (mean=0.3237 $CD20^+$ B cells/100 tumour cells), but had the most definitive increase following treatment (post-chemotherapy mean=1.174 $CD20^+$ B cells/100 tumour cells, P=0.0044).
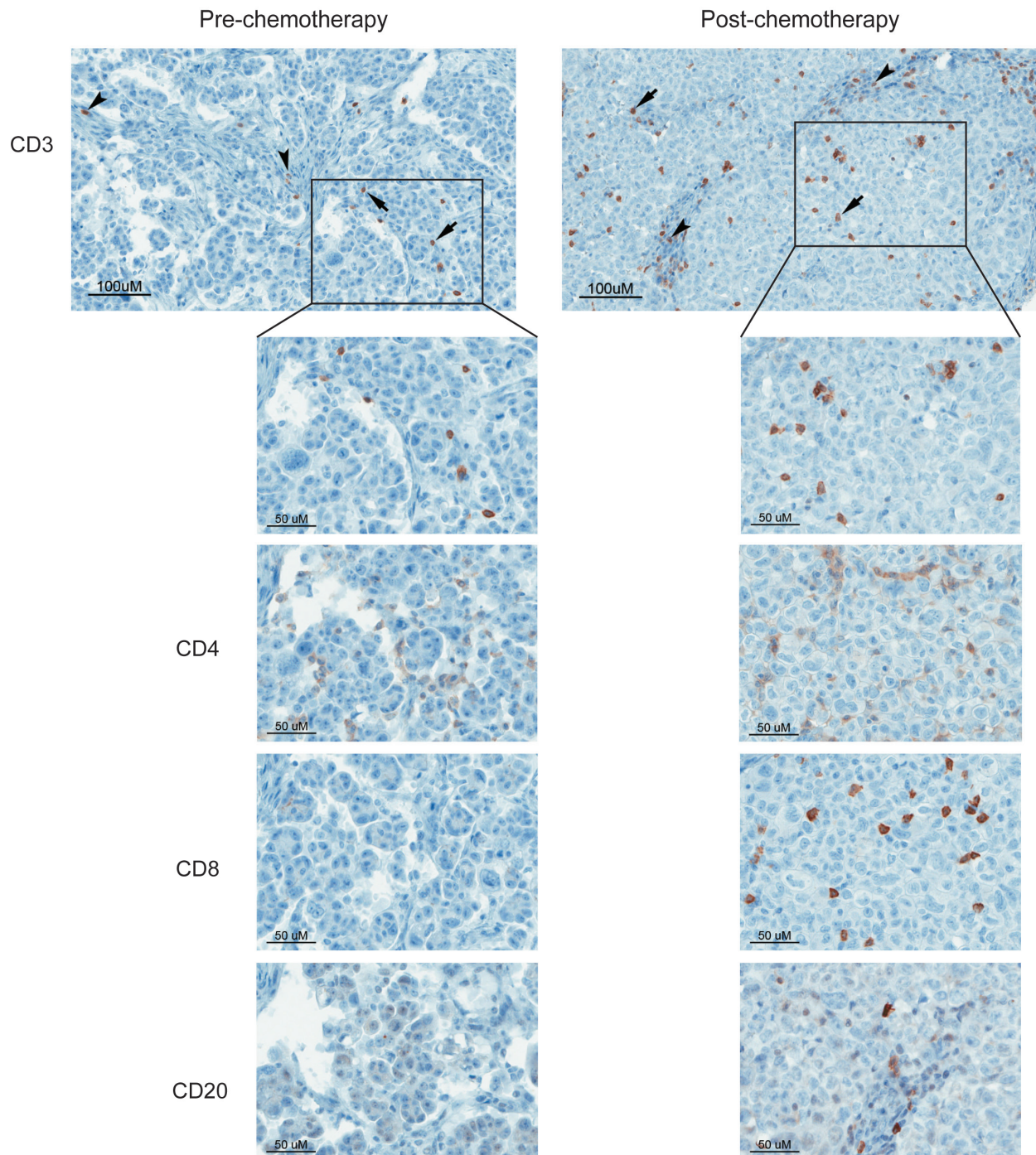
Figure 10. **Immunohistochemical staining pattern of immune cell infiltration following chemotherapy**. Representative immunohistochemical staining pattern of CD3^{+}, CD4^{+}, CD8^{+} T cells, and CD20^{+} B cells before and after chemotherapy of a neoadjuvant patient (CD3 100X magnification; CD3, CD4, CD8, CD20 200X magnification). Markers were stained in sequential order and images are in the same tumour location with examples of intraepithelial CD3^{+} T cells (arrows) and stromal CD3^{+} T cells (arrowheads).
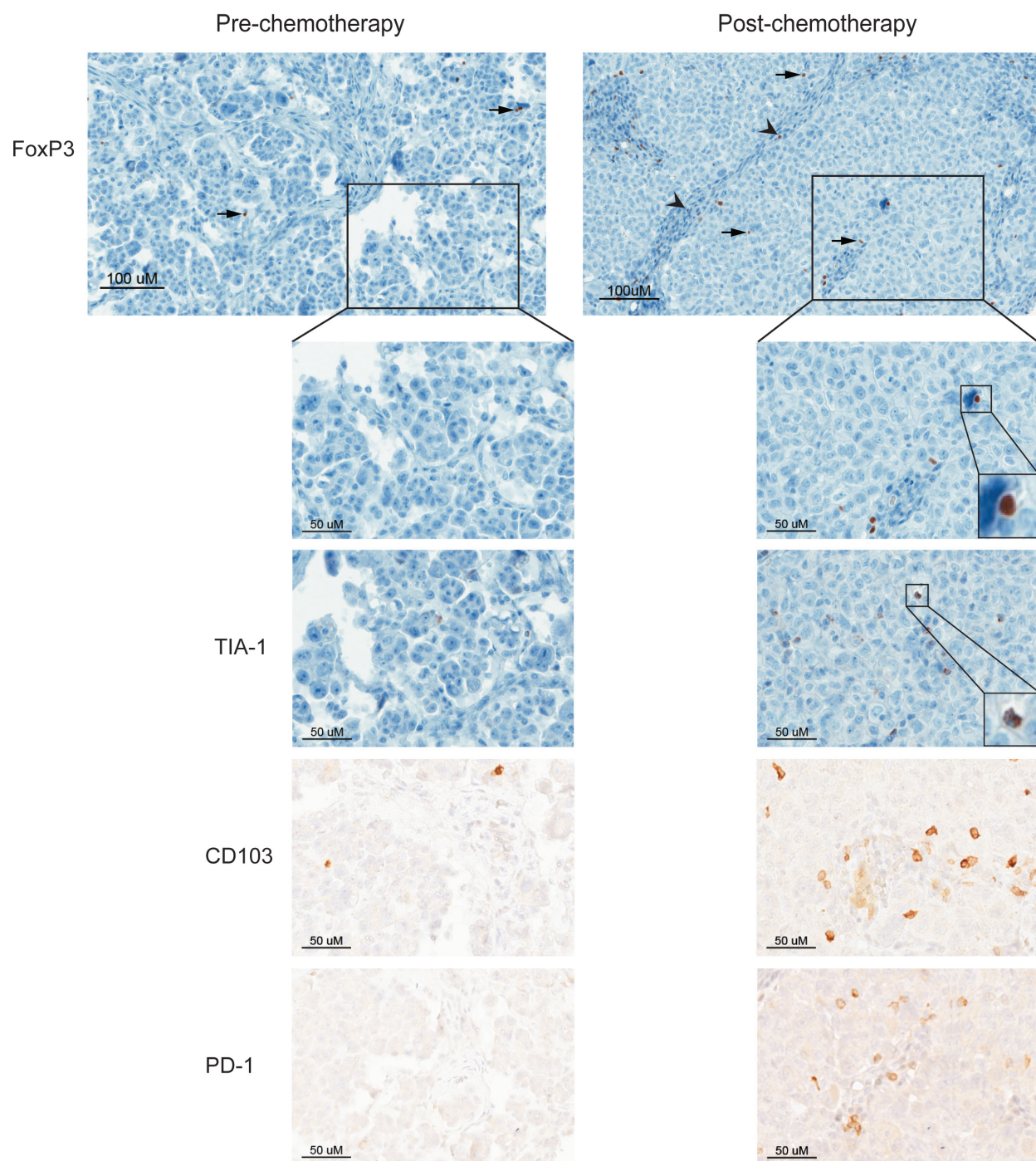
Figure 11. **Immunohistochemical staining pattern of functional TIL markers following chemotherapy**. Representative immunohistochemical staining pattern of FoxP3^{+}, TIA-1^{+}, CD103^{+}, and PD-1^{+} T cells before and after chemotherapy of a neoadjuvant patient (FoxP3 100X magnification; FoxP3, TIA-1, CD103, PD-1 200X magnification). Markers were stained in sequential order and images are in the same tumour location with examples of intraepithelial FoxP3^{+} T cells (arrows) and stromal FoxP3^{+} T cells (arrowheads).
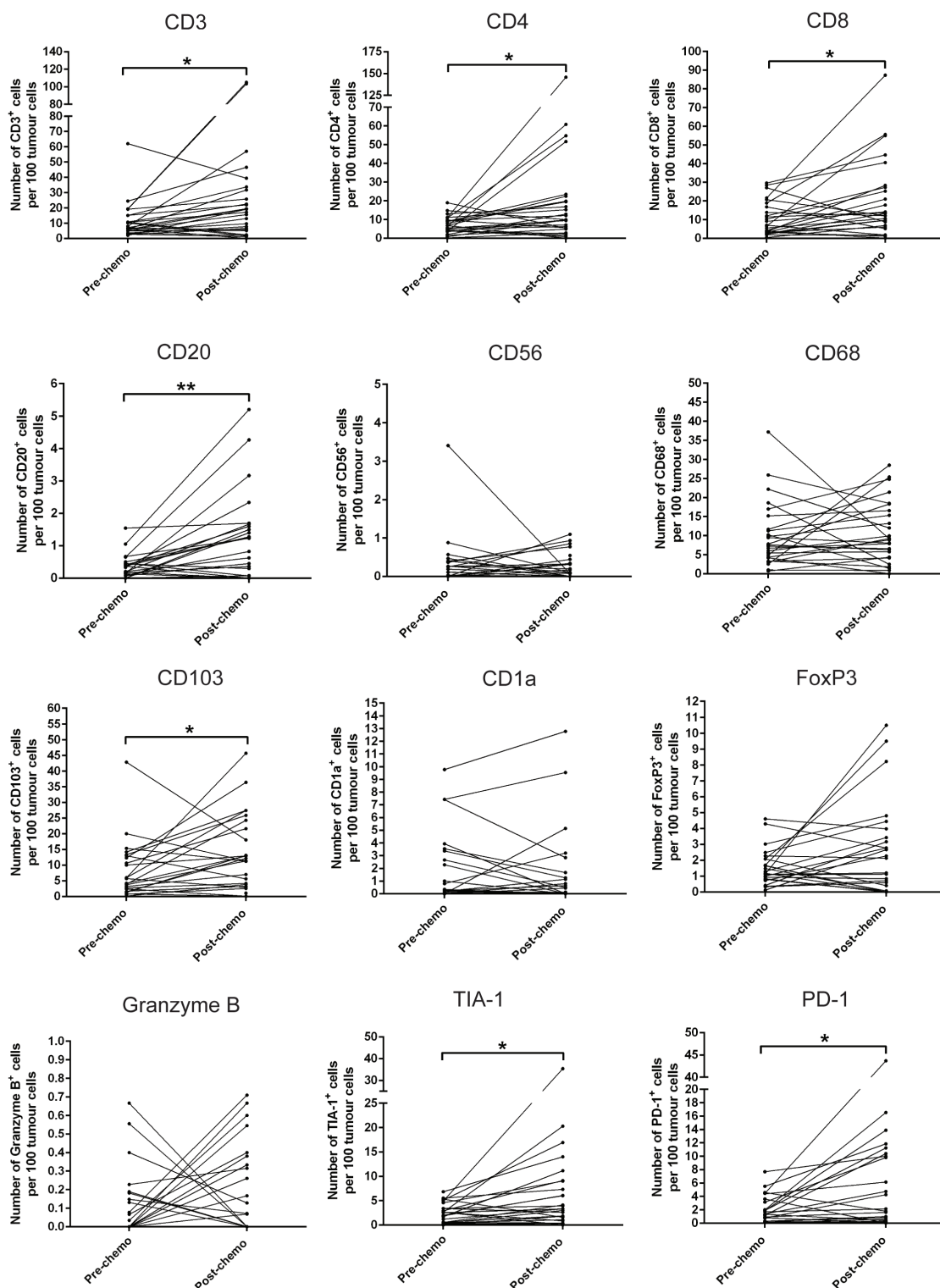
Figure 12. **Intraepithelial density of immune cells following chemotherapy**. Density of each marker within the tumour epithelium was compared in matched pre- and post-chemotherapy tumour samples (n=26, CD56, CD103, FoxP3, PD-1 n=25) using immunohistochemistry. *P* values were calculated using the Wilcoxon matched pairs test with Pratt's method and adjusted for multiple testing. Statistical significance * *P<0.05*, ** *P<0.01*, *** *P<0.001*

Table 4. **Changes in TIL density and absolute cell counts following chemotherapy in HGSC matching cohort (**n=26)

Marker	Intraepithelial Density				Total Count				Intraepithelial Count				Stromal Count			
	Median Pre-Chemo	Median Post-chemo	Median difference	P value	Median Pre-Chemo	Median Post-chemo	Median difference	P value	Median Pre-Chemo	Median Post-chemo	Median difference	P value	Median Pre-Chemo	Median Post-chemo	Median difference	P value
CD1a	0.2361	0.1292	0.00	0.8946	1.50	0.50	0.00	0.6022	1.00	0.50	-0.125	0.4538	0.00	0.00	0.00	0.9237
CD3	6.977	18.10	6.755	**0.0140**	137.8	204.8	38.00	0.2096	40.13	81.75	12.75	0.2418	99.50	131.3	13.92	0.4467
CD4	6.541	9.883	3.935	**0.0187**	64.38	90.00	15.38	0.4541	34.88	50.25	14.00	0.3034	27.13	28.50	1.25	0.9237
CD8	6.808	12.80	6.654	**0.0147**	103.0	174.8	40.50	0.1222	38.63	42.63	1.750	0.3034	39.00	74.75	14.00	0.1528
CD20	0.2026	1.026	0.4920	**0.0044**	9.50	21.00	4.75	0.1560	1.125	3.125	1.125	0.0696	6.125	18.25	4.25	0.1596
CD56	0.1132	0.09524	0.00	0.8946	2.00	1.00	-0.750	0.1902	0.750	0.500	-0.250	0.6796	0.500	0.250	0.00	0.4467
CD68	7.435	9.017	1.00	0.5908	127.30	103.1	-14.25	0.4914	38.00	31.63	-3.750	0.7977	84.75	66.50	0.3750	0.8476
CD103	4.222	11.34	3.683	**0.0432**	46.00	67.50	6.50	0.3686	20.50	36.00	1.50	0.7663	15.75	25.00	10.75	0.4467
FoxP3	1.179	2.126	0.0889	0.2149	54.00	47.50	4.00	0.9842	6.50	6.75	-0.75	0.9315	45.50	28.50	-5.00	0.9237
Granzyme B	Too few differences for calculation				3.125	5.250	3.00	**0.0449**	0.0	0.125	0.0	0.5698	2.250	4.00	3.00	0.1152
TIA-1	2.278	3.309	1.813	**0.0132**	24.13	34.63	15.13	**0.0449**	11.75	13.25	7.50	0.1680	11.75	24.63	5.50	0.1528
PD-1	1.333	1.800	0.6816	**0.0140**	11.00	11.75	1.417	0.2569	6.50	6.50	1.25	0.1680	3.50	4.500	0.0	0.9237
cleaved Caspase-3 tumour cells	N/A				2.50	4.00	0.0	0.4914	N/A				N/A			
cleaved Caspase-3 apoptotic cells	N/A				17.50	3.250	-14.00	**0.0112**	N/A				N/A			
MHC I	N/A				1.00	1.667	0.00	0.7617	N/A				N/A			
MHC II	N/A				1.00	1.00	0.25	**0.0448**	N/A				N/A			

P values are calculated using Wilcoxon matched pairs test with Pratt's method and adjusted for multiple testing. Bolded values indicate statistical significance of *P*<0.05, *P*<0.01, *P*<0.001

To investigate the functional phenotype of tumour-infiltrating T cells, we analysed

the markers GzmB, TIA-1, FoxP3, CD103, and PD-1. We observed very few intraepithelial

GzmB^{+} cells present in tumours prior to (mean=0.103 GzmB^{+} cells/100 tumour cells) and

following chemotherapy (mean=0.179 GzmB^{+} cells/100 tumour cells). The differences in GzmB

intraepithelial density infiltration between pre- and post-chemotherapy samples were too few that

Wilcoxon analysis was not achievable (Figure 12). In contrast to GzmB[+] TIL, TIA-1^{+} TIL were

more abundantly found in tumours (pre-chemotherapy mean=2.420 TIA-1^{+} cells/100 tumour

cells, post-chemotherapy mean=6.281 TIA-1^{+} cells/100 tumour cells) and significantly increased

following chemotherapy (P=0.0132) (Figure 12 and Table 4). Furthermore, we assessed the

infiltration of CD103^{+} T cells, which have been identified as being important in recognizing

and killing tumour cells in cancer[279, 280, 281]. CD103^{+} T cells were frequently found in the tumour

epithelium (mean=7.931 CD103^{+} T cells/100 tumour cells) of pre-chemotherapy samples and

moderately increased following chemotherapy (post-chemotherapy mean=13.64 CD103^{+} T

cells/100 tumours, P=0.0432) (Figures 12 and Table 4).

Next, we investigated markers that have been associated with immune suppression,

including immunosuppressive FoxP3^{+} Tregs and the T cell exhaustion marker PD-1. Pre-

chemotherapy tumours had modest numbers of FoxP3^{+} Tregs (mean=1.547 FoxP3^{+} T cells/100

tumour cells), and did not significantly change following treatment (mean=2.623 FoxP3^{+} T

cells/100 tumour cells) (Figures 12 and Table 4). There were also modest numbers of PD-1^{+} TIL

in pre-chemotherapy tumours (mean=1.934 PD-1^{+} TIL/100 tumour cells), but there was a strong

increase in intraepithelial PD-1^{+} TIL in post-chemotherapy tumours (mean=6.071 PD-1^{+} TIL/100

tumour cells, P=0.014) (Figure 12 and Table 4). Thus, there was an overall increase in TIA-1^{+},

CD103^{+}, and PD-1^{+} TIL, but no overall change in FoxP3^{+} Tregs following chemotherapy.

Changes in CD68^{+} macrophages, CD56^{+} NK cells, and CD1a^{+} DCs were also explored.

CD68^{+} macrophages were frequently found in pre-tumour samples (mean=9.876 CD68^{+}

macrophages/100 tumour cells), but no significant change was found following chemotherapy

(mean=10.80 CD68^{+} macrophages/100 tumour cells) (Figure 12 and Table 4). In contrast,

very few CD56^{+} NK cells were observed in both pre- and post-chemotherapy tumours (pre-chemotherapy mean=0.3195 CD56^{+} NK cells/100 tumour cells, post-chemotherapy mean=0.2447 CD56^{+} cells/100 tumour cells) and their densities remained stable following treatment. Similarly, few CD1a^{+} DCs were present within the tumours (pre-chemotherapy mean=1.685 CD1a^{+} DCs/100 tumour cells, post-chemotherapy mean=1.550 CD1a^{+} DCs/100 tumour cells) and their densities did not alter either. Intraepithelial densities of these subsets did not change following chemotherapy. In addition, we analysed the tumour cell expression of MHC class I and II. Although MHC class I expression on tumours did not change with chemotherapy, we found MHC class II expression was increased ($P=0.0112$), as indicated by stronger staining intensity (Figure 13 and Table 4).
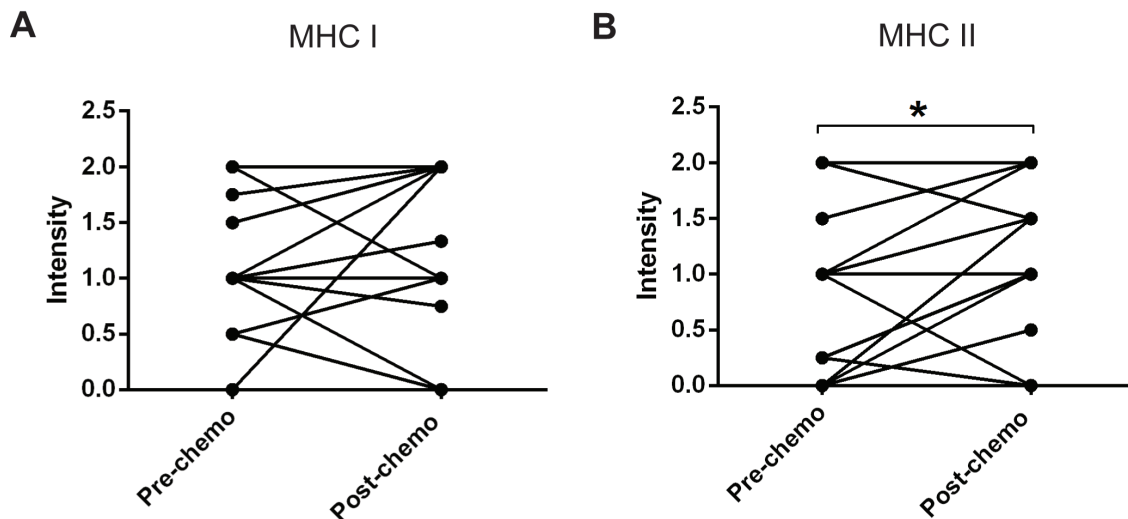
Figure 13. **MHC class I & II expression following carboplatin and paclitaxel treatment**. A comparison of MHC I and II expression of tumour cells between matched pre- and post-chemotherapy tumour samples (n=24) by immunohistochemistry. Expression was evaluated by staining intensity levels of 0 = negative, 1 = weak, 2 = strong. P values were calculated using the Wilcoxon matched pairs test with Pratt's method. Statistical significance * $P<0.05$, ** $P<0.01$, *** $P<0.001$.

Lastly, we assessed the absolute number of TIL in total, intraepithelial, and stromal cell count. After multiple testing and adjustment of the P values, we observed significant increases in total cell infiltration of GzmB[+] ($P=0.0449$)and TIA-1^{+} (P=0.0449) TIL (Appendix C). In contrast, there were no significant changes in absolute intraepithelial and stromal cell infiltrations in any of the markers.

Originally, we intended to analyze TIL from both pelvic and extra-pelvic sites because a potential caveat is that TIL can vary between pelvic and extra-pelvic sites, which could confound our results. However, comparisons of pelvic tumour samples alone would not allow for strong statistical analysis due to a limited number of available matching pre- and post-chemotherapy samples and variable tumour viability from pelvic sites (n=3). By contrast, within the 26 case cohort, 18 cases had matching pre- and post-chemotherapy tumour samples from extra-pelvic tumour sites. These patients showed similar trends to those seen in the larger cohort (Appendix D), thus, the observed changes in TIL patterns appeared to be independent of tumour sites.

3.3.3. Relationships between TIL subsets following chemotherapy

The increased TIL densities observed following chemotherapy led us to investigate about the relationships between TIL subsets. First, we evaluated PD-1$^+$ T cell population, since PD-1 represents an important immunomodulatory target. To evaluate this, we compared the proportion of PD-1$^+$ cells to CD3$^+$, CD8$^+$, and CD103$^+$ T cells present in pre- and post-chemotherapy samples. Despite an increase in PD-1$^+$ TIL following chemotherapy, we found the ratio of PD-1$^+$ cells to CD3$^+$ (P=0.2643), CD8$^+$ (P=0.7310), and CD103$^+$ (P=0.1266) T cells did not change (Figure 14). This indicated that the percentage of T cells that were PD-1$^+$ remained stable during treatment.
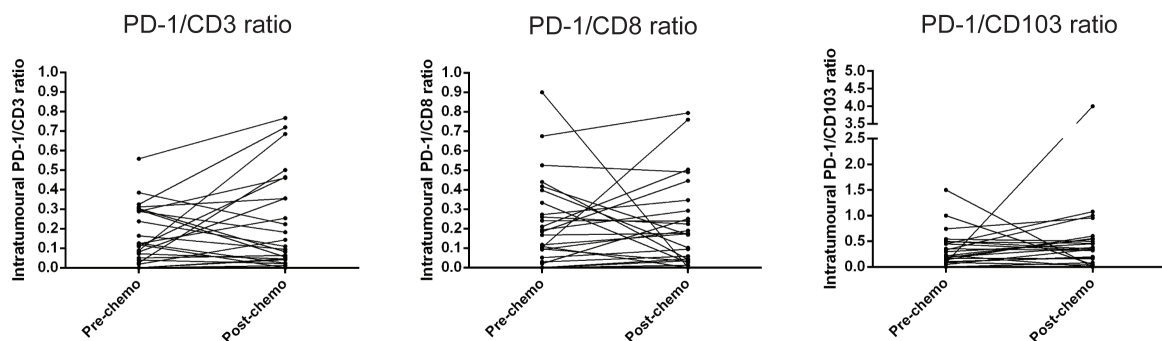
Figure 14. **Ratio of PD-1$^+$ to T$_{eff}$ cells following chemotherapy**. Proportion of intraepithelial PD-1$^+$ immue cell density to CD3$^+$, CD8$^+$, and CD103$^+$ T cells prior to and following chemotherapy. P values were calculated using the Wilcoxon matched pairs test with Pratt's method. Statistical significance * P<0.05, ** P<0.01, *** P<0.001.

Next, we explored whether increases in TIL following chemotherapy were *de novo* responses. In total, 11/26 (42%) patients showed an increase in B cell infiltration (Figure 15). Of these 11 patients, 7/26 (27%) were scored as negative for CD20$^+$ B cells at baseline yet were positive for CD20$^+$ B cells following chemotherapy. The other 4/26 patients (15%) were positive for CD20$^+$ B cells at baseline and showed a ≥2-fold increase after chemotherapy. As for T cells, 14/26 (54%) and 13/26 (50%) patients showed an increase in CD3$^+$ and CD8$^+$ TIL respectively. In all these patients, the observed increases reflected enhancement of pre-existing CD3$^+$ or CD8$^+$ TIL rather than the induction of *de novo* responses. Finally, we observed that the majority of TIA-1$^+$ and PD-1$^+$ TIL increases also had pre-existing TIL and found 9/26 (34.5%) patients and 10/25 (40%) patients showed a ≥2-fold increase in TIA-1$^+$ and PD-1$^+$ TIL densities following treatment respectively. Thus, with the exception of seven cases in which *de novo* CD20$^+$ B cell responses were seen, the observed increases in TIL reflected the enhancement of pre-existing TIL responses.

Finally, we assessed whether certain TIL subsets changed together following chemotherapy. Using hierarchical clustering, we found that T cell subsets changed together following treatment; specifically, changes in CD3$^+$ T cells were associated with similar changes in CD4$^+$, CD8$^+$ T cells, or both (Figure 16). Additionally, changes in CD8$^+$ T cells were associated with increases in CD103$^+$, TIA-1$^+$, and PD-1$^+$ TIL. A subset of those patients also had increase in CD20$^+$ B cells and CD68$^+$ macrophages. In contrast, changes in T cell infiltrations did not associate with changes in FoxP3$^+$ Treg infiltration following treatment. We also observed which TIL subsets were present together in pre- and post-chemotherapy tumours separately (Appendix E, F). We found that T cells, CD68$^+$ macrophages, and CD103$^+$ TIL were commonly present together in high abundances, while FoxP3$^+$ Tregs were found at moderate levels in both pre- and post-chemotherapy tumours. However, pre-chemotherapy tumours had low abundances of CD20$^+$ TIL and moderate abundances of TIA-1$^+$ and PD-1$^+$ TIL, while post-chemotherapy tumours exhibited higher levels of CD20$^+$, TIA-1$^+$, and PD-1$^+$ TIL. Thus, these results suggest post-chemotherapy tumours contain a network of immune infiltrates in the tumour

microenvironment different from pre-chemotherapy tumours.
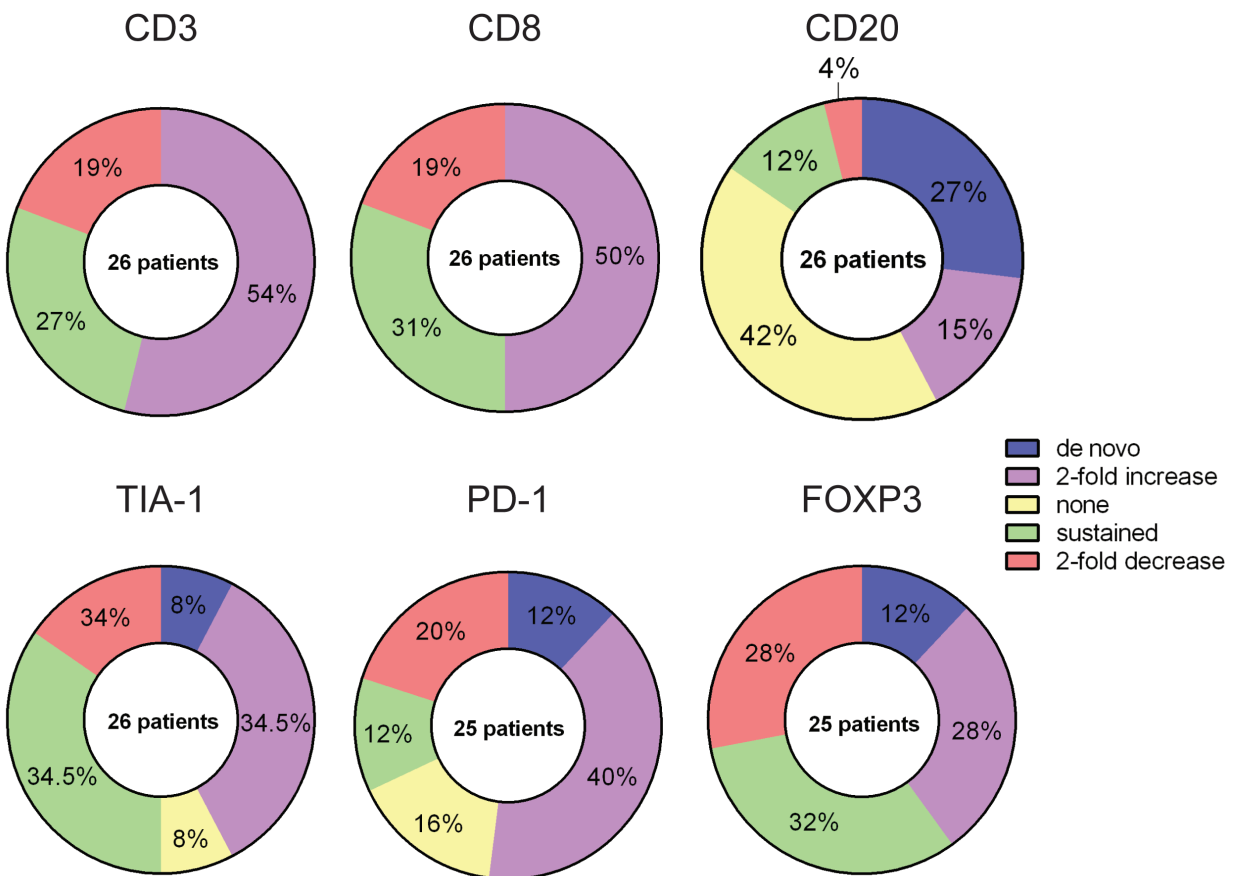
Figure 15. **Types of TIL responses following chemotherapy**. The types of lymphocyte infiltration following chemotherapy were defined as: *de novo* (no TIL before chemotherapy, but TIL present after chemotherapy), ≥2-fold TIL increase after chemotherapy, none (no TIL before and after chemotherapy), sustained (neither ≥2-fold TIL increase/decrease after chemotherapy), and ≥2-fold TIL decrease after chemotherapy. The percentage of cases showing each TIL response are reported for the matched cohort (n=26).
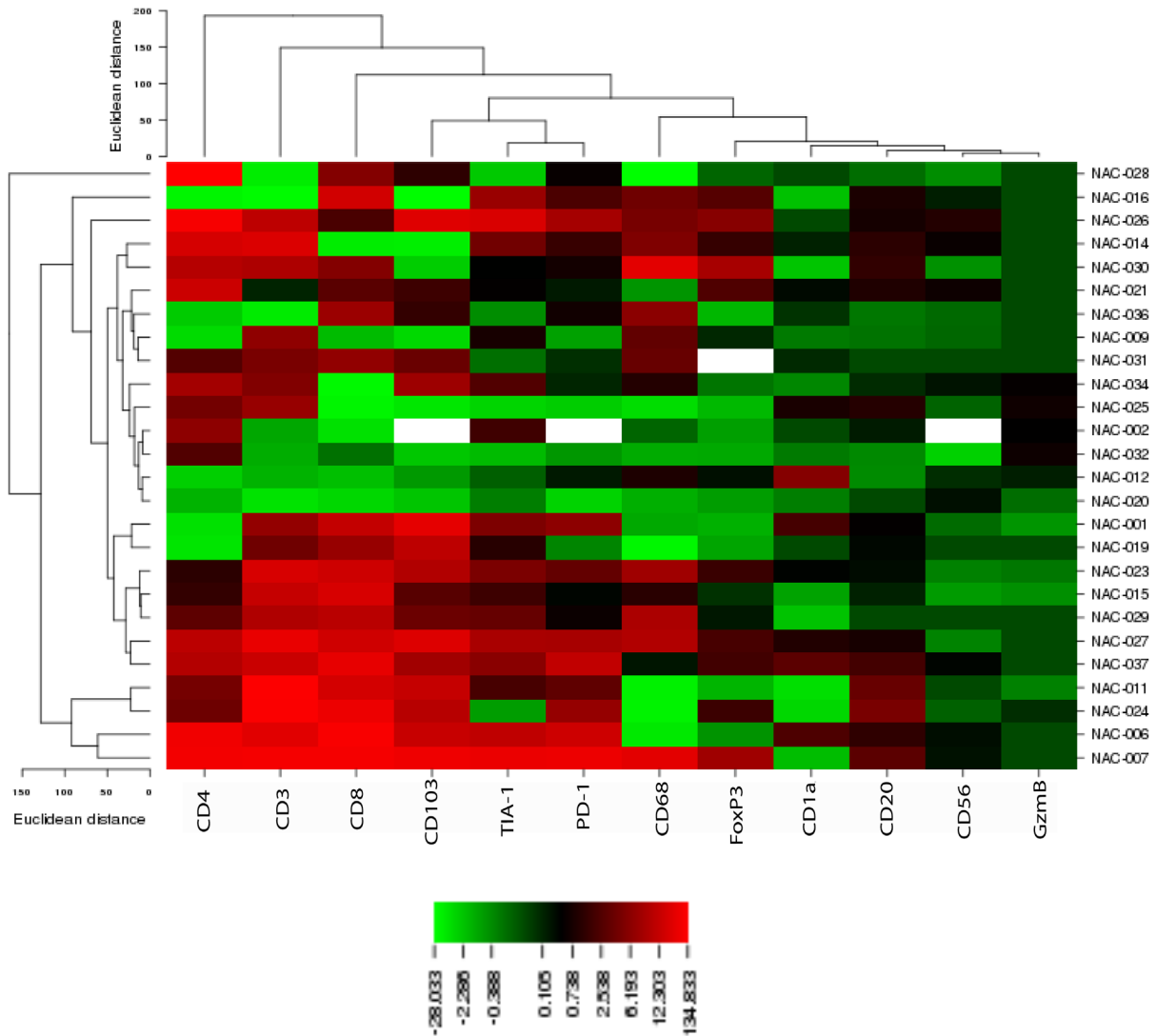
Figure 16. **Hierarchical clustering to assess associations between TIL subsets during chemotherapy**. A heatmap depicts the differences in TIL infiltration (difference= TIL density in post-chemotherapy – TIL density in pre-chemotherapy) in matching cohort (n=26). Unsupervised clustering algorithm with complete-linkage method and Euclidean distances was used. The rows represent patient cases and columns represent TIL markers indicating decreases (green) and increases (red). Missing data due to unavailable tissue are represented in white.

3.3.4. Increased T cell infiltration correlates with prolonged survival

Although our sample size was small, we assessed trends in survival associated with
TIL infiltration. A previous study from our lab found patients with high $CD8^+$ and $CD20^+$ TIL
experienced a prolonged survival, but no study to date has investigated if these correlations are
maintained following chemotherapy[164]. Thus, we investigated if TIL were correlated with overall
survival in post-chemotherapy tumours. We performed Kaplan-Meier analysis on intraepithelial
CD3, CD8, CD20, TIA-1, PD-1 and FoxP3 TIL densities in post-chemotherapy tumours from a
combination of the matching (n=26) and non-matching "post-chemotherapy only" (n=18) cohorts
(total n=44). For each marker, X-tile software was used to determine an optimal cut-off to
identify high and low TIL densities. None of the cut-offs generated were significant (Appendix
G), but survival analyses were performed nevertheless to observe trends. Patients with high
$CD8^+$ TIL densities (>2.18 $CD8^+$ cells/200 tumour cells) had prolonged survival compared
to patients with low $CD8^+$ TIL ($\leq$2.18 $CD8^+$ cells/100 tumour cells) (P=0.0297, HR=0.3288)
(Figure 17). The other TIL subsets were not statistically correlated with survival, although
patients with high $CD20^+$ TIL showed a trend toward increased survival (P=0.0731, HR=0.4925).
By contrast, patients with high $TIA-1^+$ TIL showed a trend toward decreased survival (P=0.0919,
HR=1.983). We also investigated whether changes in TIL densities following chemotherapy
correlated with overall survival, using the log-rank test in the matching cohort (n=26). Patients
with two-fold or greater increase in intraepithelial $CD8^+$ TIL density following chemotherapy
showed increased survival compared to patients who maintained a similar $CD8^+$ TIL density
(P=0.0148) (Appendix H). However, there was no difference in overall survival between
patients who had an increase in $CD8^+$ T cell density compared to those with decreased $CD8^+$ T
cell density. This suggests that this sample size (n=26) is not sufficient to distinguish between
patients with an increase, decrease, or sustained TIL infiltration.
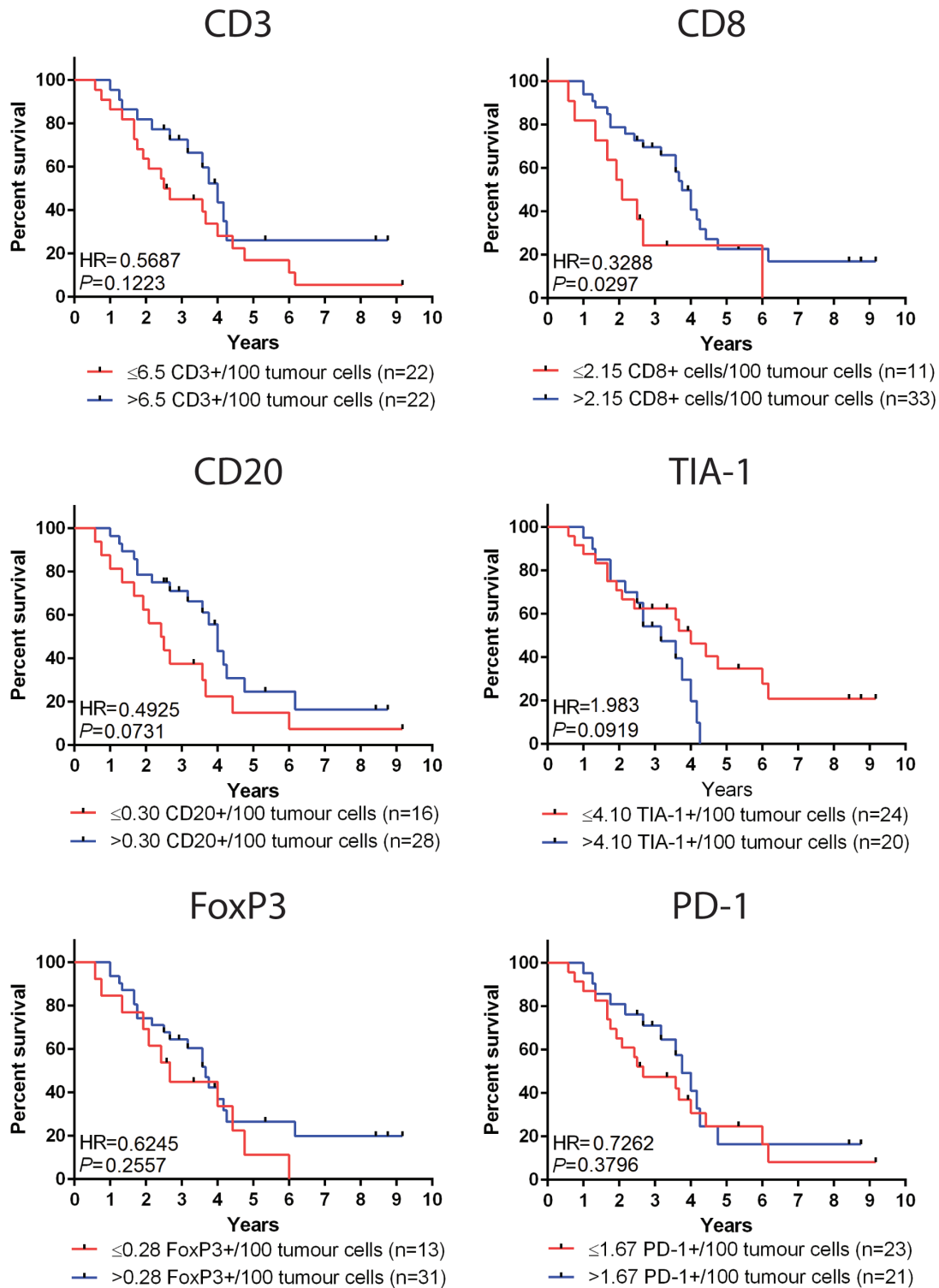
Figure 17. **Kaplan-Meier analysis of intraepithelial TIL density in post-chemotherapy tumours and overall survival**. Survival analysis includes the combined matched cohort (n=26) and non-matching cohort (n=18). For each graph, the blue line represents the cases with TIL density above the cut-off (number of positive cells/100 tumour cells), and the red line represents the cases with TIL density below or equal to the cut-off.

3.4. Discussion

Neoadjuvant chemotherapy has become increasingly popular for clinical management of advanced ovarian cancer. Currently, only a few studies have investigated the effects of chemotherapy on the immune response against cancer[262, 263, 264]. In this study, we observed that, as expected, post-chemotherapy tumours often displayed morphological changes attributable to carboplatin plus paclitaxel treatment. We found tumours exhibited higher frequency of fibrosis, histocytes or foamy macrophages, scatter clusters of tumour cells, and higher abundance of immune aggregates within the stroma, which is in agreement with other studies [282, 283, 284].

Some tumours exhibited a heightened response to chemotherapy as indicated by the presences of scattered, solitary, small tumour clusters, making inclusion of certain patient cases for analysis difficult. For these cases, whole sections were used for IHC because of minimal tissue, or they were entirely omitted from the experiment to avoid exhausting the viable tumour in the FFPE blocks. This is one of the factors contributing to the limited numbers in our patient cohort. Additionally, many of the neoadjuvant-treated patients had their pre-chemotherapy biopsies across BC and were unavailable to us for our matched comparison analysis. As neoadjuvant chemotherapy is becoming more prominent in clinic, there will be more available post-chemotherapy tumour tissue from neoadjuvant-treated patients available for future studies.

Genomic instability and high intratumoural heterogeneity is common in HGSC and a number of different tumour cell clones have been found within the same patients' tumours[285]. To account for intra-heterogeneity of TIL subsets, we opted to assess TIL from both pelvic and extra-pelvic sites whenever tumour was available. Interestingly, a study to be published in the near future from our lab and Sohrab Shah's suggest that despite high heterogeneity in tumour clones exist from one tumour site to another within a single HGSC patient, however, the immune infiltrates are remarkably consistent from one tumour site to another. Therefore, despite the low number of cases in our cohort to study TIL in pelvic and extra-pelvic sites separately, our approach in studying changes in TIL following treatment from all tumour sites remains a valid approach as seen from the similar results in our 18 patient case sub-cohort (pre- and post-

chemotherapy extra-pelvic tumours) .

We observed an increase in intraepithelial T cells following chemotherapy, while Treg infiltration remained unchanged. This is in concordance with the increase in CD4^{+} and CD8^{+} T cells following chemotherapy and unchanged FoxP3^{+} infiltration reported by Polcher et al[264]. While Polcher et al reported the mean absolute intraepithelial TIL counts, we did not find significant results within our mean absolute intraepithelial CD4^{+}, CD8^{+}, and FoxP^{+} TIL counts following treatment. This may be due to the high level of heterogeneity in respect to the abundance of viable tumour cells. We, therefore, quantified intraepithelial TIL density to standardize our cell counts. With this correction, our intraepithelial density results confirmed Polcher et al's observations. Studies in breast cancer have reported similar results of increasing TIL following exposure to chemotherapy agents, such as anthracycline and paclitaxel[261, 262, 286]. One study involving esophageal squamous cell carcinoma found 5-fluorouracil plus cisplatin induced CD4^{+} and CD8^{+} T cell infiltration into the tumour epithelium[287]. In contrast to effector TIL, there are mixed results regarding intraepithelial FoxP3^{+} infiltration; both decreased and unchanged intraepithelial FoxP3^{+} TIL have been reported following anthracycline treatment[262, 263, 286]. Furthermore, in contrast to Polcher et al's study, we did not observe an increase in GzmB[+] infiltration[264]. In fact, there was a lack of GzmB^{+} cells present in both pre- and post-chemotherapy tumours. Instead, we observed an increase in TIL expressing TIA-1 (a cytolytic granule-associated RNA-binding protein), following chemotherapy. Ours is the first study to report an effect of chemotherapy on this specific cytotoxic-associated molecule.

There is emerging evidence which states that chemotherapeutic agents can induce anti-tumour immune response[240]. Certain chemotherapeutic agents cause immunogenic cell death (ICD), such as HMGB1, calreticulin, and ATP, to be released from apoptotic tumour cells, and stimulate DCs to present new tumour antigens and activate T cells. This leads to an IFN-γ mediated immune response involving cytotoxic and γδT cells infiltrating the remaining tumour to eradicate the therapy resistant tumour cells. In murine models, ATP released from dying cancer cells exposed to anthracycline stimulated CD11c^{+} CD11b^{+}Ly6C^{hi} cells, characteristic of DC cells,

to present tumour antigens to T cells for cytotoxic eradication of tumour cells[245]. However, using CD1a as a marker for immature DC, we did not see an increase in immature DC cells. This could be due to the fact that the post-chemotherapy tumours in our neoadjuvant chemotherapy cohort were surgically removed following 3 weeks of the last carboplatin plus paclitaxel administration, while the murine studies observed infiltration of DC within hour or days of anthracycline chemotherapy. Additionally, we did not observe a change in CD68^{+} macrophage abundance following chemotherapy, which is in contrast to studies observing macrophage infiltration following anthracycline chemotherapy in neoadjuvant breast cancer patients[286, 288]. A possible explanation is that one would expect to see an increase in macrophages infiltrating the tumour immediately following chemotherapy to clear dead tumour cells; however, this cohort's post-chemotherapy tumours were resected 3 weeks after the last dose of chemotherapy. Thus, even though the mechanisms for induction of immune infiltration by various chemotherapies have not been fully elucidated, our study and others across different cancer types consistently observe increased T cell infiltration following chemotherapy.

The anti-tumour immune response does not only involve T cells. Our previous study has found that HGSC patients with CD20^{+} TIL (B cells) in addition to CD8^{+} TIL have a better prognosis than patients with CD8^{+} TIL alone[164]. Here, we showed for the first time that chemotherapy recruits CD20^{+} B cell infiltration into tumour epithelium. Very little has been reported regarding the relationship between chemotherapy and B cells. CD20^{+} B cells can facilitate T cells during tumour eradication by producing autoantibodies against newly exposed tumour antigens, acting as antigen presenting cells to T cells, and directly killing tumour cells[289]. On the other hand, a reduction in B cells has been reported in a few studies following chemotherapy treatment along with a decrease in CD4^{+} T cells[286, 288]. A recent study found regulatory B cells and macrophages cooperate to inhibit the recruitment of T cells into the tumour during the course of chemotherapy[152]. This study found macrophages that were isolated from anti-CD20 and cisplatin treated non-squamous cell tumours in mice recruited the most CD8^{+} T cells compared to macrophages isolated from the control group[152]. These mixed results

in various cancers and tumour models regarding infiltrating B cells indicate a need for more research in understanding the role of different B cell subsets in tumour immunity.

PD-1, a marker for T cell activation or exhaustion, has been a prominent research topic because of anti-PD-1 and PD-1 blockades in tumour regression seen in clinical trials. Here, we assessed the infiltration of PD-1^{+} cells and found PD-1^{+} cells significantly increased within the tumour epithelium following chemotherapy. However, we found that the percentage of T cells that were PD-1^{+} remained the same in both pre- and post-chemotherapy tumours, suggesting that tumours exposed to chemotherapy attract both effector CD8^{+} T cells and exhausted PD-1^{+} TIL, with no preference for one over the other. Studies have reported a immunosuppressive role of PD-1 on tumour reactive T cells[221, 223]. One study found tumour antigen-specific T cells reactive against a cancer-testis antigen in ovarian cancer, NY-ESO-1, that were PD-1^{+} and exhibited impaired IFN-γ and TNF-α production, suggestive of T cell exhaustion[223]. Similarly, studies in other cancer types have found cancer-type specific TIL harboured a higher frequency of PD-1^{+} and exhibited a lack of responsiveness from stimulation[220, 290, 291]. It has been observed that PD-1^{+} expression increases on tumour-reactive T cells as the stage of the disease progressed[292, 293]. In contrast to a majority of the literature, a recent study suggested PD-1 could be a marker for tumour reactive T cells. In this study, T cells that were PD-1^{+} in addition to other exhaustion markers, such as lymphocyte-activation gene 3 (LAG-3) and T cell immunoglobulin and mucin domain 3 (TIM-3), were found specifically in the tumour epithelium and were able to elicit a response when stimulated with autologous tumour[221]. CD8^{+} PD-1^{+} T cells, isolated from melanoma tumours, were able to lyse autologous tumour cells and had higher levels of IFN-γ released compared to CD8^{+}PD-1^{-} T cells. Collectively, these studies suggest antigen-specific T cells frequently express PD-1, although their ability to kill tumour warrants further investigation.

In conclusion, TIL represent a dynamic cellular network that undergoes changes in certain immune cell populations following chemotherapy. This body of work has shown that tumour-specific T cells that harbour cytotoxic potential, such as TIA-1, are recruited following treatment. Besides effector T cell recruitment, B cells are also recruited possibly through the

release of newly exposed antigens from ICD. Future work elucidating the function of tumour-infiltrating B cells and their effect on effector CD8^{+} T cells is needed. Despite the increase in cytotoxic T cells following chemotherapy, these tumour-reactive T cells frequently express PD-1 which may render them dysfunctional. Future experiments using a combination of markers such as PD-1, LAG3, and TIM-3 to characterize the state of exhaustion of intraepithelial T cells will be important in providing evidence for the use of PD-1 blockade in HGSC treatment. If these T cells are exhausted, one potential therapy would be to administer PD-1 blockade following first-line chemotherapy treatment to patients to ensure an active anti-tumour immune response, and ultimately immunosurveillance, would be sustained, thus potentially reducing recurrences. Another alternative treatment plan would be to administer a combination of PD-1 blockade and tumour vaccines to patients following neoadjuvant chemotherapy in those who had suboptimally debulked tumours at interval debulking. This body of work has provided preliminary results that multiple TIL subsets are changed during chemotherapy and elucidating the immunological events that occur is critical for designing novel treatments and warrants further investigation.

4. Conclusion and future directions

4.1 Summary and perspectives

The aim of this thesis was to identify the composition and phenotypes of intraepithelial immune infiltrates in HGSC. By deciphering the changes in TIL composition that occur during chemotherapy, we hope to design immunotherapies that specifically enhance effector T cell activity and relieve immunosuppression in order to eradicate residual tumour deposits, and thereby reduce recurrences.

In Chapter 2, the primary objective was to investigate the prevalence of intraepithelial cytotoxic T cells (CTLs), identified as CD8+ GzmB+ T cells, and their association with the presence of cleaved caspase-3+ apoptotic cells in primary HGSC tumours. Given that CD8+ T cells are associated with improved survival, we hypothesized that the majority of CD8+ T cells would possess a cytotoxic phenotype and contain GzmB granules. Contrary to our predictions, we found that the majority of the CD8+ T cells do not possess this classical GzmB+ phenotype, indicating cytotoxic CD8+ GzmB+ T cells are low in numbers in primary HGSC tumours. One explanation could be that some CD8+ GzmB+ T cells may have released GzmB to tumour cells, resulting in a GzmB- appearance by IHC. To assess this, IHC staining of CD107a (degranulation marker) could be used to assess the prevalence of CTLs that have released their cytotoxic granules[294]. Besides the release of GzmB, T cells have alternative mechanisms to induce apoptosis, including cytotoxic molecules such as granzyme A, K, and granulysin, and the direct binding of FasL on CTLs to Fas on target cells[295]. More recently, TIA-1, a cytotoxic granule-associated RNA binding protein, was found to be prominent in intraepithelial TIL and associated with good prognosis in colon and ovarian cancers[49, 143]. The mechanism by which TIA-1 induces cytotoxicity is less understood, but TIA-1 has been shown to activate cell death by fragmenting DNA[136, 137]. Perhaps CTLs induce apoptosis in tumour cells by multiple mechanisms, such as granzymes, TIA-1, and FasL/Fas pathway, to elicit a T-cell mediated anti-tumour response.

In Chapter 3, we investigated the immune composition before and after carboplatin plus paclitaxel chemotherapy in neoadjuvant-treated HGSC patients. Here, we observed an

increased density in T cells, B cells, TIA-1^{+} cells, and PD-1^{+} cells following chemotherapy, while GzmB^{+} cells, FoxP3^{+} Tregs, and CD68^{+} macrophage infiltration remained unchanged (Figure 18). These results suggest that there are changes that occur within the tumour microenvironment which result in the tumour to be more susceptible to TIL infiltration. Although all experiments were performed in neoadjuvant-treated patients, who generally have more advanced stage disease, we can expect that similar events, including immunogenic cell death (ICD), tumour microenvironment changes, and increased TIL infiltration, occur in adjuvant patients since they receive the same chemotherapeutic drugs. In previous clinical studies, high densities of intraepithelial TIL is correlated with increased survival in primary tumours of HGSC patients, indicating that intraepithelial TIL is an independent prognosis factor even before chemotherapy[48, 49, 224, 296]. In our study, we showed that following chemotherapy (in the absence of immunomodulatory therapies), there was an increase in intraepithelial TIL. This is encouraging, as HGSC patients may gain a more active anti-tumour immune response from standard treatment, an effect that could potentially be enhanced by immunotherapy. Given that our results showed increases in potentially exhausted PD-1^{+} T cells, a possible combination therapy would be to administer anti-PD-1 immunotherapy, which has recently gained FDA approval (Merck's Pembrolizumab), to patients following carboplatin plus paclitaxel chemotherapy to relieve T cell exhaustion and enhance the activity of intraepithelial CD8^{+} T cells.
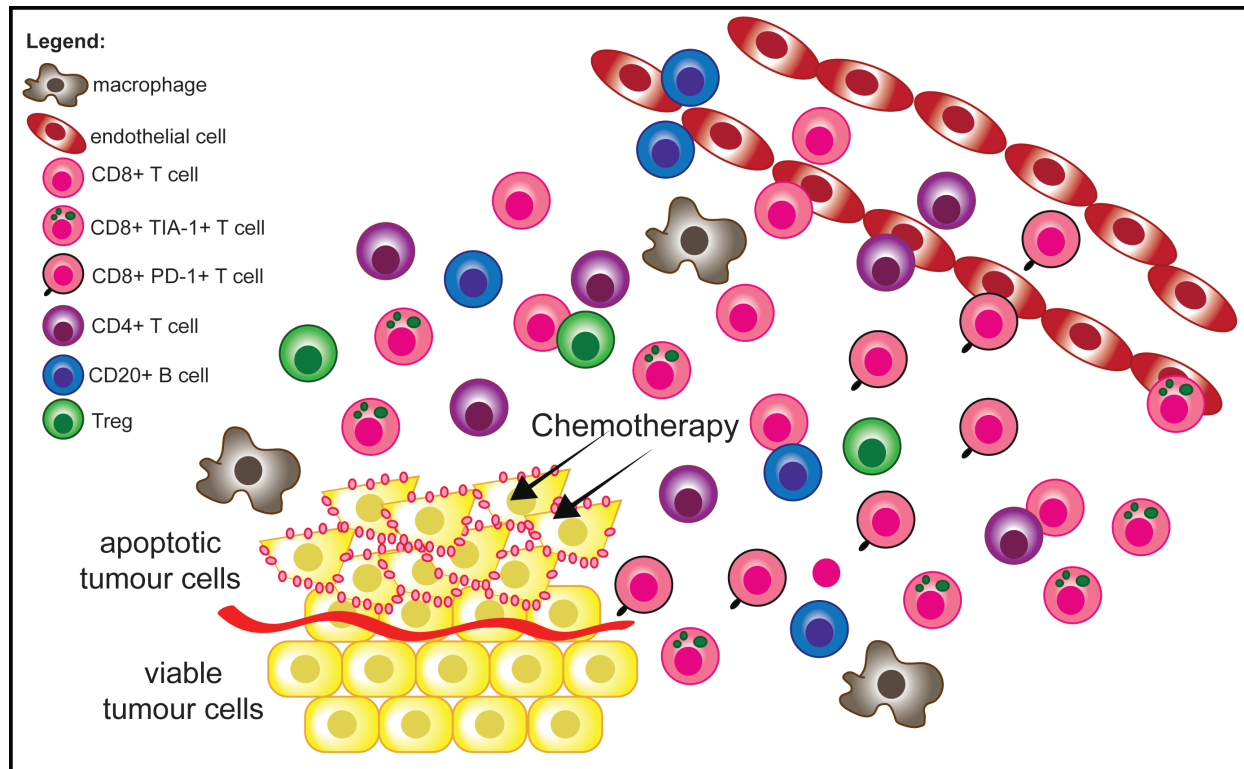
Figure 18. Recruitment of TIL following chemotherapy in HGSC. Chemotherapy recruits T cells (CD4 and CD8) and CD20+ B cells into the tumour epithelium. Tumours exposed to chemotherapy also increases in cytotoxic CD8+ TIA-1+ T cells and PD-1+ T cells following treatment. However, immunosuppressive cells such as Tregs and macrophages remain unchanged in their infiltration.

4.2. Future directions

4.2.1. Association of neoadjuvant TIL with survival

Many studies have correlated TIL with survival in HGSC, yet few have investigated whether this association still stands following standard treatment[49, 50, 51, 269]. A few studies have investigated whether TIL can predict tumour responses to chemotherapy, such as the correlation of TIL and anthracycline responses in breast cancer[265, 266, 267]. But only one has explored whether TIL are associated with response to chemotherapy in HGSC[268]. It is critical to determine which immune subsets are associated with survival in tumours that have been exposed to chemotherapy. From this, we can design immunotherapies that promote immunosurveillance at the time of remission. For example, patients who have a strong CD8+ T cell response might benefit from cancer vaccines, whereas patients who have high infiltration of Tregs and PD-1+ T cells may

85

benefit from immune modulatory therapies such as anti-CTLA-4 or anti-PD-1.

Our lab is currently investigating whether TIL patterns in chemotherapy-treated tumours are associated with survival in HGSC patients. We have assembled three HGSC cohorts to investigate this question. In addition to the cohort described here, we are analysing 40 cases of neoadjuvant-treated tumours from Princess Margaret Hospital in Toronto. We will assess the prognostic significance of the markers studied here, including CD3, CD8, CD20, TIA-1, PD-1, and FoxP3. This will be the first study to extend findings on CD20, TIA-1, and PD-1 to survival analysis in neoadjuvant-treated patients.

4.2.2. Characterizing the functional status of PD-1^{+} T cells following chemotherapy

The results presented here indicate the need for further study regarding the functional status of TIL following chemotherapy. Experiments investigating PD-1 mechanisms in HGSC could provide justification for PD-1 blockade in ovarian cancer treatment. The increase in PD-1^{+} TIL following chemotherapy in our study raises the question whether the majority of cytotoxic T cells, such as CD8^{+} TIA-1^{+} T cells, are exhausted, although PD-1 can also serve as a marker for tumour-reactive T cells[221, 223]. The first possibility is that PD-1 may be a marker for tumour-specific CTLs, whereby, it can be used in future clinical settings to identify patients who could benefit from immunotherapy. Although this concept is still in its infancy, it has been recently demonstrated by the Rosenberg and Odunsi groups[221, 223], and more studies are still needed to confirm and validate its specificity and sensitivity as a biomarker. The second possibility is that if PD-1 is up-regulated on TIA-1^{+} T cells, this would imply that exhausted CTLs have the potential to initiate an immune response against tumours but are unable to do so because of active immunosuppression from tumours with up-regulated PDL1/2 expression. If TIL are indeed immunosuppressed and rendered dysfunctional, therapies such as anti-PD-1 (Merck's Pembrolizumab) would be appropriate for restoring a robust anti-tumour immune response. Additionally, it would also provide compelling evidence for combining PD-1 blockade with chemotherapy and other immunotherapy regimens, such as tumour vaccines. To address if CTLs such as CD8^{+} TIA-1^{+} T cells are exhausted, multi-colour immunohistochemistry using a

triple-coloured stain observing CD8, TIA-1, and PD-1 markers would identify the proportion of exhausted intraepithelial CTLs present in the tumour. In future studies where frozen tumour tissue is available, T cells can be isolated and the functional status of the intraepithelial CD8^{+} TIA-1^{+} PD-1^{+} CTLs prior to and following chemotherapy can be assessed using flow cytometry with CD103 (intraepithelial marker), and additional exhaustion markers (such as LAG-3 and TIM-3) to differentiate transiently and terminally exhausted T cells[221, 297]. This flow cytometry data could provide convincing evidence that exhausted CTLs found within tumours are exhausted after chemotherapy.   Additional experiments using isolated CD8^{+} TIA-1^{+}PD-1^{+} CTLs co-cultured with autologous tumour would also allow for the assessment of their cell lysis activity and IFN-γ production as indicators for anti-tumour response[221].

The assessment of PD-L1 expression dynamics in tumours before and after chemotherapy is also important. IHC on FFPE tissue could provide further understanding of the association between PD-1^{+} TIL and PD-L1 expression following treatment. A caveat of using IHC to analyse PD-L1 expression is the lack of a reliable antibody against PD-L1. Currently, the antibody providing the best staining is produced in Liepeng Chen's laboratory and not available commercially[219, 298]. Together, these experiments can provide better understanding of the PD-1 mechanism in HGSC, as well as justification for using PD-1 blockade in ovarian cancer treatment.

4.2.3. Chemokines and their involvement in attraction of TIL following chemotherapy

Chemokines are signalling proteins that attract immune cells and other cells. The increased TIL density following chemotherapy suggests that chemoattractants may be released during the course of treatment. From a biological perspective, it would be interesting to elucidate the predominant chemokines that are released during the course of chemotherapy as well as their cellular source. This could facilitate the development of therapies that enhance the production of chemokines and attract TIL to tumours. In an *in vivo* study looking at murine melanoma tumours, temozomide was found to induce CD3^{+} T cell infiltration as well as enhanced expression of CCL5, CXCL9, and CXCL10 chemokines[299]. CCL5 is a chemokine

that attracts cells of the innate immune system, such as NK cells and MDSC, whereas CXCL9 and CXCL10 attract CTLs[300, 301]. The authors of this study also performed global transcriptome analysis of tumours from melanoma patients who received dacarbazine therapy, and found increased expression of CCL5, CXCL9, and CXCL10 in chemotherapy-sensitive tumours[299]. In our matching neoadjuvant cohort, we can investigate the change in gene expression of these chemokines in FFPE tissue using NanoString technology[302], a recently developed technology to study gene expression from mRNA extracted from FFPE tissue. Based on the findings from our IHC data, we hypothesize that there will be an up-regulation of CXCL9, CXCL10, as well as CXCL13, which is a B cell chemoattractant, in post-chemotherapy tumours versus pre-chemotherapy samples.

4.2.4. Potential combination therapies

With advances in genomics and molecular biology, new discoveries in gene mutations, tumour-antigens, and further elucidation of immunostimulatory and immunosuppressive factors in the tumour microenvironment, we are gaining a broader picture of the different players involved in cancer progression and regression. For example, the PARP inhibitor olaparib can effectively induce cell death in tumours by inhibiting the remaining DNA repair pathways in *BRCA* deficient tumours[114, 115]. Interestingly, tumours with *BRCA* mutations are correlated with increased TIL infiltration[48]. Moreover, chemotherapy has been shown to increase PD-1^{+} TIL within the tumour, indicating a possible future treatment plan would involve the combination of PARP inhibitors with anti-PD-1 therapies to effectively target the DNA repair system as well as relieving T cell exhaustion. More research is still needed to target these tumours, leaving room for immunotherapy development.

4.3. Conclusion

The integration of immunotherapies into standard treatment for HGSC remains a challenge. One must consider the state of the tumours and their sensitivity towards immune attack, the active immunosuppression within the tumour microenvironment, the modulation of

the immune system and the tumour microenvironment by chemotherapy, and the tumour reactive capability of T and B cells post-treatment.

This is the first study to investigate the cytotoxic phenotype of intraepithelial CTLs and the effects of neoadjuvant chemotherapy on the immune composition in HGSC. Additionally, we are the first to report that T cells are not the only players that are involved in the immune infiltration into the tumour epithelium, but intraepithelial B cells, cytotoxic TIA-1$^+$, and PD-1$^+$ immune cells are also key players in intraepithelial immune infiltration that are influenced by chemotherapy in HGSC.

Bibliography

1.   Committee CCSsA. Canadian Cancer Statistics 2014. In: Statistics C, editor. Toronto: Canadian Cancer Society; 2014.

2.   Kobel M, Kalloger SE, Huntsman DG, Santos JL, Swenerton KD, Seidman JD, *et al.* Differences in tumor type in low-stage versus high-stage ovarian carcinomas. *International journal of gynecological pathology : official journal of the International Society of Gynecological Pathologists* 2010, **29**(3)**:** 203-211.

3.   Horner MJ RL, Krapcho M, Neyman N, Aminou R, Howlader N, Altekruse SF, Feuer EJ, Huang L, Mariotto A, Miller BA, Lewis DR, Eisner MP, Stinchcomb DG, Edwards BK SEER Cancer Statistics Review, 1975-2006. 2009 [cited 2009]Available from: http://seer.cancer.gov/csr/1975_2006/

4.   Seidman JD, Horkayne-Szakaly I, Haiba M, Boice CR, Kurman RJ, Ronnett BM. The histologic type and stage distribution of ovarian carcinomas of surface epithelial origin. *International journal of gynecological pathology : official journal of the International Society of Gynecological Pathologists* 2004, **23**(1)**:** 41-44.

5.   Gilks CB, Prat J. Ovarian carcinoma pathology and genetics: recent advances. *Human pathology* 2009, **40**(9)**:** 1213-1223.

6.   Malpica A, Deavers MT, Lu K, Bodurka DC, Atkinson EN, Gershenson DM, *et al.* Grading ovarian serous carcinoma using a two-tier system. *The American journal of surgical pathology* 2004, **28**(4)**:** 496-504.

7.   Malpica A, Deavers MT, Tornos C, Kurman RJ, Soslow R, Seidman JD, *et al.* Interobserver and intraobserver variability of a two-tier system for grading ovarian serous carcinoma. *The American journal of surgical pathology* 2007, **31**(8)**:** 1168-1174.

8.   Integrated genomic analyses of ovarian carcinoma. *Nature* 2011, **474**(7353)**:** 609-615.

9.   Heintz AP, Odicino F, Maisonneuve P, Beller U, Benedet JL, Creasman WT, *et al.* Carcinoma of the ovary. *International journal of gynaecology and obstetrics: the official organ of the International Federation of Gynaecology and Obstetrics* 2003, **83 Suppl 1:** 135-166.

10.   Cannistra SA. Cancer of the ovary. *The New England journal of medicine* 2004, **351**(24)**:** 2519-2529.

11.   Sakamoto A, Sasaki H, Furusato M, Suzuki M, Hirai Y, Tsugane S, *et al.* Observer disagreement in histological classification of ovarian tumors in Japan. *Gynecologic oncology* 1994, **54**(1)**:** 54-58.

12.	Gurung A, Hung T, Morin J, Gilks CB. Molecular abnormalities in ovarian carcinoma: clinical, morphological and therapeutic correlates. *Histopathology* 2013, **62**(1)**:** 59-70.

13.	Han G, Gilks CB, Leung S, Ewanowich CA, Irving JA, Longacre TA*, et al.* Mixed ovarian epithelial carcinomas with clear cell and serous components are variants of high-grade serous carcinoma: an interobserver correlative and immunohistochemical study of 32 cases. *The American journal of surgical pathology* 2008, **32**(7)**:** 955-964.

14.	Sugiyama T, Kamura T, Kigawa J, Terakawa N, Kikuchi Y, Kita T*, et al.* Clinical characteristics of clear cell carcinoma of the ovary: a distinct histologic type with poor prognosis and resistance to platinum-based chemotherapy. *Cancer* 2000, **88**(11)**:** 2584-2589.

15.	Komiyama S, Aoki D, Tominaga E, Susumu N, Udagawa Y, Nozawa S. Prognosis of Japanese patients with ovarian clear cell carcinoma associated with pelvic endometriosis: clinicopathologic evaluation. *Gynecologic oncology* 1999, **72**(3)**:** 342-346.

16.	Ogawa S, Kaku T, Amada S, Kobayashi H, Hirakawa T, Ariyoshi K*, et al.* Ovarian endometriosis associated with ovarian carcinoma: a clinicopathological and immunohistochemical study. *Gynecologic oncology* 2000, **77**(2)**:** 298-304.

17.	Orezzoli JP, Russell AH, Oliva E, Del Carmen MG, Eichhorn J, Fuller AF. Prognostic implication of endometriosis in clear cell carcinoma of the ovary. *Gynecologic oncology* 2008, **110**(3)**:** 336-344.

18.	Jones S, Wang TL, Shih Ie M, Mao TL, Nakayama K, Roden R*, et al.* Frequent mutations of chromatin remodeling gene ARID1A in ovarian clear cell carcinoma. *Science (New York, NY)* 2010, **330**(6001)**:** 228-231.

19.	Wiegand KC, Shah SP, Al-Agha OM, Zhao Y, Tse K, Zeng T*, et al.* ARID1A mutations in endometriosis-associated ovarian carcinomas. *The New England journal of medicine* 2010, **363**(16)**:** 1532-1543.

20.	Yamamoto S, Tsuda H, Takano M, Iwaya K, Tamai S, Matsubara O. PIK3CA mutation is an early event in the development of endometriosis-associated ovarian clear cell adenocarcinoma. *The Journal of pathology* 2011, **225**(2)**:** 189-194.

21.	Stany MP, Vathipadiekal V, Ozbun L, Stone RL, Mok SC, Xue H*, et al.* Identification of novel therapeutic targets in microdissected clear cell ovarian cancers. *PloS one* 2011, **6**(7)**:** e21121.

22.	Anglesio MS, George J, Kulbe H, Friedlander M, Rischin D, Lemech C*, et al.* IL6-STAT3-HIF signaling and therapeutic response to the angiogenesis inhibitor sunitinib in ovarian clear cell cancer. *Clinical cancer research : an official journal of the American Association for Cancer Research* 2011, **17**(8)**:** 2538-2548.

23.   McMeekin DS, Burger RA, Manetta A, DiSaia P, Berman ML. Endometrioid adenocarcinoma of the ovary and its relationship to endometriosis. *Gynecologic oncology* 1995, **59**(1)**:** 81-86.

24.   Falkenberry SS, Steinhoff MM, Gordinier M, Rappoport S, Gajewski W, Granai CO. Synchronous endometrioid tumors of the ovary and endometrium. A clinicopathologic study of 22 cases. *The Journal of reproductive medicine* 1996, **41**(10)**:** 713-718.

25.   Jimbo H, Yoshikawa H, Onda T, Yasugi T, Sakamoto A, Taketani Y. Prevalence of ovarian endometriosis in epithelial ovarian cancer. *International journal of gynaecology and obstetrics: the official organ of the International Federation of Gynaecology and Obstetrics* 1997, **59**(3)**:** 245-250.

26.   Kobel M, Kalloger SE, Baker PM, Ewanowich CA, Arseneau J, Zherebitskiy V*, et al.* Diagnosis of ovarian carcinoma cell type is highly reproducible: a transcanadian study. *The American journal of surgical pathology* 2010, **34**(7)**:** 984-993.

27.   D'Angelo E, Prat J. Classification of ovarian carcinomas based on pathology and molecular genetics. *Clinical & translational oncology : official publication of the Federation of Spanish Oncology Societies and of the National Cancer Institute of Mexico* 2010, **12**(12)**:** 783-787.

28.   McConechy MK, Ding J, Senz J, Yang W, Melnyk N, Tone AA*, et al.* Ovarian and endometrial endometrioid carcinomas have distinct CTNNB1 and PTEN mutation profiles. *Modern pathology : an official journal of the United States and Canadian Academy of Pathology, Inc* 2014, **27**(1)**:** 128-134.

29.   Catasus L, Bussaglia E, Rodrguez I, Gallardo A, Pons C, Irving JA*, et al.* Molecular genetic alterations in endometrioid carcinomas of the ovary: similar frequency of beta-catenin abnormalities but lower rate of microsatellite instability and PTEN alterations than in uterine endometrioid carcinomas. *Human pathology* 2004, **35**(11)**:** 1360-1368.

30.   Moreno-Bueno G, Gamallo C, Perez-Gallego L, de Mora JC, Suarez A, Palacios J. beta-Catenin expression pattern, beta-catenin gene mutations, and microsatellite instability in endometrioid ovarian carcinomas and synchronous endometrial carcinomas. *Diagnostic molecular pathology : the American journal of surgical pathology, part B* 2001, **10**(2)**:** 116-122.

31.   McConechy MK, Anglesio MS, Kalloger SE, Yang W, Senz J, Chow C*, et al.* Subtype-specific mutation of PPP2R1A in endometrial and ovarian carcinomas. *The Journal of pathology* 2011, **223**(5)**:** 567-573.

32.   Shih Ie M, Panuganti PK, Kuo KT, Mao TL, Kuhn E, Jones S*, et al.* Somatic mutations of PPP2R1A in ovarian and uterine carcinomas. *The American journal of pathology* 2011, **178**(4)**:** 1442-1447.

33.   Wiegand KC, Hennessy BT, Leung S, Wang Y, Ju Z, McGahren M, *et al.* A functional proteogenomic analysis of endometrioid and clear cell carcinomas using reverse phase protein array and mutation analysis: protein expression is histotype-specific and loss of ARID1A/BAF250a is associated with AKT phosphorylation. *BMC cancer* 2014, **14:** 120.

34.   McConechy MK, Ding J, Cheang MC, Wiegand KC, Senz J, Tone AA, *et al.* Use of mutation profiles to refine the classification of endometrial carcinomas. *The Journal of pathology* 2012, **228**(1)**:** 20-30.

35.   Kobel M, Kalloger SE, Santos JL, Huntsman DG, Gilks CB, Swenerton KD. Tumor type and substage predict survival in stage I and II ovarian carcinoma: insights and implications. *Gynecologic oncology* 2010, **116**(1)**:** 50-56.

36.   Cuatrecasas M, Villanueva A, Matias-Guiu X, Prat J. K-ras mutations in mucinous ovarian tumors: a clinicopathologic and molecular study of 95 cases. *Cancer* 1997, **79**(8)**:** 1581-1586.

37.   Mayr D, Hirschmann A, Lohrs U, Diebold J. KRAS and BRAF mutations in ovarian tumors: a comprehensive study of invasive carcinomas, borderline tumors and extraovarian implants. *Gynecologic oncology* 2006, **103**(3)**:** 883-887.

38.   Gemignani ML, Schlaerth AC, Bogomolniy F, Barakat RR, Lin O, Soslow R, *et al.* Role of KRAS and BRAF gene mutations in mucinous ovarian carcinoma. *Gynecologic oncology* 2003, **90**(2)**:** 378-381.

39.   Anglesio MS, Kommoss S, Tolcher MC, Clarke B, Galletta L, Porter H, *et al.* Molecular characterization of mucinous ovarian tumours supports a stratified treatment approach with HER2 targeting in 19% of carcinomas. *The Journal of pathology* 2013, **229**(1)**:** 111-120.

40.   McAlpine JN, Wiegand KC, Vang R, Ronnett BM, Adamiak A, Kobel M, *et al.* HER2 overexpression and amplification is present in a subset of ovarian mucinous carcinomas and can be targeted with trastuzumab therapy. *BMC cancer* 2009, **9:** 433.

41.   Pectasides D, Fountzilas G, Aravantinos G, Kalofonos HP, Efstathiou E, Salamalekis E, *et al.* Advanced stage mucinous epithelial ovarian cancer: the Hellenic Cooperative Oncology Group experience. *Gynecologic oncology* 2005, **97**(2)**:** 436-441.

42.   Pignata S, Ferrandina G, Scarfone G, Scollo P, Odicino F, Cormio G, *et al.* Activity of chemotherapy in mucinous ovarian cancer with a recurrence free interval of more than 6 months: results from the SOCRATES retrospective study. *BMC cancer* 2008, **8:** 252.

43.   Singer G, Stohr R, Cope L, Dehari R, Hartmann A, Cao DF, *et al.* Patterns of p53 mutations separate ovarian serous borderline tumors and low- and high-grade carcinomas and provide support for a new model of ovarian carcinogenesis: a mutational analysis with immunohistochemical correlation. *The American journal of surgical pathology* 2005, **29**(2)**:** 218-224.

44.   Singer G, Oldt R, 3rd, Cohen Y, Wang BG, Sidransky D, Kurman RJ*, et al.* Mutations in BRAF and KRAS characterize the development of low-grade ovarian serous carcinoma. *Journal of the National Cancer Institute* 2003, **95**(6)**:** 484-486.

45.   Crispens MA, Bodurka D, Deavers M, Lu K, Silva EG, Gershenson DM. Response and survival in patients with progressive or recurrent serous ovarian tumors of low malignant potential. *Obstetrics and gynecology* 2002, **99**(1)**:** 3-10.

46.   Kobel M, Bak J, Bertelsen BI, Carpen O, Grove A, Hansen ES*, et al.* Ovarian carcinoma histotype determination is highly reproducible, and is improved through the use of immunohistochemistry. *Histopathology* 2014, **64**(7)**:** 1004-1013.

47.   Kobel M, Kalloger SE, Lee S, Duggan MA, Kelemen LE, Prentice L*, et al.* Biomarker-based ovarian carcinoma typing: a histologic investigation in the ovarian tumor tissue analysis consortium. *Cancer epidemiology, biomarkers & prevention : a publication of the American Association for Cancer Research, cosponsored by the American Society of Preventive Oncology* 2013, **22**(10)**:** 1677-1686.

48.   Clarke B, Tinker AV, Lee CH, Subramanian S, van de Rijn M, Turbin D*, et al.* Intraepithelial T cells and prognosis in ovarian carcinoma: novel associations with stage, tumor type, and BRCA1 loss. *Modern pathology : an official journal of the United States and Canadian Academy of Pathology, Inc* 2009, **22**(3)**:** 393-402.

49.   Milne K, Kobel M, Kalloger SE, Barnes RO, Gao D, Gilks CB*, et al.* Systematic analysis of immune infiltrates in high-grade serous ovarian cancer reveals CD20, FoxP3 and TIA-1 as positive prognostic factors. *PloS one* 2009, **4**(7)**:** e6412.

50.   Sato E, Olson SH, Ahn J, Bundy B, Nishikawa H, Qian F*, et al.* Intraepithelial CD8+ tumor-infiltrating lymphocytes and a high CD8+/regulatory T cell ratio are associated with favorable prognosis in ovarian cancer. *Proceedings of the National Academy of Sciences of the United States of America* 2005, **102**(51)**:** 18538-18543.

51.   Zhang W, Tian J, Hao Q. HMGB1 combining with tumor-associated macrophages enhanced lymphangiogenesis in human epithelial ovarian cancer. *Tumour biology : the journal of the International Society for Oncodevelopmental Biology and Medicine* 2014, **35**(3)**:** 2175-2186.

52.   Guth U, Huang DJ, Bauer G, Stieger M, Wight E, Singer G. Metastatic patterns at autopsy in patients with ovarian carcinoma. *Cancer* 2007, **110**(6)**:** 1272-1280.

53.   Bast RC, Jr., Knapp RC. Use of the CA 125 antigen in diagnosis and monitoring of ovarian carcinoma. *European journal of obstetrics, gynecology, and reproductive biology* 1985, **19**(6)**:** 354-356.

54.   Meyer T, Rustin GJ. Role of tumour markers in monitoring epithelial ovarian cancer. *British journal of cancer* 2000, **82**(9)**:** 1535-1538.

55.   Ozols RF. Recurrent ovarian cancer: evidence-based treatment. *Journal of clinical oncology : official journal of the American Society of Clinical Oncology* 2002, **20**(5)**:** 1161-1163.

56.   George SH, Shaw P. BRCA and Early Events in the Development of Serous Ovarian Cancer. *Frontiers in oncology* 2014, **4: 5**.

57.   Havrilesky L, Darcy k M, Hamdan H, Priore RL, Leon J, Bell J*, et al.* Prognostic significance of p53 mutation and p53 overexpression in advanced epithelial ovarian cancer: a Gynecologic Oncology Group Study. *Journal of clinical oncology : official journal of the American Society of Clinical Oncology* 2003, **21**(20)**:** 3814-3825.

58.   Salani R, Kurman RJ, Giuntoli R, 2nd, Gardner G, Bristow R, Wang TL*, et al.* Assessment of TP53 mutation using purified tissue samples of ovarian serous carcinomas reveals a higher mutation rate than previously reported and does not correlate with drug resistance. *International journal of gynecological cancer : official journal of the International Gynecological Cancer Society* 2008, **18**(3)**:** 487-491.

59.   Yemelyanova A, Vang R, Kshirsagar M, Lu D, Marks MA, Shih Ie M*, et al.* Immunohistochemical staining patterns of p53 can serve as a surrogate marker for TP53 mutations in ovarian carcinoma: an immunohistochemical and nucleotide sequencing analysis. *Modern pathology : an official journal of the United States and Canadian Academy of Pathology, Inc* 2011, **24**(9)**:** 1248-1253.

60.   Pietsch EC, Sykes SM, McMahon SB, Murphy ME. The p53 family and programmed cell death. *Oncogene* 2008, **27**(50)**:** 6507-6521.

61.   Antoniou A, Pharoah PD, Narod S, Risch HA, Eyfjord JE, Hopper JL*, et al.* Average risks of breast and ovarian cancer associated with BRCA1 or BRCA2 mutations detected in case Series unselected for family history: a combined analysis of 22 studies. *American journal of human genetics* 2003, **72**(5)**:** 1117-1130.

62.   Foulkes WD, Narod SA. Ovarian cancer risk and family history. *Lancet* 1997, **349**(9055)**:** 878.

63.   King MC, Marks JH, Mandell JB. Breast and ovarian cancer risks due to inherited mutations in BRCA1 and BRCA2. *Science (New York, NY)* 2003, **302**(5645)**:** 643-646.

64.   Sogaard M, Kjaer SK, Gayther S. Ovarian cancer and genetic susceptibility in relation to the BRCA1 and BRCA2 genes. Occurrence, clinical importance and intervention. *Acta obstetricia et gynecologica Scandinavica* 2006, **85**(1)**:** 93-105.

65.   Hilton JL, Geisler JP, Rathe JA, Hattermann-Zogg MA, DeYoung B, Buller RE. Inactivation of BRCA1 and BRCA2 in ovarian cancer. *Journal of the National Cancer Institute* 2002, **94**(18)**:** 1396-1406.

66.   Press JZ, De Luca A, Boyd N, Young S, Troussard A, Ridge Y, *et al.* Ovarian carcinomas with genetic and epigenetic BRCA1 loss have distinct molecular abnormalities. *BMC cancer* 2008, **8:** 17.

67.   Risch HA, McLaughlin JR, Cole DE, Rosen B, Bradley L, Kwan E, *et al.* Prevalence and penetrance of germline BRCA1 and BRCA2 mutations in a population series of 649 women with ovarian cancer. *American journal of human genetics* 2001, **68**(3)**:** 700-710.

68.   Roy R, Chun J, Powell SN. BRCA1 and BRCA2: different roles in a common pathway of genome protection. *Nature reviews Cancer* 2012, **12**(1)**:** 68-78.

69.   Collins N, Wooster R, Stratton MR. Absence of methylation of CpG dinucleotides within the promoter of the breast cancer susceptibility gene BRCA2 in normal tissues and in breast and ovarian cancers. *British journal of cancer* 1997, **76**(9)**:** 1150-1156.

70.   Plate JM, Plate AE, Shott S, Bograd S, Harris JE. Effect of gemcitabine on immune cells in subjects with adenocarcinoma of the pancreas. *Cancer immunology, immunotherapy : CII* 2005, **54**(9)**:** 915-925.

71.   Ben David Y, Chetrit A, Hirsh-Yechezkel G, Friedman E, Beck BD, Beller U, *et al.* Effect of BRCA mutations on the length of survival in epithelial ovarian tumors. *Journal of clinical oncology : official journal of the American Society of Clinical Oncology* 2002, **20**(2)**:** 463-466.

72.   Boyd J, Sonoda Y, Federici MG, Bogomolniy F, Rhei E, Maresco DL, *et al.* Clinicopathologic features of BRCA-linked and sporadic ovarian cancer. *JAMA : the journal of the American Medical Association* 2000, **283**(17)**:** 2260-2265.

73.   Quinn JE, James CR, Stewart GE, Mulligan JM, White P, Chang GK, *et al.* BRCA1 mRNA expression levels predict for overall survival in ovarian cancer after chemotherapy. *Clinical cancer research : an official journal of the American Association for Cancer Research* 2007, **13**(24)**:** 7413-7420.

74.   Cairns RA, Harris IS, Mak TW. Regulation of cancer cell metabolism. *Nature reviews Cancer* 2011, **11**(2)**:** 85-95.

75.   Nik NN, Vang R, Shih Ie M, Kurman RJ. Origin and pathogenesis of pelvic (ovarian, tubal, and primary peritoneal) serous carcinoma. *Annual review of pathology* 2014, **9:** 27-45.

76.   McGee ZA, Jensen RL, Clemens CM, Taylor-Robinson D, Johnson AP, Gregg CR. Gonococcal infection of human fallopian tube mucosa in organ culture: relationship of mucosal tissue TNF-alpha concentration to sloughing of ciliated cells. *Sexually transmitted diseases* 1999, **26**(3)**:** 160-165.

77. Salvador S, Gilks B, Kobel M, Huntsman D, Rosen B, Miller D. The fallopian tube: primary site of most pelvic high-grade serous carcinomas. *International journal of gynecological cancer : official journal of the International Gynecological Cancer Society* 2009, **19**(1)**:** 58-64.

78. Strandell A, Thorburn J, Wallin A. The presence of cytokines and growth factors in hydrosalpingeal fluid. *Journal of assisted reproduction and genetics* 2004, **21**(7)**:** 241-247.

79. Nash MA, Ferrandina G, Gordinier M, Loercher A, Freedman RS. The role of cytokines in both the normal and malignant ovary. *Endocrine-related cancer* 1999, **6**(1)**:** 93-107.

80. Medeiros F, Muto MG, Lee Y, Elvin JA, Callahan MJ, Feltmate C*, et al.* The tubal fimbria is a preferred site for early adenocarcinoma in women with familial ovarian cancer syndrome. *The American journal of surgical pathology* 2006, **30**(2)**:** 230-236.

81. Finch A, Shaw P, Rosen B, Murphy J, Narod SA, Colgan TJ. Clinical and pathologic findings of prophylactic salpingo-oophorectomies in 159 BRCA1 and BRCA2 carriers. *Gynecologic oncology* 2006, **100**(1)**:** 58-64.

82. Leeper K, Garcia R, Swisher E, Goff B, Greer B, Paley P. Pathologic findings in prophylactic oophorectomy specimens in high-risk women. *Gynecologic oncology* 2002, **87**(1)**:** 52-56.

83. Olivier RI, van Beurden M, Lubsen MA, Rookus MA, Mooij TM, van de Vijver MJ*, et al.* Clinical outcome of prophylactic oophorectomy in BRCA1/BRCA2 mutation carriers and events during follow-up. *British journal of cancer* 2004, **90**(8)**:** 1492-1497.

84. Kuhn E, Kurman RJ, Vang R, Sehdev AS, Han G, Soslow R*, et al.* TP53 mutations in serous tubal intraepithelial carcinoma and concurrent pelvic high-grade serous carcinoma--evidence supporting the clonal relationship of the two lesions. *The Journal of pathology* 2012, **226**(3)**:** 421-426.

85. Piek JM, Verheijen RH, Kenemans P, Massuger LF, Bulten H, van Diest PJ. BRCA1/2-related ovarian cancers are of tubal origin: a hypothesis. *Gynecologic oncology* 2003, **90**(2)**:** 491.

86. Kauff ND, Satagopan JM, Robson ME, Scheuer L, Hensley M, Hudis CA*, et al.* Risk-reducing salpingo-oophorectomy in women with a BRCA1 or BRCA2 mutation. *The New England journal of medicine* 2002, **346**(21)**:** 1609-1615.

87. Rebbeck TR, Lynch HT, Neuhausen SL, Narod SA, Van't Veer L, Garber JE*, et al.* Prophylactic oophorectomy in carriers of BRCA1 or BRCA2 mutations. *The New England journal of medicine* 2002, **346**(21)**:** 1616-1622.

88.   Kjaer SK, Mellemkjaer L, Brinton LA, Johansen C, Gridley G, Olsen JH. Tubal sterilization and risk of ovarian, endometrial and cervical cancer. A Danish population-based follow-up study of more than 65 000 sterilized women. *International journal of epidemiology* 2004, **33**(3)**:** 596-602.

89.   Kreiger N, Sloan M, Cotterchio M, Parsons P. Surgical procedures associated with risk of ovarian cancer. *International journal of epidemiology* 1997, **26**(4)**:** 710-715.

90.   Miracle-McMahill HL, Calle EE, Kosinski AS, Rodriguez C, Wingo PA, Thun MJ*, et al.* Tubal ligation and fatal ovarian cancer in a large prospective cohort study. *American journal of epidemiology* 1997, **145**(4)**:** 349-357.

91.   Rosenblatt KA, Thomas DB. Reduced risk of ovarian cancer in women with a tubal ligation or hysterectomy. The World Health Organization Collaborative Study of Neoplasia and Steroid Contraceptives. *Cancer epidemiology, biomarkers & prevention : a publication of the American Association for Cancer Research, cosponsored by the American Society of Preventive Oncology* 1996, **5**(11)**:** 933-935.

92.   Jayson GC, Kohn EC, Kitchener HC, Ledermann JA. Ovarian cancer. *Lancet* 2014.

93.   Hoskins WJ, Bundy BN, Thigpen JT, Omura GA. The influence of cytoreductive surgery on recurrence-free interval and survival in small-volume stage III epithelial ovarian cancer: a Gynecologic Oncology Group study. *Gynecologic oncology* 1992, **47**(2)**:** 159-166.

94.   Eisenhauer EL, Abu-Rustum NR, Sonoda Y, Levine DA, Poynor EA, Aghajanian C*, et al.* The addition of extensive upper abdominal surgery to achieve optimal cytoreduction improves survival in patients with stages IIIC-IV epithelial ovarian cancer. *Gynecologic oncology* 2006, **103**(3)**:** 1083-1090.

95.   Le T, Krepart GV, Lotocki RJ, Heywood MS. Does debulking surgery improve survival in biologically aggressive ovarian carcinoma? *Gynecologic oncology* 1997, **67**(2)**:** 208-214.

96.   Bristow RE, Tomacruz RS, Armstrong DK, Trimble EL, Montz FJ. Survival effect of maximal cytoreductive surgery for advanced ovarian carcinoma during the platinum era: a meta-analysis. *Journal of clinical oncology : official journal of the American Society of Clinical Oncology* 2002, **20**(5)**:** 1248-1259.

97.   McGuire WP, Hoskins WJ, Brady MF, Kucera PR, Partridge EE, Look KY*, et al.* Cyclophosphamide and cisplatin compared with paclitaxel and cisplatin in patients with stage III and stage IV ovarian cancer. *The New England journal of medicine* 1996, **334**(1)**:** 1-6.

98.   Kim A, Ueda Y, Naka T, Enomoto T. Therapeutic strategies in epithelial ovarian cancer. *Journal of experimental & clinical cancer research : CR* 2012, **31:** 14.

99.   Rowinsky EK, Donehower RC. Paclitaxel (taxol). *The New England journal of medicine* 1995, **332**(15)**:** 1004-1014.

100.   McGuire WP, Ozols RF. Chemotherapy of advanced ovarian cancer. *Seminars in oncology* 1998, **25**(3)**:** 340-348.

101.   Muggia FM, Braly PS, Brady MF, Sutton G, Niemann TH, Lentz SL*, et al.* Phase III randomized study of cisplatin versus paclitaxel versus cisplatin and paclitaxel in patients with suboptimal stage III or IV ovarian cancer: a gynecologic oncology group study. *Journal of clinical oncology : official journal of the American Society of Clinical Oncology* 2000, **18**(1)**:** 106-115.

102.   Piccart MJ. RESPONSE: re: randomized intergroup trial of cisplatin-paclitaxel versus cisplatin-cyclophosphamide in women with advanced epithelial ovarian cancer: three-year results. *Journal of the National Cancer Institute* 2000, **92**(17)**:** 1446-1447.

103.   du Bois A, Luck HJ, Meier W, Adams HP, Mobus V, Costa S*, et al.* A randomized clinical trial of cisplatin/paclitaxel versus carboplatin/paclitaxel as first-line treatment of ovarian cancer. *Journal of the National Cancer Institute* 2003, **95**(17)**:** 1320-1329.

104.   Ozols RF, Bundy BN, Greer BE, Fowler JM, Clarke-Pearson D, Burger RA*, et al.* Phase III trial of carboplatin and paclitaxel compared with cisplatin and paclitaxel in patients with optimally resected stage III ovarian cancer: a Gynecologic Oncology Group study. *Journal of clinical oncology : official journal of the American Society of Clinical Oncology* 2003, **21**(17)**:** 3194-3200.

105.   Bristow RE, Chi DS. Platinum-based neoadjuvant chemotherapy and interval surgical cytoreduction for advanced ovarian cancer: a meta-analysis. *Gynecologic oncology* 2006, **103**(3)**:** 1070-1076.

106.   Chi DS, Musa F, Dao F, Zivanovic O, Sonoda Y, Leitao MM*, et al.* An analysis of patients with bulky advanced stage ovarian, tubal, and peritoneal carcinoma treated with primary debulking surgery (PDS) during an identical time period as the randomized EORTC-NCIC trial of PDS vs neoadjuvant chemotherapy (NACT). *Gynecologic oncology* 2012, **124**(1)**:** 10-14.

107.   Hou JY, Kelly MG, Yu H, McAlpine JN, Azodi M, Rutherford TJ*, et al.* Neoadjuvant chemotherapy lessens surgical morbidity in advanced ovarian cancer and leads to improved survival in stage IV disease. *Gynecologic oncology* 2007, **105**(1)**:** 211-217.

108.   Milam MR, Tao X, Coleman RL, Harrell R, Bassett R, Dos Reis R*, et al.* Neoadjuvant chemotherapy is associated with prolonged primary treatment intervals in patients with advanced epithelial ovarian cancer. *International journal of gynecological cancer : official journal of the International Gynecological Cancer Society* 2011, **21**(1)**:** 66-71.

109. Vergote I, Trope CG, Amant F, Kristensen GB, Ehlen T, Johnson N, *et al.* Neoadjuvant chemotherapy or primary surgery in stage IIIC or IV ovarian cancer. *The New England journal of medicine* 2010, **363**(10)**:** 943-953.

110. Stoeckle E, Boubli B, Floquet A, Brouste V, Sire M, Croce S, *et al.* Optimal timing of interval debulking surgery in advanced ovarian cancer: yet to be defined? *European journal of obstetrics, gynecology, and reproductive biology* 2011, **159**(2)**:** 407-412.

111. Robinson W, Cantillo E. Debulking surgery and intraperitoneal chemotherapy are associated with decreased morbidity in women receiving neoadjuvant chemotherapy for ovarian cancer. *International journal of gynecological cancer : official journal of the International Gynecological Cancer Society* 2014, **24**(1)**:** 43-47.

112. Rauh-Hain JA, Nitschmann CC, Worley MJ, Jr., Bradford LS, Berkowitz RS, Schorge JO, *et al.* Platinum resistance after neoadjuvant chemotherapy compared to primary surgery in patients with advanced epithelial ovarian carcinoma. *Gynecologic oncology* 2013, **129**(1)**:** 63-68.

113. Stoeckle E, Bourdarias L, Guyon F, Croce S, Brouste V, Thomas L, *et al.* Progress in survival outcomes in patients with advanced ovarian cancer treated by neo-adjuvant platinum/taxane-based chemotherapy and late interval debulking surgery. *Annals of surgical oncology* 2014, **21**(2)**:** 629-636.

114. Gelmon KA, Tischkowitz M, Mackay H, Swenerton K, Robidoux A, Tonkin K, *et al.* Olaparib in patients with recurrent high-grade serous or poorly differentiated ovarian carcinoma or triple-negative breast cancer: a phase 2, multicentre, open-label, non-randomised study. *The lancet oncology* 2011, **12**(9)**:** 852-861.

115. Ledermann J, Harter P, Gourley C, Friedlander M, Vergote I, Rustin G, *et al.* Olaparib maintenance therapy in platinum-sensitive relapsed ovarian cancer. *The New England journal of medicine* 2012, **366**(15)**:** 1382-1392.

116. O'Sullivan CC, Moon DH, Kohn EC, Lee JM. Beyond Breast and Ovarian Cancers: PARP Inhibitors for BRCA Mutation-Associated and BRCA-Like Solid Tumors. *Frontiers in oncology* 2014, **4:** 42.

117. Banerjee S, Kaye SB. New strategies in the treatment of ovarian cancer: current clinical perspectives and future potential. *Clinical cancer research : an official journal of the American Association for Cancer Research* 2013, **19**(5)**:** 961-968.

118. Ashworth A. A synthetic lethal therapeutic approach: poly(ADP) ribose polymerase inhibitors for the treatment of cancers deficient in DNA double-strand break repair. *Journal of clinical oncology : official journal of the American Society of Clinical Oncology* 2008, **26**(22)**:** 3785-3790.

119. Kaplan DH, Shankaran V, Dighe AS, Stockert E, Aguet M, Old LJ, *et al.* Demonstration of an interferon gamma-dependent tumor surveillance system in immunocompetent mice. *Proceedings of the National Academy of Sciences of the United States of America* 1998, **95**(13)**:** 7556-7561.

120. Shankaran V, Ikeda H, Bruce AT, White JM, Swanson PE, Old LJ, *et al.* IFNgamma and lymphocytes prevent primary tumour development and shape tumour immunogenicity. *Nature* 2001, **410**(6832)**:** 1107-1111.

121. Muranski P, Boni A, Antony PA, Cassard L, Irvine KR, Kaiser A, *et al.* Tumor-specific Th17-polarized cells eradicate large established melanoma. *Blood* 2008, **112**(2)**:** 362-373.

122. Dudley ME, Wunderlich JR, Robbins PF, Yang JC, Hwu P, Schwartzentruber DJ, *et al.* Cancer regression and autoimmunity in patients after clonal repopulation with antitumor lymphocytes. *Science (New York, NY)* 2002, **298**(5594)**:** 850-854.

123. Robbins PF, Morgan RA, Feldman SA, Yang JC, Sherry RM, Dudley ME, *et al.* Tumor regression in patients with metastatic synovial cell sarcoma and melanoma using genetically engineered lymphocytes reactive with NY-ESO-1. *Journal of clinical oncology : official journal of the American Society of Clinical Oncology* 2011, **29**(7)**:** 917-924.

124. Mantovani A, Romero P, Palucka AK, Marincola FM. Tumour immunity: effector response to tumour and role of the microenvironment. *Lancet* 2008, **371**(9614)**:** 771-783.

125. Segal NH, Parsons DW, Peggs KS, Velculescu V, Kinzler KW, Vogelstein B, *et al.* Epitope landscape in breast and colorectal cancer. *Cancer research* 2008, **68**(3)**:** 889-892.

126. Robbins PF, Lu YC, El-Gamil M, Li YF, Gross C, Gartner J, *et al.* Mining exomic sequencing data to identify mutated antigens recognized by adoptively transferred tumor-reactive T cells. *Nature medicine* 2013, **19**(6)**:** 747-752.

127. Lieberman J. The ABCs of granule-mediated cytotoxicity: new weapons in the arsenal. *Nature reviews Immunology* 2003, **3**(5)**:** 361-370.

128. Tschopp J, Masson D, Stanley KK. Structural/functional similarity between proteins involved in complement- and cytotoxic T-lymphocyte-mediated cytolysis. *Nature* 1986, **322**(6082)**:** 831-834.

129. Adrain C, Murphy BM, Martin SJ. Molecular ordering of the caspase activation cascade initiated by the cytotoxic T lymphocyte/natural killer (CTL/NK) protease granzyme B. *The Journal of biological chemistry* 2005, **280**(6)**:** 4663-4673.

130. Cullen SP, Adrain C, Luthi AU, Duriez PJ, Martin SJ. Human and murine granzyme B exhibit divergent substrate preferences. *The Journal of cell biology* 2007, **176**(4)**:** 435-444.

131. Martin SJ, Amarante-Mendes GP, Shi L, Chuang TH, Casiano CA, O'Brien GA, *et al.* The cytotoxic cell protease granzyme B initiates apoptosis in a cell-free system by proteolytic processing and activation of the ICE/CED-3 family protease, CPP32, via a novel two-step mechanism. *The EMBO journal* 1996, **15**(10)**:** 2407-2416.

132. Alimonti JB, Shi L, Baijal PK, Greenberg AH. Granzyme B induces BID-mediated cytochrome c release and mitochondrial permeability transition. *The Journal of biological chemistry* 2001, **276**(10)**:** 6974-6982.

133. Barry M, Heibein JA, Pinkoski MJ, Lee SF, Moyer RW, Green DR, *et al.* Granzyme B short-circuits the need for caspase 8 activity during granule-mediated cytotoxic T-lymphocyte killing by directly cleaving Bid. *Molecular and cellular biology* 2000, **20**(11)**:** 3781-3794.

134. Sutton VR, Davis JE, Cancilla M, Johnstone RW, Ruefli AA, Sedelies K, *et al.* Initiation of apoptosis by granzyme B requires direct cleavage of bid, but not direct granzyme B-mediated caspase activation. *The Journal of experimental medicine* 2000, **192**(10)**:** 1403-1414.

135. Nijman HW, van Diest PJ, Poort-Keesom RJ, von Mensdorff-Pouilly S, Verstraeten RA, Kummer A, *et al.* T cell infiltration and MHC I and II expression in the presence of tumor antigens: An immunohistochemical study in patients with serous epithelial ovarian cancer. *European journal of obstetrics, gynecology, and reproductive biology* 2001, **94**(1)**:** 114-120.

136. Tian Q, Streuli M, Saito H, Schlossman SF, Anderson P. A polyadenylate binding protein localized to the granules of cytolytic lymphocytes induces DNA fragmentation in target cells. *Cell* 1991, **67**(3)**:** 629-639.

137. Kawakami A, Tian Q, Duan X, Streuli M, Schlossman SF, Anderson P. Identification and functional characterization of a TIA-1-related nucleolysin. *Proceedings of the National Academy of Sciences of the United States of America* 1992, **89**(18)**:** 8681-8685.

138. Piecyk M, Wax S, Beck AR, Kedersha N, Gupta M, Maritim B, *et al.* TIA-1 is a translational silencer that selectively regulates the expression of TNF-alpha. *The EMBO journal* 2000, **19**(15)**:** 4154-4163.

139. Saito K, Chen S, Piecyk M, Anderson P. TIA-1 regulates the production of tumor necrosis factor alpha in macrophages, but not in lymphocytes. *Arthritis and rheumatism* 2001, **44**(12)**:** 2879-2887.

140. Kedersha NL, Gupta M, Li W, Miller I, Anderson P. RNA-binding proteins TIA-1 and TIAR link the phosphorylation of eIF-2 alpha to the assembly of mammalian stress granules. *The Journal of cell biology* 1999, **147**(7)**:** 1431-1442.

141. Yamasaki S, Stoecklin G, Kedersha N, Simarro M, Anderson P. T-cell intracellular antigen-1 (TIA-1)-induced translational silencing promotes the decay of selected mRNAs. *The Journal of biological chemistry* 2007, **282**(41)**:** 30070-30077.

142. Fitzgerald KD, Semler BL. Poliovirus infection induces the co-localization of cellular protein SRp20 with TIA-1, a cytoplasmic stress granule protein. *Virus research* 2013, **176**(1-2)**:** 223-231.

143. Zlobec I, Karamitopoulou E, Terracciano L, Piscuoglio S, Iezzi G, Muraro MG*, et al.* TIA-1 cytotoxic granule-associated RNA binding protein improves the prognostic performance of CD8 in mismatch repair-proficient colorectal cancer. *PloS one* 2010, **5**(12)**:** e14282.

144. Hasselblom S, Sigurdadottir M, Hansson U, Nilsson-Ehle H, Ridell B, Andersson PO. The number of tumour-infiltrating TIA-1+ cytotoxic T cells but not FOXP3+ regulatory T cells predicts outcome in diffuse large B-cell lymphoma. *British journal of haematology* 2007, **137**(4)**:** 364-373.

145. Bauer WJ, Heath J, Jenkins JL, Kielkopf CL. Three RNA recognition motifs participate in RNA recognition and structural organization by the pro-apoptotic factor TIA-1. *Journal of molecular biology* 2012, **415**(4)**:** 727-740.

146. Cascino I, Fiucci G, Papoff G, Ruberti G. Three functional soluble forms of the human apoptosis-inducing Fas molecule are produced by alternative splicing. *Journal of immunology* 1995, **154**(6)**:** 2706-2713.

147. Izquierdo JM, Majos N, Bonnal S, Martinez C, Castelo R, Guigo R*, et al.* Regulation of Fas alternative splicing by antagonistic effects of TIA-1 and PTB on exon definition. *Molecular cell* 2005, **19**(4)**:** 475-484.

148. Izquierdo JM, Valcarcel J. Fas-activated serine/threonine kinase (FAST K) synergizes with TIA-1/TIAR proteins to regulate Fas alternative splicing. *The Journal of biological chemistry* 2007, **282**(3)**:** 1539-1543.

149. Shah S, Divekar AA, Hilchey SP, Cho HM, Newman CL, Shin SU*, et al.* Increased rejection of primary tumors in mice lacking B cells: inhibition of anti-tumor CTL and TH1 cytokine responses by B cells. *International journal of cancer Journal international du cancer* 2005, **117**(4)**:** 574-586.

150. Moulin V, Andris F, Thielemans K, Maliszewski C, Urbain J, Moser M. B lymphocytes regulate dendritic cell (DC) function in vivo: increased interleukin 12 production by DCs from B cell-deficient mice results in T helper cell type 1 deviation. *The Journal of experimental medicine* 2000, **192**(4)**:** 475-482.

151. Inoue S, Leitner WW, Golding B, Scott D. Inhibitory effects of B cells on antitumor immunity. *Cancer research* 2006, **66**(15)**:** 7741-7747.

152. Affara NI, Ruffell B, Medler TR, Gunderson AJ, Johansson M, Bornstein S*, et al.* B cells regulate macrophage phenotype and response to chemotherapy in squamous carcinomas. *Cancer cell* 2014, **25**(6)**:** 809-821.

153. Olkhanud PB, Damdinsuren B, Bodogai M, Gress RE, Sen R, Wejksza K*, et al.* Tumor-evoked regulatory B cells promote breast cancer metastasis by converting resting CD4(+) T cells to T-regulatory cells. *Cancer research* 2011, **71**(10)**:** 3505-3515.

154. DiLillo DJ, Yanaba K, Tedder TF. B cells are required for optimal CD4+ and CD8+ T cell tumor immunity: therapeutic B cell depletion enhances B16 melanoma growth in mice. *Journal of immunology* 2010, **184**(7)**:** 4006-4016.

155. Lapointe R, Bellemare-Pelletier A, Housseau F, Thibodeau J, Hwu P. CD40-stimulated B lymphocytes pulsed with tumor antigens are effective antigen-presenting cells that can generate specific T cells. *Cancer research* 2003, **63**(11)**:** 2836-2843.

156. von Bergwelt-Baildon MS, Vonderheide RH, Maecker B, Hirano N, Anderson KS, Butler MO*, et al.* Human primary and memory cytotoxic T lymphocyte responses are efficiently induced by means of CD40-activated B cells as antigen-presenting cells: potential for clinical application. *Blood* 2002, **99**(9)**:** 3319-3325.

157. Coughlin CM, Vance BA, Grupp SA, Vonderheide RH. RNA-transfected CD40-activated B cells induce functional T-cell responses against viral and tumor antigen targets: implications for pediatric immunotherapy. *Blood* 2004, **103**(6)**:** 2046-2054.

158. Van den Bosch GA, Ponsaerts P, Nijs G, Lenjou M, Vanham G, Van Bockstaele DR*, et al.* Ex vivo induction of viral antigen-specific CD8 T cell responses using mRNA-electroporated CD40-activated B cells. *Clinical and experimental immunology* 2005, **139**(3)**:** 458-467.

159. Schultze JL, Michalak S, Seamon MJ, Dranoff G, Jung K, Daley J*, et al.* CD40-activated human B cells: an alternative source of highly efficient antigen presenting cells to generate autologous antigen-specific T cells for adoptive immunotherapy. *The Journal of clinical investigation* 1997, **100**(11)**:** 2757-2765.

160. Tamada K, Harada M, Okamoto T, Takenoyama M, Ito O, Matsuzaki G*, et al.* Specific antitumor activity of tumor-infiltrating lymphocytes expanded first in a culture with both anti-CD3 monoclonal antibody and activated B cells and then in a culture with interleukin-2. *Cancer immunology, immunotherapy : CII* 1995, **41**(6)**:** 339-347.

161. Al-Shibli KI, Donnem T, Al-Saad S, Persson M, Bremnes RM, Busund LT. Prognostic effect of epithelial and stromal lymphocyte infiltration in non-small cell lung cancer. *Clinical cancer research : an official journal of the American Association for Cancer Research* 2008, **14**(16)**:** 5220-5227.

162. Nedergaard BS, Ladekarl M, Nyengaard JR, Nielsen K. A comparative study of the cellular immune response in patients with stage IB cervical squamous cell carcinoma. Low numbers of several immune cell subtypes are strongly associated with relapse of disease within 5 years. *Gynecologic oncology* 2008, **108**(1)**:** 106-111.

163. Schmidt M, Bohm D, von Torne C, Steiner E, Puhl A, Pilch H*, et al.* The humoral immune system has a key prognostic impact in node-negative breast cancer. *Cancer research* 2008, **68**(13)**:** 5405-5413.

164. Nielsen JS, Sahota RA, Milne K, Kost SE, Nesslinger NJ, Watson PH*, et al.* CD20+ tumor-infiltrating lymphocytes have an atypical CD27- memory phenotype and together with CD8+ T cells promote favorable prognosis in ovarian cancer. *Clinical cancer research : an official journal of the American Association for Cancer Research* 2012, **18**(12)**:** 3281-3292.

165. Shimabukuro-Vornhagen A, Schlosser HA, Gryschok L, Malcher J, Wennhold K, Garcia-Marquez M*, et al.* Characterization of tumor-associated B-cell subsets in patients with colorectal cancer. *Oncotarget* 2014, **5**(13)**:** 4651-4664.

166. Ding C, Wang L, Marroquin J, Yan J. Targeting of antigens to B cells augments antigen-specific T-cell responses and breaks immune tolerance to tumor-associated antigen MUC1. *Blood* 2008, **112**(7)**:** 2817-2825.

167. Reuschenbach M, von Knebel Doeberitz M, Wentzensen N. A systematic review of humoral immune responses against tumor antigens. *Cancer immunology, immunotherapy : CII* 2009, **58**(10)**:** 1535-1544.

168. Coronella-Wood JA, Hersh EM. Naturally occurring B-cell responses to breast cancer. *Cancer immunology, immunotherapy : CII* 2003, **52**(12)**:** 715-738.

169. Curiel TJ, Coukos G, Zou L, Alvarez X, Cheng P, Mottram P*, et al.* Specific recruitment of regulatory T cells in ovarian carcinoma fosters immune privilege and predicts reduced survival. *Nature medicine* 2004, **10**(9)**:** 942-949.

170. Facciabene A, Motz GT, Coukos G. T-regulatory cells: key players in tumor immune escape and angiogenesis. *Cancer research* 2012, **72**(9)**:** 2162-2171.

171. Loser K, Apelt J, Voskort M, Mohaupt M, Balkow S, Schwarz T*, et al.* IL-10 controls ultraviolet-induced carcinogenesis in mice. *Journal of immunology* 2007, **179**(1)**:** 365-371.

172. Strauss L, Bergmann C, Szczepanski M, Gooding W, Johnson JT, Whiteside TL. A unique subset of CD4+CD25highFoxp3+ T cells secreting interleukin-10 and transforming growth factor-beta1 mediates suppression in the tumor microenvironment. *Clinical cancer research : an official journal of the American Association for Cancer Research* 2007, **13**(15 Pt 1)**:** 4345-4354.

173. Vignali DA, Collison LW, Workman CJ. How regulatory T cells work. *Nature reviews Immunology* 2008, **8**(7)**:** 523-532.

174. Garin MI, Chu CC, Golshayan D, Cernuda-Morollon E, Wait R, Lechler RI. Galectin-1: a key effector of regulation mediated by CD4+CD25+ T cells. *Blood* 2007, **109**(5)**:** 2058-2065.

175. Gondek DC, Lu LF, Quezada SA, Sakaguchi S, Noelle RJ. Cutting edge: contact-mediated suppression by CD4+CD25+ regulatory cells involves a granzyme B-dependent, perforin-independent mechanism. *Journal of immunology* 2005, **174**(4)**:** 1783-1786.

176. Grossman WJ, Verbsky JW, Tollefsen BL, Kemper C, Atkinson JP, Ley TJ. Differential expression of granzymes A and B in human cytotoxic lymphocyte subsets and T regulatory cells. *Blood* 2004, **104**(9)**:** 2840-2848.

177. Ren X, Ye F, Jiang Z, Chu Y, Xiong S, Wang Y. Involvement of cellular death in TRAIL/DR5-dependent suppression induced by CD4(+)CD25(+) regulatory T cells. *Cell death and differentiation* 2007, **14**(12)**:** 2076-2084.

178. Fallarino F, Grohmann U, Hwang KW, Orabona C, Vacca C, Bianchi R*, et al.* Modulation of tryptophan catabolism by regulatory T cells. *Nature immunology* 2003, **4**(12)**:** 1206-1212.

179. Ishida T, Ishii T, Inagaki A, Yano H, Komatsu H, Iida S*, et al.* Specific recruitment of CC chemokine receptor 4-positive regulatory T cells in Hodgkin lymphoma fosters immune privilege. *Cancer research* 2006, **66**(11)**:** 5716-5722.

180. Facciabene A, Peng X, Hagemann IS, Balint K, Barchetti A, Wang LP*, et al.* Tumour hypoxia promotes tolerance and angiogenesis via CCL28 and T(reg) cells. *Nature* 2011, **475**(7355)**:** 226-230.

181. Valzasina B, Piconese S, Guiducci C, Colombo MP. Tumor-induced expansion of regulatory T cells by conversion of CD4+CD25- lymphocytes is thymus and proliferation independent. *Cancer research* 2006, **66**(8)**:** 4488-4495.

182. Liu VC, Wong LY, Jang T, Shah AH, Park I, Yang X*, et al.* Tumor evasion of the immune system by converting CD4+CD25- T cells into CD4+CD25+ T regulatory cells: role of tumor-derived TGF-beta. *Journal of immunology* 2007, **178**(5)**:** 2883-2892.

183. Seo N, Hayakawa S, Takigawa M, Tokura Y. Interleukin-10 expressed at early tumour sites induces subsequent generation of CD4(+) T-regulatory cells and systemic collapse of antitumour immunity. *Immunology* 2001, **103**(4)**:** 449-457.

184. Zarek PE, Huang CT, Lutz ER, Kowalski J, Horton MR, Linden J*, et al.* A2A receptor signaling promotes peripheral tolerance by inducing T-cell anergy and the generation of adaptive regulatory T cells. *Blood* 2008, **111**(1)**:** 251-259.

185.   Ghiringhelli F, Puig PE, Roux S, Parcellier A, Schmitt E, Solary E, *et al.* Tumor cells convert immature myeloid dendritic cells into TGF-beta-secreting cells inducing CD4+CD25+ regulatory T cell proliferation. *The Journal of experimental medicine* 2005, **202**(7)**:** 919-929.

186.   Colvin EK. Tumor-associated macrophages contribute to tumor progression in ovarian cancer. *Frontiers in oncology* 2014, **4:** 137.

187.   Lewis CE, Pollard JW. Distinct role of macrophages in different tumor microenvironments. *Cancer research* 2006, **66**(2)**:** 605-612.

188.   Mantovani A, Sozzani S, Locati M, Allavena P, Sica A. Macrophage polarization: tumor-associated macrophages as a paradigm for polarized M2 mononuclear phagocytes. *Trends in immunology* 2002, **23**(11)**:** 549-555.

189.   Qian BZ, Pollard JW. Macrophage diversity enhances tumor progression and metastasis. *Cell* 2010, **141**(1)**:** 39-51.

190.   Farinha P, Masoudi H, Skinnider BF, Shumansky K, Spinelli JJ, Gill K, *et al.* Analysis of multiple biomarkers shows that lymphoma-associated macrophage (LAM) content is an independent predictor of survival in follicular lymphoma (FL). *Blood* 2005, **106**(6)**:** 2169-2174.

191.   Lissbrant IF, Stattin P, Wikstrom P, Damber JE, Egevad L, Bergh A. Tumor associated macrophages in human prostate cancer: relation to clinicopathological variables and survival. *International journal of oncology* 2000, **17**(3)**:** 445-451.

192.   Tsutsui S, Yasuda K, Suzuki K, Tahara K, Higashi H, Era S. Macrophage infiltration and its prognostic implications in breast cancer: the relationship with VEGF expression and microvessel density. *Oncology reports* 2005, **14**(2)**:** 425-431.

193.   Takaishi K, Komohara Y, Tashiro H, Ohtake H, Nakagawa T, Katabuchi H, *et al.* Involvement of M2-polarized macrophages in the ascites from advanced epithelial ovarian carcinoma in tumor progression via Stat3 activation. *Cancer science* 2010, **101**(10)**:** 2128-2136.

194.   Kawamura K, Komohara Y, Takaishi K, Katabuchi H, Takeya M. Detection of M2 macrophages and colony-stimulating factor 1 expression in serous and mucinous ovarian epithelial tumors. *Pathology international* 2009, **59**(5)**:** 300-305.

195.   Klimp AH, Hollema H, Kempinga C, van der Zee AG, de Vries EG, Daemen T. Expression of cyclooxygenase-2 and inducible nitric oxide synthase in human ovarian tumors and tumor-associated macrophages. *Cancer research* 2001, **61**(19)**:** 7305-7309.

196.   Wang X, Deavers M, Patenia R, Bassett RL, Jr., Mueller P, Ma Q, *et al.* Monocyte/macrophage and T-cell infiltrates in peritoneum of patients with ovarian cancer or benign pelvic disease. *Journal of translational medicine* 2006, **4:** 30.

197. Lan C, Huang X, Lin S, Huang H, Cai Q, Wan T, *et al.* Expression of M2-polarized macrophages is associated with poor prognosis for advanced epithelial ovarian cancer. *Technology in cancer research & treatment* 2013, **12**(3)**:** 259-267.

198. Le Page C, Marineau A, Bonza PK, Rahimi K, Cyr L, Labouba I, *et al.* BTN3A2 expression in epithelial ovarian cancer is associated with higher tumor infiltrating T cells and a better prognosis. *PloS one* 2012, **7**(6)**:** e38541.

199. Chambers SK, Kacinski BM, Ivins CM, Carcangiu ML. Overexpression of epithelial macrophage colony-stimulating factor (CSF-1) and CSF-1 receptor: a poor prognostic factor in epithelial ovarian cancer, contrasted with a protective effect of stromal CSF-1. *Clinical cancer research : an official journal of the American Association for Cancer Research* 1997, **3**(6)**:** 999-1007.

200. Schutyser E, Struyf S, Proost P, Opdenakker G, Laureys G, Verhasselt B, *et al.* Identification of biologically active chemokine isoforms from ascitic fluid and elevated levels of CCL18/pulmonary and activation-regulated chemokine in ovarian carcinoma. *The Journal of biological chemistry* 2002, **277**(27)**:** 24584-24593.

201. Wang X, Zhao X, Wang K, Wu L, Duan T. Interaction of monocytes/macrophages with ovarian cancer cells promotes angiogenesis in vitro. *Cancer science* 2013, **104**(4)**:** 516-523.

202. Allavena P, Chieppa M, Bianchi G, Solinas G, Fabbri M, Laskarin G, *et al.* Engagement of the mannose receptor by tumoral mucins activates an immune suppressive phenotype in human tumor-associated macrophages. *Clinical & developmental immunology* 2010, **2010:** 547179.

203. Dijkgraaf EM, Heusinkveld M, Tummers B, Vogelpoel LT, Goedemans R, Jha V, *et al.* Chemotherapy alters monocyte differentiation to favor generation of cancer-supporting M2 macrophages in the tumor microenvironment. *Cancer research* 2013, **73**(8)**:** 2480-2492.

204. Azuma M, Ito D, Yagita H, Okumura K, Phillips JH, Lanier LL, *et al.* B70 antigen is a second ligand for CTLA-4 and CD28. *Nature* 1993, **366**(6450)**:** 76-79.

205. Hathcock KS, Laszlo G, Dickler HB, Bradshaw J, Linsley P, Hodes RJ. Identification of an alternative CTLA-4 ligand costimulatory for T cell activation. *Science (New York, NY)* 1993, **262**(5135)**:** 905-907.

206. Schwartz RH. Costimulation of T lymphocytes: the role of CD28, CTLA-4, and B7/BB1 in interleukin-2 production and immunotherapy. *Cell* 1992, **71**(7)**:** 1065-1068.

207. Qureshi OS, Zheng Y, Nakamura K, Attridge K, Manzotti C, Schmidt EM, *et al.* Trans-endocytosis of CD80 and CD86: a molecular basis for the cell-extrinsic function of CTLA-4. *Science (New York, NY)* 2011, **332**(6029)**:** 600-603.

208. Phan GQ, Yang JC, Sherry RM, Hwu P, Topalian SL, Schwartzentruber DJ, *et al.* Cancer regression and autoimmunity induced by cytotoxic T lymphocyte-associated antigen 4 blockade in patients with metastatic melanoma. *Proceedings of the National Academy of Sciences of the United States of America* 2003, **100**(14)**:** 8372-8377.

209. Ribas A, Camacho LH, Lopez-Berestein G, Pavlov D, Bulanhagui CA, Millham R, *et al.* Antitumor activity in melanoma and anti-self responses in a phase I trial with the anti-cytotoxic T lymphocyte-associated antigen 4 monoclonal antibody CP-675,206. *Journal of clinical oncology : official journal of the American Society of Clinical Oncology* 2005, **23**(35)**:** 8968-8977.

210. Hodi FS, O'Day SJ, McDermott DF, Weber RW, Sosman JA, Haanen JB, *et al.* Improved survival with ipilimumab in patients with metastatic melanoma. *The New England journal of medicine* 2010, **363**(8)**:** 711-723.

211. Phase II study of Ipilimumab monotherapy in recurrent platinum sensitive ovarian cancer patients (NCT01611558). 2014 2014 [cited]clinical trials website]. Available from: http://clinicaltrials.gov/ct2/show/NCT01611558

212. Devaud C, John LB, Westwood JA, Darcy PK, Kershaw MH. Immune modulation of the tumor microenvironment for enhancing cancer immunotherapy. *Oncoimmunology* 2013, **2**(8)**:** e25961.

213. Pardoll DM. The blockade of immune checkpoints in cancer immunotherapy. *Nature reviews Cancer* 2012, **12**(4)**:** 252-264.

214. Curiel TJ, Wei S, Dong H, Alvarez X, Cheng P, Mottram P, *et al.* Blockade of B7-H1 improves myeloid dendritic cell-mediated antitumor immunity. *Nature medicine* 2003, **9**(5)**:** 562-567.

215. Liu Y, Zeng B, Zhang Z, Zhang Y, Yang R. B7-H1 on myeloid-derived suppressor cells in immune suppression by a mouse model of ovarian cancer. *Clinical immunology (Orlando, Fla)* 2008, **129**(3)**:** 471-481.

216. Thompson RH, Gillett MD, Cheville JC, Lohse CM, Dong H, Webster WS, *et al.* Costimulatory B7-H1 in renal cell carcinoma patients: Indicator of tumor aggressiveness and potential therapeutic target. *Proceedings of the National Academy of Sciences of the United States of America* 2004, **101**(49)**:** 17174-17179.

217. Hamanishi J, Mandai M, Iwasaki M, Okazaki T, Tanaka Y, Yamaguchi K, *et al.* Programmed cell death 1 ligand 1 and tumor-infiltrating CD8+ T lymphocytes are prognostic factors of human ovarian cancer. *Proceedings of the National Academy of Sciences of the United States of America* 2007, **104**(9)**:** 3360-3365.

218. Dong H, Strome SE, Salomao DR, Tamura H, Hirano F, Flies DB, *et al.* Tumor-associated B7-H1 promotes T-cell apoptosis: a potential mechanism of immune evasion. *Nature medicine* 2002, **8**(8)**:** 793-800.

219.   Taube JM, Anders RA, Young GD, Xu H, Sharma R, McMiller TL, *et al.* Colocalization of inflammatory response with B7-h1 expression in human melanocytic lesions supports an adaptive resistance mechanism of immune escape. *Science translational medicine* 2012, **4**(127)**:** 127ra137.

220.   Ahmadzadeh M, Johnson LA, Heemskerk B, Wunderlich JR, Dudley ME, White DE, *et al.* Tumor antigen-specific CD8 T cells infiltrating the tumor express high levels of PD-1 and are functionally impaired. *Blood* 2009, **114**(8)**:** 1537-1544.

221.   Gros A, Robbins PF, Yao X, Li YF, Turcotte S, Tran E, *et al.* PD-1 identifies the patient-specific CD8+ tumor-reactive repertoire infiltrating human tumors. *The Journal of clinical investigation* 2014, **124**(5)**:** 2246-2259.

222.   Sfanos KS, Bruno TC, Meeker AK, De Marzo AM, Isaacs WB, Drake CG. Human prostate-infiltrating CD8+ T lymphocytes are oligoclonal and PD-1+. *The Prostate* 2009, **69**(15)**:** 1694-1703.

223.   Matsuzaki J, Gnjatic S, Mhawech-Fauceglia P, Beck A, Miller A, Tsuji T, *et al.* Tumor-infiltrating NY-ESO-1-specific CD8+ T cells are negatively regulated by LAG-3 and PD-1 in human ovarian cancer. *Proceedings of the National Academy of Sciences of the United States of America* 2010, **107**(17)**:** 7875-7880.

224.   Zhang L, Conejo-Garcia JR, Katsaros D, Gimotty PA, Massobrio M, Regnani G, *et al.* Intratumoral T cells, recurrence, and survival in epithelial ovarian cancer. *The New England journal of medicine* 2003, **348**(3)**:** 203-213.

225.   Wolf D, Wolf AM, Rumpold H, Fiegl H, Zeimet AG, Muller-Holzner E, *et al.* The expression of the regulatory T cell-specific forkhead box transcription factor FoxP3 is associated with poor prognosis in ovarian cancer. *Clinical cancer research : an official journal of the American Association for Cancer Research* 2005, **11**(23)**:** 8326-8331.

226.   Kryczek I, Wei S, Zhu G, Myers L, Mottram P, Cheng P, *et al.* Relationship between B7-H4, regulatory T cells, and patient outcome in human ovarian carcinoma. *Cancer research* 2007, **67**(18)**:** 8900-8905.

227.   Kryczek I, Zou L, Rodriguez P, Zhu G, Wei S, Mottram P, *et al.* B7-H4 expression identifies a novel suppressive macrophage population in human ovarian carcinoma. *The Journal of experimental medicine* 2006, **203**(4)**:** 871-881.

228.   Bak SP, Alonso A, Turk MJ, Berwin B. Murine ovarian cancer vascular leukocytes require arginase-1 activity for T cell suppression. *Molecular immunology* 2008, **46**(2)**:** 258-268.

229.   Obermajer N, Muthuswamy R, Odunsi K, Edwards RP, Kalinski P. PGE(2)-induced CXCL12 production and CXCR4 expression controls the accumulation of human MDSCs in ovarian cancer environment. *Cancer research* 2011, **71**(24)**:** 7463-7470.

230. Yang R, Cai Z, Zhang Y, Yutzy WHt, Roby KF, Roden RB. CD80 in immune suppression by mouse ovarian carcinoma-associated Gr-1+CD11b+ myeloid cells. *Cancer research* 2006, **66**(13)**:** 6807-6815.

231. Mellman I, Coukos G, Dranoff G. Cancer immunotherapy comes of age. *Nature* 2011, **480**(7378)**:** 480-489.

232. Schreiber RD, Old LJ, Smyth MJ. Cancer immunoediting: integrating immunity's roles in cancer suppression and promotion. *Science (New York, NY)* 2011, **331**(6024)**:** 1565-1570.

233. Thomas ED, Buckner CD, Banaji M, Clift RA, Fefer A, Flournoy N*, et al.* One hundred patients with acute leukemia treated by chemotherapy, total body irradiation, and allogeneic marrow transplantation. *Blood* 1977, **49**(4)**:** 511-533.

234. Thomas ED, Buckner CD, Clift RA, Fefer A, Johnson FL, Neiman PE*, et al.* Marrow transplantation for acute nonlymphoblastic leukemia in first remission. *The New England journal of medicine* 1979, **301**(11)**:** 597-599.

235. Gupta V, Lazarus HM, Keating A. Myeloablative conditioning regimens for AML allografts: 30 years later. *Bone marrow transplantation* 2003, **32**(10)**:** 969-978.

236. Schiavoni G, Sistigu A, Valentini M, Mattei F, Sestili P, Spadaro F*, et al.* Cyclophosphamide synergizes with type I interferons through systemic dendritic cell reactivation and induction of immunogenic tumor apoptosis. *Cancer research* 2011, **71**(3)**:** 768-778.

237. Ghiringhelli F, Menard C, Puig PE, Ladoire S, Roux S, Martin F*, et al.* Metronomic cyclophosphamide regimen selectively depletes CD4+CD25+ regulatory T cells and restores T and NK effector functions in end stage cancer patients. *Cancer immunology, immunotherapy : CII* 2007, **56**(5)**:** 641-648.

238. Ghiringhelli F, Menard C, Terme M, Flament C, Taieb J, Chaput N*, et al.* CD4+CD25+ regulatory T cells inhibit natural killer cell functions in a transforming growth factor-beta-dependent manner. *The Journal of experimental medicine* 2005, **202**(8)**:** 1075-1085.

239. Chang CL, Hsu YT, Wu CC, Lai YZ, Wang C, Yang YC*, et al.* Dose-dense chemotherapy improves mechanisms of antitumor immune response. *Cancer research* 2013, **73**(1)**:** 119-127.

240. Kroemer G, Galluzzi L, Kepp O, Zitvogel L. Immunogenic cell death in cancer therapy. *Annual review of immunology* 2013, **31:** 51-72.

241. Martins I, Wang Y, Michaud M, Ma Y, Sukkurwala AQ, Shen S*, et al.* Molecular mechanisms of ATP secretion during immunogenic cell death. *Cell death and differentiation* 2014, **21**(1)**:** 79-91.

242.   Obeid M, Tesniere A, Ghiringhelli F, Fimia GM, Apetoh L, Perfettini JL*, et al.* Calreticulin exposure dictates the immunogenicity of cancer cell death. *Nature medicine* 2007, **13**(1)**:** 54-61.

243.   Tesniere A, Apetoh L, Ghiringhelli F, Joza N, Panaretakis T, Kepp O*, et al.* Immunogenic cancer cell death: a key-lock paradigm. *Current opinion in immunology* 2008, **20**(5)**:** 504-511.

244.   Apetoh L, Ghiringhelli F, Tesniere A, Obeid M, Ortiz C, Criollo A*, et al.* Toll-like receptor 4-dependent contribution of the immune system to anticancer chemotherapy and radiotherapy. *Nature medicine* 2007, **13**(9)**:** 1050-1059.

245.   Ma Y, Adjemian S, Yang H, Catani JP, Hannani D, Martins I*, et al.* ATP-dependent recruitment, survival and differentiation of dendritic cell precursors in the tumor bed after anticancer chemotherapy. *Oncoimmunology* 2013, **2**(6)**:** e24568.

246.   Michaud M, Martins I, Sukkurwala AQ, Adjemian S, Ma Y, Pellegatti P*, et al.* Autophagy-dependent anticancer immune responses induced by chemotherapeutic agents in mice. *Science (New York, NY)* 2011, **334**(6062)**:** 1573-1577.

247.   Obeid M, Tesniere A, Panaretakis T, Tufi R, Joza N, van Endert P*, et al.* Ecto-calreticulin in immunogenic chemotherapy. *Immunological reviews* 2007, **220:** 22-34.

248.   Panaretakis T, Kepp O, Brockmeier U, Tesniere A, Bjorklund AC, Chapman DC*, et al.* Mechanisms of pre-apoptotic calreticulin exposure in immunogenic cell death. *The EMBO journal* 2009, **28**(5)**:** 578-590.

249.   Kepp O, Tesniere A, Schlemmer F, Michaud M, Senovilla L, Zitvogel L*, et al.* Immunogenic cell death modalities and their impact on cancer treatment. *Apoptosis : an international journal on programmed cell death* 2009, **14**(4)**:** 364-375.

250.   Obeid M, Panaretakis T, Tesniere A, Joza N, Tufi R, Apetoh L*, et al.* Leveraging the immune system during chemotherapy: moving calreticulin to the cell surface converts apoptotic death from "silent" to immunogenic. *Cancer research* 2007, **67**(17)**:** 7941-7944.

251.   Garg AD, Krysko DV, Verfaillie T, Kaczmarek A, Ferreira GB, Marysael T*, et al.* A novel pathway combining calreticulin exposure and ATP secretion in immunogenic cancer cell death. *The EMBO journal* 2012, **31**(5)**:** 1062-1079.

252.   Wemeau M, Kepp O, Tesniere A, Panaretakis T, Flament C, De Botton S*, et al.* Calreticulin exposure on malignant blasts predicts a cellular anticancer immune response in patients with acute myeloid leukemia. *Cell death & disease* 2010, **1:** e104.

253. Zappasodi R, Pupa SM, Ghedini GC, Bongarzone I, Magni M, Cabras AD*, et al.* Improved clinical outcome in indolent B-cell lymphoma patients vaccinated with autologous tumor cells experiencing immunogenic death. *Cancer research* 2010, **70**(22)**:** 9062-9072.

254. Elliott MR, Chekeni FB, Trampont PC, Lazarowski ER, Kadl A, Walk SF*, et al.* Nucleotides released by apoptotic cells act as a find-me signal to promote phagocytic clearance. *Nature* 2009, **461**(7261)**:** 282-286.

255. Scaffidi P, Misteli T, Bianchi ME. Release of chromatin protein HMGB1 by necrotic cells triggers inflammation. *Nature* 2002, **418**(6894)**:** 191-195.

256. Yamazaki T, Hannani D, Poirier-Colame V, Ladoire S, Locher C, Sistigu A*, et al.* Defective immunogenic cell death of HMGB1-deficient tumors: compensatory therapy with TLR4 agonists. *Cell death and differentiation* 2014, **21**(1)**:** 69-78.

257. Sims GP, Rowe DC, Rietdijk ST, Herbst R, Coyle AJ. HMGB1 and RAGE in inflammation and cancer. *Annual review of immunology* 2010, **28:** 367-388.

258. Apetoh L, Ghiringhelli F, Tesniere A, Criollo A, Ortiz C, Lidereau R*, et al.* The interaction between HMGB1 and TLR4 dictates the outcome of anticancer chemotherapy and radiotherapy. *Immunological reviews* 2007, **220:** 47-59.

259. Martins I, Kepp O, Schlemmer F, Adjemian S, Tailler M, Shen S*, et al.* Restoration of the immunogenicity of cisplatin-induced cancer cell death by endoplasmic reticulum stress. *Oncogene* 2011, **30**(10)**:** 1147-1158.

260. Tesniere A, Schlemmer F, Boige V, Kepp O, Martins I, Ghiringhelli F*, et al.* Immunogenic death of colon cancer cells treated with oxaliplatin. *Oncogene* 2010, **29**(4)**:** 482-491.

261. Demaria S, Volm MD, Shapiro RL, Yee HT, Oratz R, Formenti SC*, et al.* Development of tumor-infiltrating lymphocytes in breast cancer after neoadjuvant paclitaxel chemotherapy. *Clinical cancer research : an official journal of the American Association for Cancer Research* 2001, **7**(10)**:** 3025-3030.

262. Ladoire S, Arnould L, Apetoh L, Coudert B, Martin F, Chauffert B*, et al.* Pathologic complete response to neoadjuvant chemotherapy of breast carcinoma is associated with the disappearance of tumor-infiltrating foxp3+ regulatory T cells. *Clinical cancer research : an official journal of the American Association for Cancer Research* 2008, **14**(8)**:** 2413-2420.

263. Ladoire S, Mignot G, Dabakuyo S, Arnould L, Apetoh L, Rebe C*, et al.* In situ immune response after neoadjuvant chemotherapy for breast cancer predicts survival. *The Journal of pathology* 2011, **224**(3)**:** 389-400.

264.   Polcher M, Braun M, Friedrichs N, Rudlowski C, Bercht E, Fimmers R, *et al.* Foxp3(+) cell infiltration and granzyme B(+)/Foxp3(+) cell ratio are associated with outcome in neoadjuvant chemotherapy-treated ovarian carcinoma. *Cancer immunology, immunotherapy : CII* 2010, **59**(6): 909-919.

265.   Ono M, Tsuda H, Shimizu C, Yamamoto S, Shibata T, Yamamoto H, *et al.* Tumor-infiltrating lymphocytes are correlated with response to neoadjuvant chemotherapy in triple-negative breast cancer. *Breast cancer research and treatment* 2012, **132**(3): 793-805.

266.   Yamaguchi R, Tanaka M, Yano A, Tse GM, Yamaguchi M, Koura K, *et al.* Tumor-infiltrating lymphocytes are important pathologic predictors for neoadjuvant chemotherapy in patients with breast cancer. *Human pathology* 2012, **43**(10): 1688-1694.

267.   West NR, Milne K, Truong PT, Macpherson N, Nelson BH, Watson PH. Tumor-infiltrating lymphocytes predict response to anthracycline-based chemotherapy in estrogen receptor-negative breast cancer. *Breast cancer research : BCR* 2011, **13**(6): R126.

268.   Bosmuller H, Haitchi-Petnehazy S, Webersinke G, Marschon R, Roithmeier F, Stummvoll W, *et al.* Intratumoral lymphocyte density in serous ovarian carcinoma is superior to ERCC1 expression for predicting response to platinum-based therapy. *Virchows Archiv : an international journal of pathology* 2011, **459**(2): 183-191.

269.   Adams SF, Levine DA, Cadungog MG, Hammond R, Facciabene A, Olvera N, *et al.* Intraepithelial T cells and tumor proliferation: impact on the benefit from surgical cytoreduction in advanced serous ovarian cancer. *Cancer* 2009, **115**(13): 2891-2902.

270.   Pages F, Galon J, Dieu-Nosjean MC, Tartour E, Sautes-Fridman C, Fridman WH. Immune infiltration in human tumors: a prognostic factor that should not be ignored. *Oncogene* 2010, **29**(8): 1093-1102.

271.   Salama P, Phillips M, Platell C, Iacopetta B. Low expression of Granzyme B in colorectal cancer is associated with signs of early metastastic invasion. *Histopathology* 2011, **59**(2): 207-215.

272.   Dudley ME, Gross CA, Langhan MM, Garcia MR, Sherry RM, Yang JC, *et al.* CD8+ enriched "young" tumor infiltrating lymphocytes can mediate regression of metastatic melanoma. *Clinical cancer research : an official journal of the American Association for Cancer Research* 2010, **16**(24): 6122-6131.

273.   Khammari A, Labarriere N, Vignard V, Nguyen JM, Pandolfino MC, Knol AC, *et al.* Treatment of metastatic melanoma with autologous Melan-A/MART-1-specific cytotoxic T lymphocyte clones. *The Journal of investigative dermatology* 2009, **129**(12): 2835-2842.

274. Pardo J, Bosque A, Brehm R, Wallich R, Naval J, Mullbacher A, *et al.* Apoptotic pathways are selectively activated by granzyme A and/or granzyme B in CTL-mediated target cell lysis. *The Journal of cell biology* 2004, **167**(3)**:** 457-468.

275. Sarin A, Haddad EK, Henkart PA. Caspase dependence of target cell damage induced by cytotoxic lymphocytes. *Journal of immunology* 1998, **161**(6)**:** 2810-2816.

276. Trapani JA, Jans DA, Jans PJ, Smyth MJ, Browne KA, Sutton VR. Efficient nuclear targeting of granzyme B and the nuclear consequences of apoptosis induced by granzyme B and perforin are caspase-dependent, but cell death is caspase-independent. *The Journal of biological chemistry* 1998, **273**(43)**:** 27934-27938.

277. Kume T, Oshima K, Yamashita Y, Shirakusa T, Kikuchi M. Relationship between Fas-ligand expression on carcinoma cell and cytotoxic T-lymphocyte response in lymphoepithelioma-like cancer of the stomach. *International journal of cancer Journal international du cancer* 1999, **84**(4)**:** 339-343.

278. Zucchetto A, Cattarossi I, Nanni P, Zaina E, Prato G, Gilestro M, *et al.* Cluster analysis of immunophenotypic data: the example of chronic lymphocytic leukemia. *Immunology letters* 2011, **134**(2)**:** 137-144.

279. French JJ, Cresswell J, Wong WK, Seymour K, Charnley RM, Kirby JA. T cell adhesion and cytolysis of pancreatic cancer cells: a role for E-cadherin in immunotherapy? *British journal of cancer* 2002, **87**(9)**:** 1034-1041.

280. Le Floc'h A, Jalil A, Vergnon I, Le Maux Chansac B, Lazar V, Bismuth G, *et al.* Alpha E beta 7 integrin interaction with E-cadherin promotes antitumor CTL activity by triggering lytic granule polarization and exocytosis. *The Journal of experimental medicine* 2007, **204**(3)**:** 559-570.

281. Ling KL, Dulphy N, Bahl P, Salio M, Maskell K, Piris J, *et al.* Modulation of CD103 expression on human colon carcinoma-specific CTL. *Journal of immunology* 2007, **178**(5)**:** 2908-2915.

282. Bromley AB, Altman AD, Chu P, Nation JG, Nelson GS, Ghatage P, *et al.* Architectural patterns of ovarian/pelvic high-grade serous carcinoma. *International journal of gynecological pathology : official journal of the International Society of Gynecological Pathologists* 2012, **31**(5)**:** 397-404.

283. McCluggage WG, Lyness RW, Atkinson RJ, Dobbs SP, Harley I, McClelland HR, *et al.* Morphological effects of chemotherapy on ovarian carcinoma. *Journal of clinical pathology* 2002, **55**(1)**:** 27-31.

284. Sassen S, Schmalfeldt B, Avril N, Kuhn W, Busch R, Hofler H, *et al.* Histopathologic assessment of tumor regression after neoadjuvant chemotherapy in advanced-stage ovarian cancer. *Human pathology* 2007, **38**(6)**:** 926-934.

285.   Bashashati A, Ha G, Tone A, Ding J, Prentice LM, Roth A*, et al.* Distinct evolutionary trajectories of primary high-grade serous ovarian cancers revealed through spatial mutational profiling. *The Journal of pathology* 2013, **231**(1)**:** 21-34.

286.   Ruffell B, Au A, Rugo HS, Esserman LJ, Hwang ES, Coussens LM. Leukocyte composition of human breast cancer. *Proceedings of the National Academy of Sciences of the United States of America* 2012, **109**(8)**:** 2796-2801.

287.   Tsuchikawa T, Md MM, Yamamura Y, Shichinohe T, Hirano S, Kondo S. The immunological impact of neoadjuvant chemotherapy on the tumor microenvironment of esophageal squamous cell carcinoma. *Annals of surgical oncology* 2012, **19**(5)**:** 1713-1719.

288.   DeNardo DG, Brennan DJ, Rexhepaj E, Ruffell B, Shiao SL, Madden SF*, et al.* Leukocyte complexity predicts breast cancer survival and functionally regulates response to chemotherapy. *Cancer discovery* 2011, **1**(1)**:** 54-67.

289.   Nelson BH. CD20+ B cells: the other tumor-infiltrating lymphocytes. *Journal of immunology* 2010, **185**(9)**:** 4977-4982.

290.   Inozume T, Hanada K, Wang QJ, Ahmadzadeh M, Wunderlich JR, Rosenberg SA*, et al.* Selection of CD8+PD-1+ lymphocytes in fresh human melanomas enriches for tumor-reactive T cells. *Journal of immunotherapy (Hagerstown, Md : 1997)* 2010, **33**(9)**:** 956-964.

291.   Myklebust JH, Irish JM, Brody J, Czerwinski DK, Houot R, Kohrt HE*, et al.* High PD-1 expression and suppressed cytokine signaling distinguish T cells infiltrating follicular lymphoma tumors from peripheral T cells. *Blood* 2013, **121**(8)**:** 1367-1376.

292.   Kronig H, Julia Falchner K, Odendahl M, Brackertz B, Conrad H, Muck D*, et al.* PD-1 expression on Melan-A-reactive T cells increases during progression to metastatic disease. *International journal of cancer Journal international du cancer* 2012, **130**(10)**:** 2327-2336.

293.   Chapon M, Randriamampita C, Maubec E, Badoual C, Fouquet S, Wang SF*, et al.* Progressive upregulation of PD-1 in primary and metastatic melanomas associated with blunted TCR signaling in infiltrating T lymphocytes. *The Journal of investigative dermatology* 2011, **131**(6)**:** 1300-1307.

294.   Koch M, Beckhove P, Op den Winkel J, Autenrieth D, Wagner P, Nummer D*, et al.* Tumor infiltrating T lymphocytes in colorectal cancer: Tumor-selective activation and cytotoxic activity in situ. *Annals of surgery* 2006, **244**(6)**:** 986-992; discussion 992-983.

295.   Chavez-Galan L, Arenas-Del Angel MC, Zenteno E, Chavez R, Lascurain R. Cell death mechanisms induced by cytotoxic lymphocytes. *Cellular & molecular immunology* 2009, **6**(1)**:** 15-25.

296.   Stumpf M, Hasenburg A, Riener MO, Jutting U, Wang C, Shen Y, *et al.* Intraepithelial CD8-positive T lymphocytes predict survival for patients with serous stage III ovarian carcinomas: relevance of clonal selection of T lymphocytes. *British journal of cancer* 2009, **101**(9)**:** 1513-1521.

297.   Webb JR, Milne K, Watson P, Deleeuw RJ, Nelson BH. Tumor-infiltrating lymphocytes expressing the tissue resident memory marker CD103 are associated with increased survival in high-grade serous ovarian cancer. *Clinical cancer research : an official journal of the American Association for Cancer Research* 2014, **20**(2)**:** 434-444.

298.   Bigelow E, Bever KM, Xu H, Yager A, Wu A, Taube J, *et al.* Immunohistochemical staining of B7-H1 (PD-L1) on paraffin-embedded slides of pancreatic adenocarcinoma tissue. *Journal of visualized experiments : JoVE* 2013(71).

299.   Hong M, Puaux AL, Huang C, Loumagne L, Tow C, Mackay C, *et al.* Chemotherapy induces intratumoral expression of chemokines in cutaneous melanoma, favoring T-cell infiltration and tumor control. *Cancer research* 2011, **71**(22)**:** 6997-7009.

300.   Harlin H, Meng Y, Peterson AC, Zha Y, Tretiakova M, Slingluff C, *et al.* Chemokine expression in melanoma metastases associated with CD8+ T-cell recruitment. *Cancer research* 2009, **69**(7)**:** 3077-3085.

301.   Mukaida N, Sasaki S, Baba T. Chemokines in cancer development and progression and their potential as targeting molecules for cancer treatment. *Mediators of inflammation* 2014, **2014:** 170381.

302.   Scott DW, Wright GW, Williams PM, Lih CJ, Walsh W, Jaffe ES, *et al.* Determining cell-of-origin subtypes of diffuse large B-cell lymphoma using gene expression in formalin-fixed paraffin-embedded tissue. *Blood* 2014, **123**(8)**:** 1214-1217.

Appendices

Appendix A.

Spearman's r correlations between the presence of total CD8$^+$ GzmB$^+$ T cells and total CD8$^+$ T cells and GzmB$^+$ immune cells.
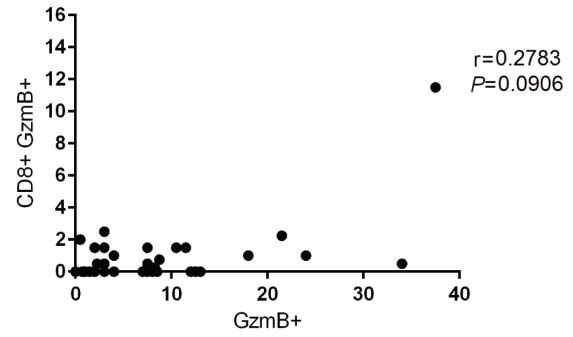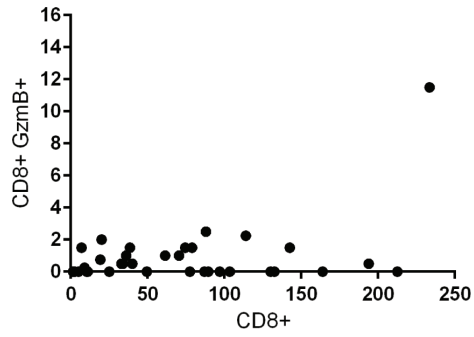
Appendix B.

Power analysis was performed on 12 immune markers (excluding cleaved caspase-3, MHC I, and MHC II) because these markers had absolute cell quantifications. The types of cells presenting cleaved caspase-3 were unidentifiable (they were collectively termed apoptotic bodies), and MHC I and II were scored on intensity levels.

Sensitivity Analysis (the level of effect size detection with 80% power)

Number of markers	Alpha (α)	Sample Size	Effect Size (mean of the differences standard/deviation of differences
1	0.05000	26	0.57
2	0.02500	26	0.64
3	0.01667	26	0.67
4	0.01250	26	0.70
5	0.01000	26	0.72
6	0.00833	26	0.74
7	0.00714	26	0.75
8	0.00625	26	0.76
9	0.00556	26	0.78
10	0.00500	26	0.78
11	0.00455	26	0.79
12	0.00417	26	0.79

With a sample size of n=26, one is predicted to be able to detect an effect size of 0.8 with 80% confidence after adjustment to account for multiple testing.

t tests – Means: Wilcoxon signed–rank test (matched pairs)
Tail(s) = Two. Parent distribution = Normal. α err prob = 0.004. Power (1–β err prob) = 0.8
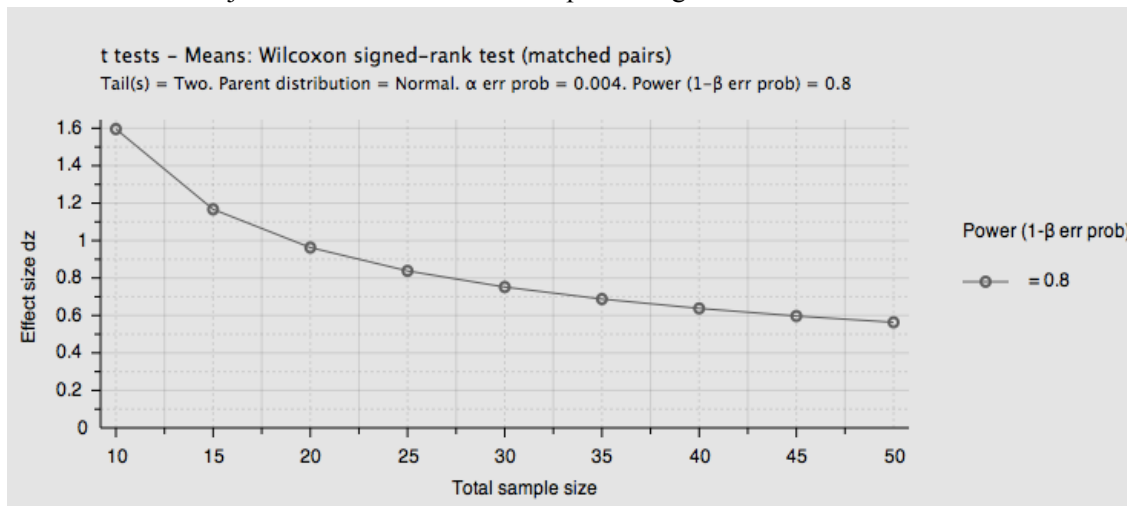
For my results, I have 80% power to detect a standardized effect size of 0.8.

t tests – Means: Wilcoxon signed-rank test (matched pairs)
Tail(s) = Two. Parent distribution = Normal. Total sample size = 26. α err prob = 0.004
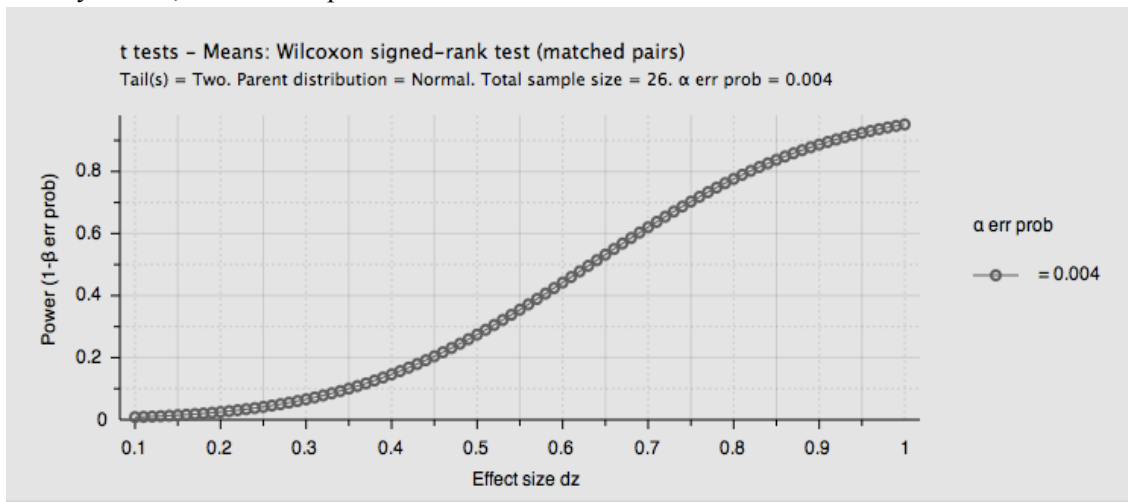
Appendix C.

Multiple testing analysis for intraepithelial TIL density, total cell count, absolute intraepithelial cell count, and absolute stromal cell count following chemotherapy in all tumour sites (n=26). Unadjusted *P* values represent Wilcoxon matched-pairs test prior to multiple testing, and adjusted *P* values represent Wilcoxon matched-pairs test after multiple testing use (false discovery rate).

P values	Intraepithelial density		Total cell count		Intraepithelial cell count		Stromal cell count	
Markers	Unadjusted	Adjusted	Unadjusted	Adjusted	Unadjusted	Adjusted	Unadjusted	Adjusted
CD1a	0.8169	0.8946	0.5269	0.6022	0.2647	0.4538	0.9237	0.9237
CD3	**0.0039**	**0.0140**	0.1048	0.2096	0.0806	0.2418	0.2472	0.4467
CD4	**0.0102**	**0.0187**	0.3122	0.4541	0.1358	0.3034	0.7172	0.9237
CD8	**0.0067**	**0.0147**	**0.0382**	0.1222	0.1517	0.3034	**0.0382**	0.1528
CD20	**0.0004**	**0.0044**	0.0585	0.1560	**0.0058**	0.0696	0.0532	0.1596
CD56	0.8946	0.8946	0.0832	0.1902	0.5097	0.6796	0.2485	0.4467
CD68	0.4834	0.5908	0.3976	0.4914	0.7312	0.7977	0.5651	0.8476
CD103	**0.0275**	**0.0432**	0.2304	0.3686	0.6386	0.7663	0.2606	0.4467
FoxP3	0.1563	0.2149	0.9842	0.9842	0.9315	0.9315	0.8893	0.9237
GzmB	N/A	N/A	**0.0060**	**0.0449**	0.3799	0.5698	**0.0096**	0.1152
TIA-1	**0.0024**	**0.0132**	**0.0085**	**0.0449**	**0.0420**	0.1680	**0.0307**	0.1528
PD-1	**0.0051**	**0.0140**	0.1445	0.2569	**0.0414**	0.1680	0.8374	0.9237
Cleaved caspase-3 tumour cells	-	-	0.3993	0.4914	-	-	-	-
Cleaved caspase-3 apoptotic bodies	-	-	**0.0007**	**0.0112**	-	-	-	-
MHC I	-	-	0.7141	0.7617	-	-	-	-
MHC II	-	-	**0.0112**	**0.0448**	-	-	-	-

P values are calculated using Wilcoxon matched pairs test with Pratt's method and bolded values indicate statistical significance of *P<0.05, P<0.01, P<0.001*
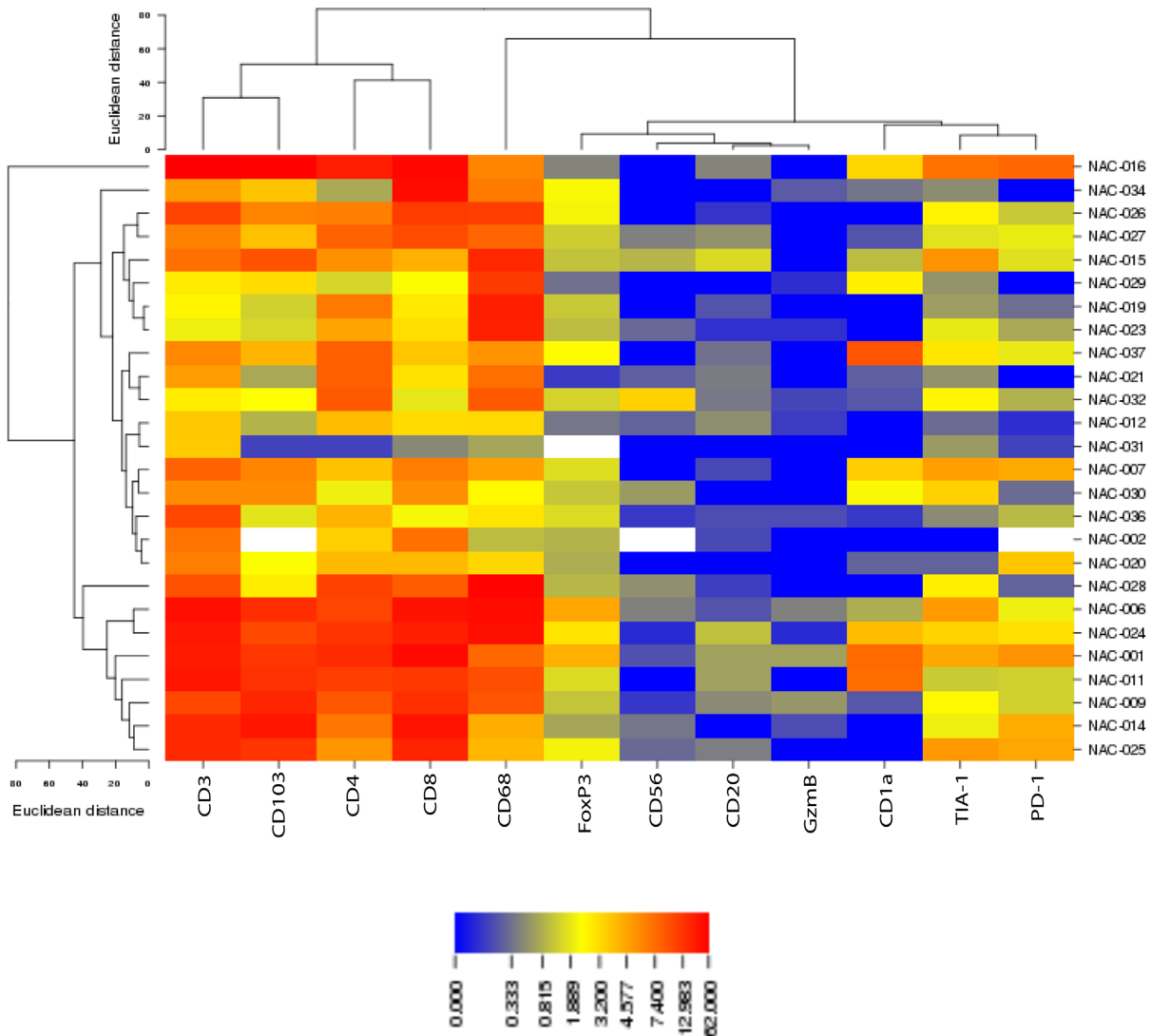
Appendix D.

A comparison of adjusted statistical significances following multiple testing (false discovery rate) in immune infiltration following chemotherapy in extra-pelvic sites only and all tumour sites.

P-values	Extra-pelvic sites only (n=18)				All tumour sites (n=26)			
Marker	Density	Total	IT	S	Density	Total	IT	S
CD1a	0.5693	0.3140	0.3990	0.5157	0.8946	0.6022	0.4538	0.9237
CD3	**0.0188**	**0.0357**	0.3990	0.1726	**0.0140**	0.2096	0.2418	0.4467
CD4	0.3922	0.7763	0.8072	0.8046	**0.0187**	0.4541	0.3034	0.9237
CD8	0.0569	**0.0357**	0.5208	**0.0240**	**0.0147**	0.1222	0.3034	0.1528
CD20	**0.0180**	**0.0357**	0.2076	**0.0240**	**0.0044**	0.1560	0.0696	0.1596
CD56	0.9355	0.1957	0.8072	0.2026	0.8946	0.1902	0.6796	0.4467
CD68	0.5197	0.5134	0.2379	0.9070	0.5908	0.4914	0.7977	0.8476
CD103	0.2648	0.3717	0.8072	0.1726	**0.0432**	0.3686	0.7663	0.4467
FoxP3	0.9355	0.7918	0.8072	0.7633	0.2149	0.9842	0.9315	0.9237
Granzyme B	0.5691	**0.0064**	0.7442	**0.0096**	N/A	**0.0449**	0.5698	0.1152
TIA-1	**0.0144**	**0.0299**	0.2076	**0.0240**	**0.0132**	**0.0449**	0.1680	0.1528
PD-1	**0.0417**	0.1625	0.2379	0.9070	**0.0140**	0.2569	0.1680	0.9237
cl. Casp-3 tumour cells		0.1625	-	-	-	0.4914	-	-
cl. Casp-3 apoptotic cells		**0.0016**	-	-	-	**0.0112**	-	-
MHC I		0.9999	-	-	-	0.7617	-	-
MHC II		0.1607	-	-	-	**0.0448**	-	-

P values are calculated using Wilcoxon matched pairs test with Pratt's method and bolded values indicate statistical significance of *P*<0.05, *P*<0.01, *P*<0.001

Appendix E.
Hierarchical clustering to assess associations between TIL subsets in pre-chemotherapy tumours.
A heatmap illustrates the intraepithelial TIL densities in pre-chemotherapy tumours from the
matching cohort (n=26). Unsupervised clustering algorithm with complete-linkage method
and Euclidean distances was used. The rows represent patient cases and columns represent TIL
markers indicating 0 (blue) to 62 (orange).

Appendix F.
Hierarchical clustering to assess associations between TIL subsets in post-chemotherapy tumours. A heatmap illustrates the intraepithelial TIL densities in post-chemotherapy tumours from the matching cohort (n=26). Unsupervised clustering algorithm with complete-linkage method and Euclidean distances was used. The rows represent patient cases and columns represent TIL markers indicating 0 (blue) to 146 (orange).
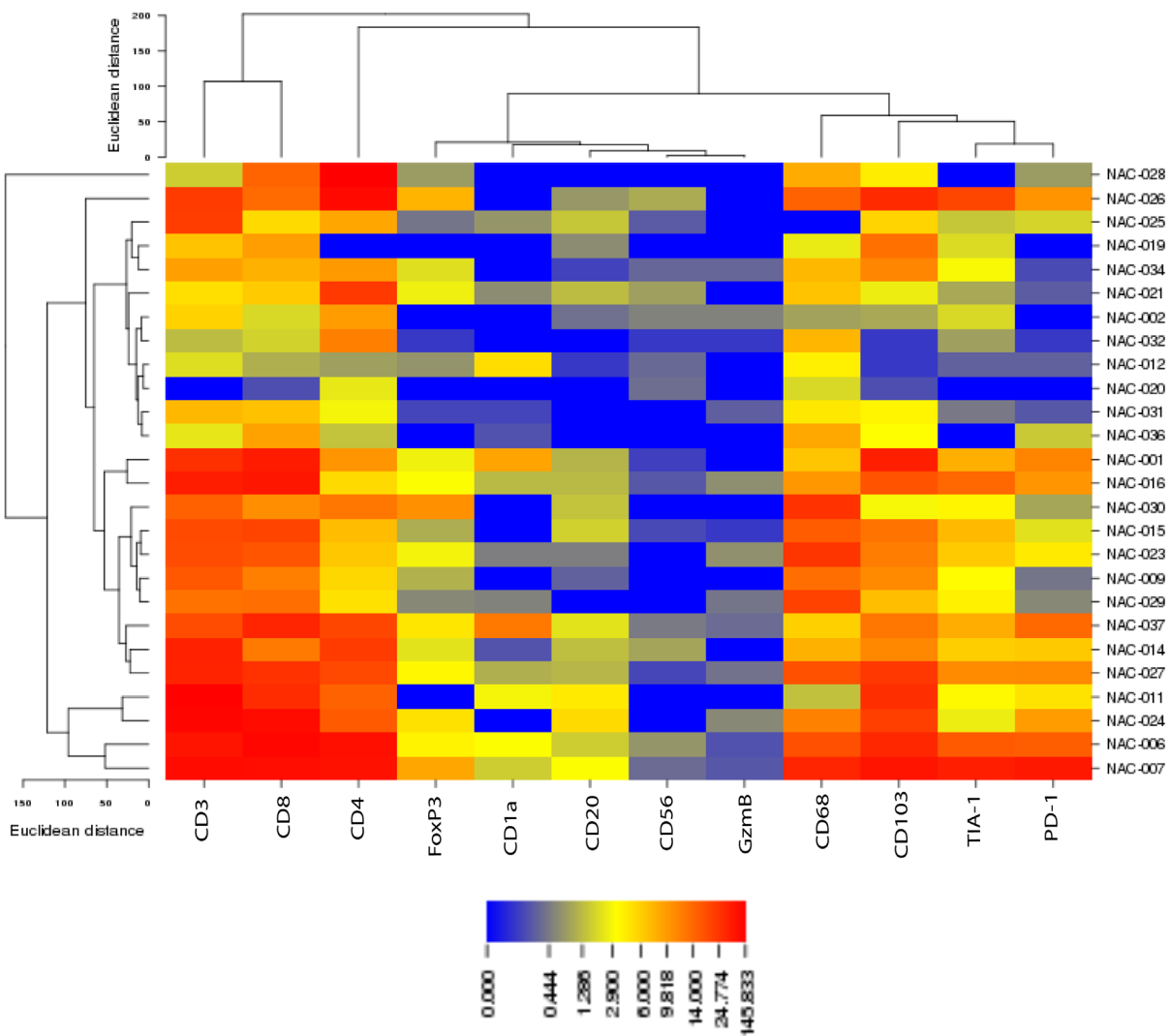
Appendix G.

Intraepithelial TIL density cut-offs using X-tile to differentiate patients between high and low TIL densities. Monte-Carlo *P* value indicates if the cut-point is robust in segregating patients into low and high TIL densities. Chi-sq Hi/Lo is the chi square test for the survival curves generated using the cut-offs.

Marker	Cut-Point	Monte-Carlo *P* value	Chi-sq Hi/Lo
CD3	6.50	0.4028	2.3210
CD8	2.15	0.4795	1.5341
CD20	0.30	0.2542	3.1684
TIA-1	4.10	0.4028	2.6284
PD-1	1.67	0.5839	0.7461
FoxP3	0.28	0.5839	1.1917

Appendix H.
Kaplan-Meier analysis of change in TIL infiltration following chemotherapy. For each graph, cases that have increased-*de novo* responses or 2-fold increase TIL (blue), 2-fold decrease (red), and 0 or sustained TIL (black) following chemotherapy.

CD3

P=0.2673

CD8

P=0.0259   P=0.0148

(Increase, n=13; decrease, n=5; unchanged, n=8)

CD20

P=0.6698

TIA-1

P=0.8851

FoxP3

P=0.7848

PD-1

P=0.8969

126